

USING NONSTANDARD BASIS FUNCTIONS IN
DESCRIPTION OF SIGNALS AND SYSTEMS

By
Alexandros Soumelidis

SUBMITTED IN PARTIAL FULFILLMENT OF THE
REQUIREMENTS FOR THE DEGREE OF
DOCTOR OF PHILOSOPHY
AT
BUDAPEST UNIVERSITY OF TECHNOLOGY AND ECONOMICS
BUDAPEST, HUNGARY
MARCH 2002

© Copyright by Alexandros Soumelidis, 2002

BUDAPEST UNIVERSITY OF TECHNOLOGY AND ECONOMICS
DEPARTMENT OF
TRANSPORT AUTOMATION

The undersigned hereby certify that they have read and recommend to the Faculty of Transportation Engineering for acceptance a thesis entitled “**Using nonstandard basis functions in description of signals and systems**” by **Alexandros Soumelidis** in partial fulfillment of the requirements for the degree of **Doctor of Philosophy**.

Dated: March 2002

Thesis Supervisor:

József Bokor

Reviewers:

Table of Contents

Table of Contents	v
Acknowledgements	ix
Abstract	xi
Notation	xiii
Introduction	1
1 Signal representations	3
1.1 Signals and systems	3
1.2 Signal representations basics	9
1.2.1 Continuous representations	12
1.2.2 Discrete representations	14
1.3 Representation of continuous-time signals	17
1.3.1 The \mathcal{L}^p signal spaces	18
1.3.2 Frequency domain representations	21
1.4 Representation of discrete-time signals	30
2 Representation of signals in \mathcal{H}^2	31
2.1 Representations of discrete-time signals and systems	31
2.2 Standard basis in \mathcal{H}^2	38
2.3 The discrete Laguerre system	39
2.3.1 Generalization of the standard basis	39
2.3.2 The Blaschke-function, and the argument transform	44
2.3.3 Identification by Laguerre representation	52
2.4 Generalized orthogonal bases	53
2.4.1 Generalizing the Laguerre system	53
2.4.2 Takenaka-Malmquist system: general considerations	55
2.4.3 Takenaka-Malmquist system: the finite case	59

2.4.4	Takenaka-Malmquist system: the periodic case	63
2.4.5	Argument-transform for the generalized orthogonal basis	67
2.4.6	General orthogonal basis in the z -domain	73
3	Realizing the GOB representation	79
3.1	Computing the GOB coefficients in z -domain	79
3.2	Computing the GOB coefficients: examples	85
3.3	Obtaining frequency domain data	93
3.4	Applying the inverse argument transform	102
4	Applying GOB representations: detection	113
4.1	Detection, feature enhancement and noise suppression	113
4.2	Using a priori knowledge in representations	117
4.3	Detection scheme by using generalized orthogonal bases	122
4.3.1	Detection scheme upon the representation coefficients	135
4.3.2	Detection by building reproducing kernel in GOB	143
4.4	Noise suppression, feature enhancement	151
5	Applying GOB representations: identification	153
5.1	System identification and nonstandard representations	153
5.2	Identification of functions in \mathcal{H}^2	157
5.3	Obtaining approximate pole information	160
5.4	Iterative improving of poles	161
5.4.1	Construction of a bi-orthogonal system defined by partial fraction	162
5.4.2	Iteration on pole structure and parameters	168
5.4.3	The discrete Cauchy formula	169
5.4.4	Realization and examples	172
5.5	\mathcal{H}^∞ representations in generalized orthogonal basis	174
6	New results	181
6.1	Thesis I.	181
6.2	Thesis II.	182
6.3	Thesis III.	183
6.4	Thesis IV.	184
6.5	Thesis V.	185
6.6	Thesis VI.	186
	Bibliography	187

To my wife Éva,

and

the memory of my father

Acknowledgements

This thesis has been prepared as a result of long time research work done in the Systems and Control Laboratory, Computer and Automation Research Institute of the Hungarian Academy of Sciences in collaboration with laboratory staff members, and researchers of other institutes. The author would like to express major gratitude to all the persons, who contributed in any way to forming an interesting and stimulating environment which is essential for any systematic research.

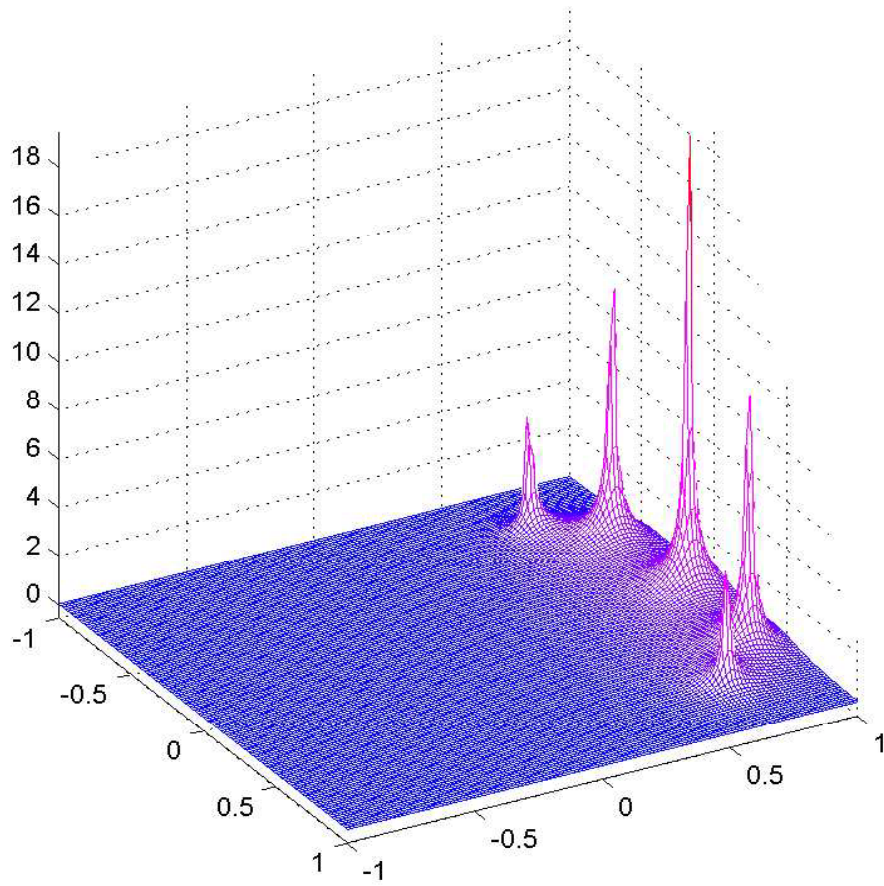
This work would never have come into existence without the help, encouragement, stimulation, and sometimes pressure of the thesis supervisor József Bokor, head of the Systems and Control Laboratory. Special gratitude to Ferenc Schipp, professor of the Eötvös Loránd University of Budapest for his stimulating ideas, and the mathematical support, that has been indispensable for the "non-mathematician" author to clarify his ideas.

The author is most grateful to Laboratory staff members András Edelmayer, Zoltán Szabó, and Péter Gáspár for their valuable help given in the course of the everyday work.

Special thanks to our industrial partners for the inspiring problems that I have the opportunity to confront, and their practical experience that has been shared with me, both helped me in to keep to reality.

Let me express gratefulness to my teachers, my former and present principals, especially to László Keviczky, who started my path in the field of systems sciences, and to the memory of József Hatvany, who started about twenty years ago my career in the Institute.

Finally, I'd like to express my heartfelt gratitude to my wife for her *patience* and *love* that have supported me not only in the period of writing this thesis, but in all the things that are — not always easily tolerable — properties of a "researcher". Thanks also for my daughter Christina, for the happy and joyful moments bringing in my life.



"Things are not to be searched on basis of words but words have to be found to things, since things become perfect not because of words but give perfection to words."

Myson, an ancient Greek philosopher

Abstract

The subject of the thesis is the application of nonstandard basis functions in description of signals and systems. After an introduction the the general concept of representations, the frequency domain representations of discrete-time signals is elaborated, and a system of functions, called generalized orthogonal basis (GOB) functions, that forma an orthonormal basis in the space $\mathcal{H}^2(\mathbb{D})$ is introduced.

The signal representations based upon this system are applied in the detection and identification field in association with signals and systems emerging in application areas, such as industry, engineering, energy production, vehicles control, etc. The main motivation to apply representations upon nonstandard bases is the ability of these constructions to incorporate a priori information upon the characteristics of the system to be analyzed, which can result in high sensitivity on that characteristics themselves. The a priori information involved into the methods studied in the thesis is the location of system poles, that is a dominant constituent in determination of the system dynamics.

The thesis proposes also methods to realize detection and identification tasks on the basis of nonstandard representations, as well as examines the realization and convergence aspects emerging in association with them.

Notation

\mathbb{Z}	the set of integer numbers
\mathbb{N}	the set of nonnegative integers, i.e. $\mathbb{N} := \{n \in \mathbb{Z} : x \geq 0\}$
\mathbb{N}^*	the set of positive integers, i.e. $\mathbb{N}^* := \{n \in \mathbb{Z} : x > 0\}$
\mathbb{R}	the set of real numbers
\mathbb{R}^*	the set of non-negative real numbers, i.e. $\mathbb{R}^* := \{x \in \mathbb{R} : x \geq 0\}$
\mathbb{R}^-	the set of non-positive real numbers, i.e. $\mathbb{R}^- := \{x \in \mathbb{R} : x \leq 0\}$
\mathbb{C}	the set of complex numbers
\mathbb{T}	the unit circle on the complex plane, i.e. $\mathbb{T} := \{z \in \mathbb{C} : z = 1\}$
\mathbb{D}	the open unit disc on the complex plane, i.e. $\mathbb{D} := \{z \in \mathbb{C} : z < 1\}$
$\mathbb{I}(\cdot)$	a closed interval within (\cdot)
\mathcal{D}	the domain of a function
\mathcal{R}	the range of a function
\mathcal{L}^p	the Banach space of real functions with p -norm
\mathcal{L}^1	the Banach space of real functions with absolute norm
\mathcal{L}^2	the Banach space of real functions with square norm
\mathcal{L}^∞	the Banach space of real functions with maximum norm
\mathcal{A}	the set of complex functions analytic in the unit circle
\mathcal{H}^p	the Hardy space with p -norm
\mathcal{H}^2	the Hardy space with square norm
\mathcal{H}_\perp^2	the orthogonal complement of the Hardy space \mathcal{H}^2
\mathcal{H}^∞	the Hardy space with maximum norm

Introduction

The subject of this thesis work has been the use of *nonstandard basis functions* in the *description* of *signals* and *systems* emerging in many application areas, of the industry, engineering, energy production, vehicles, etc. *Description* has been used to indicate the variety of the application: description mostly means to use a mathematical language to make possible the recognition of it, hence incorporates the modelling and identification of systems, and can be completed into the direction of the goals of the recognition, the decision making upon its state and operation, i.e. detection of phenomena and control. Within this variety the current thesis focuses mostly on the identification and the detection field. Furthermore the thesis deals with *signals* and *systems*: the goal is in most cases the cognition of systems, however this can only be done through the signals belonging the them. Observations, measurements can usually be considered as signals, and signal processing tasks can be used for the purpose to recognize the structure and the behavior of the underlying system. This thesis mostly concentrates upon the signals, however the connection with the systems will always be kept in mind.

Finally the expression *nonstandard basis functions* will be analyzed: this notion in the title suggest that the nonstandard basis functions are used contrary to standard ones. Standard basis in the mathematics and the systems science usually means a trigonometric basis that is strictly connected to the concept of Fourier series and Fourier transform. The motivation to use something different originated from several sources.

In the mathematics this field began to evolve at the beginning of the 20th century in

connection with the convergence problems of the Fourier series in several function spaces, for example in \mathcal{L}^∞ . Another motor of the development was the demand for finding several orthogonal systems, which can represent any function belonging to interesting Hilbert spaces — as the spaces \mathcal{L}^2 and \mathcal{H}^2 — which has led to the construction of the Schauder, Franklin, Walsh, Haar, and other systems [51], [70].

Within the systems science system identification has been the area, that has principally acted in the generation and development of the principle what is now called *nonstandard representations* or *nonstandard basis functions*. The demand to use of nonstandard bases has arisen because of convergence problems were being emerged in the spaces applied to find robust solutions instead of the classical optimal ones, namely the \mathcal{L}^∞ and \mathcal{H}^∞ [31], [43], [16], [38], [7].

Besides this the motivation of this thesis to concentrate upon the nonstandard bases contain a new component: the nonstandard bases offer a new opportunity to provide them with characteristics that are in connection with *a priori* information about the system to be described. Equipped with this information the representations built upon the bases will be sensitive to these characteristics, which can be advantageous in identification and detection problems.

Organization of the thesis: First a general introduction will be given to the representations of signals (Chapter 1), than the discussion will be concretized to the frequency domain representations in $\mathcal{H}^2(\mathbb{D})$ by using information upon the system poles (Chapter 2), and the notion of the generalized orthogonal bases (GOB) is introduced. Chapter 3 is devoted to realization and algorithmic problems emerging in association with the GOB representations. The next to chapters deal with application areas of the generalized orthogonal bases, Chapter 4 is devoted to the detection type methods, and Chapter 5 to system identification. Finally a summary of the scientific results is presented (Chapter 6).

Chapter 1

Signal representations

In this chapter a brief introduction is given to signals representations and their connection with the systems. The goal is to lay the foundation for the specific area selected as research field in the framework of the thesis, the discrete-time frequency-domain signal and system representations, hence the introduction focuses on selected topics within the systems science and signal theory. This does not mean that the fields omitted are not appreciated, however the restrictions on space do not allow the comprehensive study of the whole domain. In this chapter, following a general introduction to signal representations, the representations of continuous-time signals are mainly concerned, the discrete-time representations remain subject of the principal chapters of the thesis.

1.1 Signals and systems

In mediam res . . . the main subject of the present thesis work is the *representation* of *signals* in several systems of functions with some specific *purpose*. This statement immediately involves a number of questions, at least as follow: what is the meaning of *signal*; what does *representation* mean; and what is the *purpose* of doing this.

Signal is a rather diversified notion both in the common sense and in several disciplines of science. In the common sense signal can on the one hand be a message, a symbolic

action that is used to transfer ideas between humans (e.g. a sentence, a gesture), or in static sense the symbol itself in its visual or acoustic incarnation (e.g. a picture, a sound). On the other hand signal can be a message that characterize an event, a series of events, i.e. the state or the behavior of a natural or artificial object, organism existing in the real world. *Signals* are subject of a number of disciplines of science, namely that of *semiotics* or *semiology*; they've got their name from "σημείον", the Greek equivalent of the word signal. *Semiotics* is originated from the American mathematician Ch. S. Pierce and elaborated by philosopher Ch. Morris. Its subject comprise everything from the simplest symbols used in human communication until the most complex languages including the artificial ones introduced by computer science. Besides the *syntactics* and *semantics* of the systems of signals it deals also with *pragmatics*, i.e. examines what is the reaction of humans as answer to signals. More "theoretic" or "philosophic" discipline is *semiology*, which has established by F. de Saussure and became part of structuralism, a significant trend of the philosophy of the 20th century. *Semiology* began from structural linguistics and developed until the meta-linguistic forms of the human communication by the work of e.g. R. Barthes, M. Foucault and others. One of the main statements of the structural *semiology* is that signals (including images, gestures, music, ritual or traditional objects, and systems built from them) can be described as abstract objects and systems independently of their concrete meaning, i.e. the semantics representing by them.

In the current thesis work the discipline of *signal theory* — or more technically — the field of *signal processing* is studied, which rather have their source within the technological science which evolved in the middle of the 20th century, along with system science, information, and communication theory. Creator was a scientific community rather than individuals, however there are some undoubtedly significant personals distinguished as e.g. W. Wiener, C.E. Shannon, R. E. Kalman, D. Gabor, and others. Signal theory and system theory is strictly connected to each other, it is no surprising, that in many cases rather

vague dividing line can be found between them.

In *signal theory* the central notion is *signal*, which can be defined as a physical quantity observed in connection with objects or systems of the physical reality as function of time. Hence the notion of signal corresponds to the notion of the mathematical *function* with the independent variable of *time*. The notion of signal is an abstraction, any physical property in connection with signals — the underlying semantics — is ignored, only the changes against time are considered. In this respect signal theory shows some relations with semiology as outlined above.

The goals of signal theory are rather diversified. Signal theory observes and analyzes signals with the purpose to obtain information of the source object. What kind of information is required to produce by signal analysis depends upon the question analyzed, e.g. exploring its structure, determining its operation under specific conditions, or mapping its behavior within its environment, etc. The information acquired usually serves as starting point for making decisions upon the future of the underlying system, for example changing its structure, controlling its operation, repairing it, or even drop it in the waste. Signal theory concentrate on the process of acquiring information, and disregard the particular application of this. Of course system theory cannot isolate itself in an ivory tower, it must correspond to the requirements raised by particular application fields. Signal theory determines basic tasks to solve in a level of abstraction, namely — with some simplification — by applying the abstractions of the mathematical theory of functions and operators, such that the resulted analysis methods be useful in various application fields.

In the near past the signal analysis methods was divided in two main branches, the time-domain as well as the frequency domain ones with connection link between them the Fourier-transform. Signal theory became successful when the digital methods had begun to spread, and one of the most important factor in development was the efficiency of Fast Fourier Transform (FFT) algorithm. The modern view of signals consider the frequency

domain description as one of the imaginable *representations* of the signals, and investigate for further useful, and for specific applications more efficient, representations. These efforts resulted in numerous improvements in signal theory, for example difficulties arisen by time-varying spectra or the principle of uncertainty has been eliminated.

Representation of a particular signal is constructed on the basis of a — countable or not countable — set of signals. Selecting the basic set by fulfilling specific features, results in an increased sensitivity of the representation against these features, this fact can immediately be utilized in detection, feature enhancement, noise rejection, and similar algorithms. Furthermore the representing function set can possess properties, which can characterize the approximations based upon it, i.e. if the representing set forms a metric function space, the metric can be used to judge the goodness of the approximation. The methods used in connection with system identification and modelling, as well as digital signal analysis algorithms are frequently based upon approximations, hence representations on metric spaces have great importance in the practice.

The notion of signals is frequently mentioned in association with *systems*. Signal theory is connected to systems theory in numerous ways: the system inputs and outputs, as well as the internal variables, e.g. the state variables, are considered as signals; and the systems are considered as operators mapping a signal space to another one. A significant part of the methods used in the system theory — for example system identification, or system change detection — are common with that of signal processing; furthermore a lot of signal processing method contain in the depth some type of system concept — e.g. state-space considerations. In the present thesis work the main emphasis is concentrated upon signal processing methods, however the direct connections with the systems either in conceptual or in the application level will not be omitted.

To be explicit, *signals* in the more general view can be regarded as real functions of

time:

$$x = f(t) \quad (t \in \mathbb{R})$$

In many cases the t domain is restricted to finite open or closed intervals, e.g.

$$x = f(t) \quad (t \in [a, b] \quad a, b \in \mathbb{R})$$

This is the fact when a signal is *periodic* with the period $[a, b]$. Signals can also be considered to be *multi-dimensional*, when multiple signals, synchronous in time, are advantageous to be handled simultaneously, as it is typical in system descriptions; in this case f is a vector-valued function. In many cases it is advantageous to consider *complex* valued signals. This can on the one hand be only formal action to make possible the usage of methods working originally on complex variables; in this case the imaginary part usually has no physical meaning. On the other hand combining two signals in a complex valued one can possess physical meaning; signals with $\pi/2$ phase shift originated from a rotating system is a typical example.

The signal concept stated above is that of *continuous-time signal*, in contrast with the so-called *discrete-time signal*. Continuous-time signals are functions upon the whole real line, or any interval of it. Discrete-time signals are considered to be sequences upon a countable (infinite or finite) set of indexes, i.e.

$$x = \{x_n\} \quad (n = 0, 1, \dots, N \quad N \in \mathbb{N})$$

The indices have a strict correspondence with some points of the real time-line, i.e. with time instants, when the corresponding signal value is valid. In these time instants a new signal value is generated either by completing a measurement if original data acquisition is performed, or completing a computation for derived signals. The procedure of turning from the continuum time-scale to the discrete one is called *sampling*. In the field of signal theory

usually uniform sampling is realized, i.e. sampling is performed periodically starting at a time instant (t_0) with equal time-period (Δt):

$$x_n = f(t_0 + n\Delta t) \quad (t_0, \Delta t \in \mathbb{R} \quad n = 0, 1, \dots, N \quad N \in \mathbb{N})$$

Non-uniform or event-driven sampling is usual characteristic of acquiring information in other disciplines, for example in the field of discrete-event systems. Studying these type of systems and the signals associated with them is not subject of the current thesis work.

To be precise, an other standpoint of classification can also be mentioned: signals can be of *deterministic* or *stochastic* nature. In this thesis work the signals will mainly be considered to be deterministic, any stochastic nature will be concentrated in the notion of *noise*. Noises occur usually as (mainly additive) error-terms, which can vary by time, hence satisfy the characteristics of signal, however they are not treated as signals, only some statistical properties are considered. Their interpretation is usually quite simple: normally distributed stationary noise process is a common assumption.

The following sections of this chapter will give a summary of the commonly studied signal types in the signal theory, embedded them in the notion of signal spaces and underlying representations. Signal spaces are defined because the classes of continuous- or discrete-time signals are too broad to be tractable with the mathematical methods of functions. Besides the viewpoints given up to this point (e.g. continuity, periodicity) further characteristics are used to widen the classification, e.g. boundedness by amplitude and by energy as the commonly used ones.

The use of spaces of signals with bounded energy is a quite natural requirement originating from physics. In the nature physical systems contain strictly finite amount of energy, and there is no process, which utilizes infinite energy. The roots of the finite energy principle resort to Gauss: it has a strict correspondence with the least-square methods. Least square methods — independently of any energetical consideration — are very popular in many

fields not only in signal theory, and suited as conceptual basis to the classical optimization theory. Wiener and Kalman filtering, a lot of methods for filter design, an detection are based upon it. Although the concept of optimality has nowadays been revised, and instead of strict optimality — which can be oversensitive to some changes — worst-case or robust optimality is preferred, least-square methods have not lost their significance. The principles of finite energy or least square optimality is embedded in the \mathcal{L}^2 , ℓ^2 , and \mathcal{H}^2 representations, which will be discussed in the following sections.

Boundedness of amplitude also corresponds to some physical principles; the physical quantities has in the practice some upper bound, e.g. maximal torque for a motor drive, or maximal tolerable pressure for a mechanical part. Boundedness in mathematics is usually connected to uniform continuity or convergence, and worst-case optimality. Optimization by this principle forms the basis of the robust design, detection, etc. methods, which have become popular in the past decade. The function spaces corresponding to the principle of boundedness are denoted by \mathcal{L}^∞ , ℓ^∞ , and \mathcal{H}^∞ , the reason, and the detailed description will follow later. The delay of spreading these methods relative to that of least square ones is due to the mathematical difficulties arisen in the representations.

1.2 Signal representations basics

The representation of a signal — i.e. a function of time $f(t)$ — essentially means its realization with the elements of a predefined collection of functions. This collection can contain finite, countable, or continuum elements; let's call it *representing set*. Of course, the above statement is not exact, because we haven't defined what does exactly mean the realization. This, usually in the traditionally evolved practice, means some type of linear operation upon the elements of the set.

In the case when the representing set is countable (finite or infinite) the customary

procedure is to form a linear combination of the elements, i.e. the representation of function $f(t)$ on the countable set of functions $\{\varphi_n(t)\}$ has the form of

$$f(t) = \sum_{n=1}^N c_n \varphi_n(t) \quad (N \in \mathbb{N}) \quad (1.2.1)$$

where $\{c_n\}$ are the coefficients of the representation. Of course, (1.2.1) can only be considered as a formal specification, it does not per se guarantee either the exactness of the realization or the convergence in the infinite case. The set of all the real functions is too broad to examine these questions, conditions for the exactness and convergence can only be given for smaller function classes. These type of representations are called *discrete* ones, to emphasize that the representing set contains countable number of individual functions. One must not confuse the attribute "discrete" used here with "discrete-time", which characterizes the time-scale of the functions involved.

The formula (1.2.1) cannot be regarded as the more general form of the discrete representations, it has only been selected for the simplicity of the introduction. In the practice various other forms are used, for example there are two-sided forms with indexes both negative and positive, double-indexed constructs to represent two-dimensional coefficient-space, as well as there exist also complex forms. As "omnipotent" representation does not exist, there is no reason to make efforts for finding a universal formula.

The representation scheme can be considered as a linear transform from the sequence-space of the coefficients into the space of functions. If the source and destination spaces are considered to be linear ones, this transform constitutes a linear operator between the two spaces. The inverse procedure, i.e. the construction of the set of the coefficients from the function is also an important problem. In the signal processing practice the latter task is called "transform", and the representation formula establishes the "inverse transform", i.e. the time-based view is dominant.

The discrete representation of signals can also be considered as a weighted sum of

the elements of the representing function set, and the coefficients $\{c_n\}$ are the weights, showing how strongly influences the target function any given function from the set. This scheme can be generalized onto the case when a continuum collection of functions form the representing set: if the set is parameterized with a given real variable, the weighted sum will be transferred to an integral according to this variable upon a density function. Let us consider the collection of functions $\Psi(t, s)$, parameterized by the variable $s \in \mathbb{R}$, and a real function $d(s)$ with domain of \mathbb{R} ,

$$f(t) = \int_{-\infty}^{\infty} d(s) \Psi(t, s) ds \quad (1.2.2)$$

is an integral-transform between d and f with kernel $\Psi(t, s)$. The analogy with the formula of discrete representation is obvious, the value of density function $d(s)$ in any s_0 point in \mathbb{R} serves as a weight for the infinitely small segment of $\Psi(t, s)$ containing s_0 in the approximating sum — if the notions of Riemann-integration are used — in any point t . More general form can be obtained if instead of the density a distribution is used, i.e.

$$f(t) = \int_{-\infty}^{\infty} \Psi(t, s) d\mu(s), \quad (1.2.3)$$

where

$$\mu(s) = \int_{-\infty}^s d(\sigma) d\sigma. \quad (1.2.4)$$

The representations specified by (1.2.2), (1.2.3) and (1.2.4) are called *continuous representations*. This name does not mean any statement upon the continuity of either the transform or the functions acting within it in mathematical sense, the fact that the representing set is a continuum is only concerned. It can be stated that — similarly to the discrete case — these formulas does not present the general form of the continuous representations, a simple form has been selected for the sake of clarity. However there is no reason to look for a general formula, because universal representation scheme does not exist, hence specific forms will be discussed that are valid only for smaller classes of functions.

Many of the representations specified by formula (1.2.2) are known as continuous signal transforms. More exactly the inverse of the representation formula is called "transform" and the representation formula itself is the "inverse transform". Specific signal-transforms will be studied later.

In the following sub-sections some important characteristics of the continuous and discrete representations will be discussed, as well as some examples will be presented.

1.2.1 Continuous representations

For practical reasons — to allow complex-valued functions — the definition of the continuous representations (1.2.2) is used in a slightly modified form. The representation of the $f(t)$ real (or complex-valued) function according to kernel $\Psi(t, s)$ is given by

$$f(t) = \int_{-\infty}^{\infty} \check{f}(s) \Psi^*(t, s) ds \quad (1.2.5)$$

where (*) denotes the complex conjugation. The weight-function (or density-function as it has been called above) is denoted \check{f} to sign that it is a transformed form of f . The transform can be expressed as

$$\check{f}(s) = \int_{-\infty}^{\infty} f(t) \Phi(t, s) dt \quad (1.2.6)$$

where $\Phi(t, s)$ kernel is used. The existence of this transform — of course — is not guaranteed for any case. The function $\Phi(t, s)$ is called *dual kernel*. If the dual kernel is equivalent to the original kernel, i.e.

$$\Phi(t, s) \equiv \Psi(t, s)$$

it is called *self-dual*.

As it has been noticed above, (1.2.5) is not the most general form of a continuous representation. This form assumes that the domain of both f and its transform \check{f} is the entire \mathbb{R} . In practice many other conditions are used, for example the domain is restricted to a finite interval of \mathbb{R} (as in the case of periodic signals), or the domain s is multidimensional,

hence multiple integrals are used, and the domain of the transform is interpreted as a plane (as in the case of continuous wavelet-transform). These and other special cases will be discussed later, here a simplified general introduction is given, hence transform and inverse transform from \mathbb{R} to \mathbb{R} is assumed. The existence and convergence even in this case is not guaranteed, these conditions are also studied later for special cases.

The representation must reconstruct the original function from its transform. To examine the conditions of this, let us substitute the expression of the inverse (formula (1.2.6)) into (1.2.5):

$$f(t) = \int_{-\infty}^{\infty} \int_{-\infty}^{\infty} f(\tau) \Phi(\tau, s) d\tau \Psi^*(t, s) ds,$$

and make a rearrangement in the order of integrations

$$f(t) = \int_{-\infty}^{\infty} f(\tau) \int_{-\infty}^{\infty} \Phi(\tau, s) \Psi^*(t, s) ds d\tau.$$

Let us denote

$$K(t, \tau) = \int_{-\infty}^{\infty} \Phi(\tau, s) \Psi^*(t, s) ds,$$

with this, if $K(t, \tau)$ function exists,

$$f(t) = \int_{-\infty}^{\infty} f(\tau) K(t, \tau) d\tau,$$

i.e. $K(t, \tau)$ is a *reproducing kernel*.

It is well-known, that there is no reproducing kernel in the space of the real functions. Formally it can be expressed with the δ -distribution (or Dirac-delta as it is known in the technical literature)

$$\int_{-\infty}^{\infty} \Phi(\tau, s) \Psi^*(t, s) ds = \delta(\tau - t).$$

This can be considered as an "orthogonality" condition, this is the condition of the reproducing property of the representation. There are some function-spaces where there exist reproducing kernel, that is the reproducing kernel is an ordinary function; for example some Hilbert-spaces possess this property, these are called RKHS-s (it means Reproducing Kernel Hilbert-Space). Some examples will be given later.

1.2.2 Discrete representations

To produce a discrete representation of function f of the form

$$f(t) = \sum_{n=1}^N c_n \varphi_n(t) \quad (N \in \mathbb{N}) \quad (1.2.7)$$

presumes that f is expressed as the linear combination of some (finite or infinite number of) functions belonging to a linear function space. Finite number of representing functions results in a finite dimensional function-space; in this case any element of the space can be expressed by the linear combination, i.e. the elements of the space can be represented.

More exciting is the case of the infinite dimensional space. In this case the question of convergence is a cardinal thing. To speak of convergence, a topology, or metric must be assumed, hence representations in metric (or normed) spaces gets essential significance.

If in a linear space of functions there is a countable collection of functions, which represent in the form (1.2.7) all the functions belonging to the space, is called to be *separable*. Among these collections of functions must be at least one of minimal cardinal number, this is the *dimension* of the space. If a collection of functions can represent all the functions of the space, it is called *complete system*. If the elements of the complete system are linearly independent, it is said to be *basis*. The dimension of the basis is equal to the cardinal number of the minimal complete system. In the practice not all linear function-spaces are separable, and not all linear systems possess basis.

In metric (normed) spaces the convergent function series tend to functions, the question is whether all the convergent function series has limit a function belonging to the space. The answer is no, the normed spaces where this property is valid, are said to be complete, and called Banach-spaces. Exact definitions and examples for some significant Banach-spaces will be presented later in this chapter, for general introduction to Banach spaces refer e.g. to [25]. The norm of a function f belonging to the normed space \mathbb{N} will be denoted by $\|f\|$ in generality.

The existence of basis in a function space is advantageous in respect of representation, because the representation of any function in the space is unambiguous, i.e. any two representations of the same function results in the same coefficients. The representation in a basis can conveniently be performed if the space of function is a Hilbert-space, i.e. there exist the notion of the scalar-product in it (for an introduction to Hilbert spaces see e.g. [25]). Let us denote the scalar product of a f, g element of the Hilbert-space \mathcal{H} as $\langle f, g \rangle$. Let us form the scalar product of an $f \in \mathcal{H}$ with the elements of the basis $\{\varphi_n\}$, the k-th product will be

$$\langle f, \varphi_k \rangle = \left\langle \sum_n c_n \varphi_n, \varphi_k \right\rangle = \sum_n c_n \langle \varphi_n, \varphi_k \rangle,$$

or by ordering the scalar products it into a matrix scheme it results in

$$\begin{bmatrix} \langle f, \varphi_0 \rangle \\ \langle f, \varphi_1 \rangle \\ \vdots \\ \langle f, \varphi_k \rangle \\ \vdots \end{bmatrix} = \begin{bmatrix} \langle \varphi_0, \varphi_0 \rangle & \langle \varphi_1, \varphi_0 \rangle & \cdots & \langle \varphi_k, \varphi_0 \rangle & \cdots \\ \langle \varphi_0, \varphi_1 \rangle & \langle \varphi_1, \varphi_1 \rangle & \cdots & \langle \varphi_k, \varphi_1 \rangle & \cdots \\ \vdots & \vdots & \ddots & \vdots & \vdots \\ \langle \varphi_0, \varphi_k \rangle & \langle \varphi_1, \varphi_k \rangle & \cdots & \langle \varphi_k, \varphi_k \rangle & \cdots \\ \vdots & \vdots & \vdots & \vdots & \ddots \end{bmatrix} \begin{bmatrix} c_0 \\ c_1 \\ \vdots \\ c_k \\ \vdots \end{bmatrix}.$$

For finite basis dimension the system linear equations can be solved and results in a unique set of coefficients. However in infinite dimensional spaces exact solution cannot be produced.

The notion of the orthogonality can help to find solution, if the basis forms an orthonormal system, i.e. for any φ_n, φ_k elements of the basis

$$\langle \varphi_n, \varphi_k \rangle = \delta_{nk},$$

where δ_{nk} denotes the Kronecker-delta symbol,

$$\langle f, \varphi_k \rangle = \sum_n c_n \langle \varphi_n, \varphi_k \rangle = c_k,$$

that is the coefficient of the representation can be kept by the scalar product of the system with the elements of the orthonormal basis:

$$f(t) = \sum_n \langle f, \varphi_n \rangle \varphi_n(t).$$

If a basis exists in the representation space, orthonormal basis can be constructed by the Gram-Schmidt orthogonalization process, which is a recursive procedure in the infinite dimensional spaces. In a Hilbert-space any full-dimensional orthogonal system forms a basis, hence the task for finding a basis can be fulfilled by finding an orthogonal system in the space.

To solve the representation problem in a Hilbert space does not necessarily requires an orthogonal basis, a bi-orthogonal system pair of functions is sufficient. The bi-orthogonal pair $\{\psi_n\}$ of the $\{\varphi_n\}$ system is defined by

$$\langle \varphi_k, \psi_l \rangle = \delta_{kl}$$

in the Hilbert-space \mathcal{H} for any $k, l \in \mathbb{N}$ pair of indexes. To obtain the coefficients of the representation let us form the scalar product of the function to represent with the elements of the bi-orthogonal system:

$$\langle f, \psi_k \rangle = \sum_n c_n \langle \varphi_n, \psi_k \rangle = c_k,$$

hence the representation is given by

$$f(t) = \sum_n \langle f, \psi_n \rangle \varphi_n(t).$$

The representation is symmetrical in the context of the bi-orthogonal pair, i.e.

$$f(t) = \sum_n \langle f, \psi_n \rangle \varphi_n(t) = \sum_n \langle f, \varphi_n \rangle \psi_n(t),$$

both representations are equivalent.

If basis does not exist in a Hilbert-space, representation on *frames* can also be successful. Frame is a complete system of functions in $\{\varphi_n\}$ the space \mathcal{H} that satisfies the following condition: there exist some $A, B \in \mathbb{R}$, $0 < A \leq B < \infty$ that for any $f \in \mathcal{H}$

$$A \|f\|^2 \leq \sum_n |\langle f, \varphi_n \rangle|^2 \leq B \|f\|^2. \quad (1.2.8)$$

If the inequality (1.2.8) is valid for numbers $A = B$, that is

$$\sum_n |\langle f, \varphi_n \rangle|^2 = A \|f\|^2, \quad (1.2.9)$$

it is named *tight frame*. It is easy to show that any basis in the Hilbert-space is also a tight frame, for orthonormal basis (1.2.9) is accomplished with $A = 1$.

1.3 Representation of continuous-time signals

Continuous-time signals form a significant class of signals, as real-world systems — at least those belonging to the field of classical physics, i.e. participants of the macroscopic world — shows nature of continuity in time. This means, that the behavior of these systems can change — so it becomes interesting for us — in any time-interval, even in infinitely small ones. The continuous-time feature of the signals corresponds to the mathematical notion of the function upon a real variable t , identified as *time*, i.e. $f(t)$, $t \in I(\mathbb{R})$ where $I(\mathbb{R})$ means an interval of \mathbb{R} , including the whole \mathbb{R} . Continuous-time feature means that the domain of the function $f(t)$ is a continuum set. Completion it does not involve the mathematical continuity of the function, functions with breaks, jumps, and isolated points are also belong to the class of continuous-time signals.

The discrete signal representation mean the expression of signals as the linear combination upon a set of signals, hence a central notion in representations is that of *linear function spaces*. To express accuracy and convergence in representations require notions of distance measure and norm, hence the metric and normed spaces — particularly the Banach-spaces, among them — are taken of special interest. To apply projection in deriving the representation parameters require the notion of scalar product and orthogonality, hence the inner-product spaces — particularly the Hilbert-spaces — have specific significance.

An ordinary classification of signals is based upon the domain of their time-function on the one hand, furthermore the signal space which belong to on the other. According to the

domain considered the following classes are usually discussed:

- \mathbb{R} is the domain of the general class or the class of *two-sided* signals,
- \mathbb{R}^* is the domain of the *causal* signals,
- \mathbb{R}^- is the domain of the *anti-causal* signals,
- $[a, b]$ ($-\infty < a < b < \infty$, $a, b \in \mathbb{R}$) domain belongs to the class of periodic signals with period $T = b - a$ ($f(t + T) = f(t)$).

The notion *anti-causal* differs from *noncausal*, the two-sided signals, belonging to the first class of the enumeration, are considered to be noncausal.

The signal classes enumerated above are used in the practice in association with several norms, these serve as the principle of further classification. In the theory and applications the so-called \mathcal{L}^p -norms are frequently used, hence the next section will be devoted to the field of \mathcal{L}^p -spaces.

1.3.1 The \mathcal{L}^p signal spaces

The \mathcal{L}^p -norm set up in the linear space of measurable functions f with domain $\mathbb{I} \subset \mathbb{R}$ for the integer number p is defined by the Lebesgue-integral

$$\|f\|_p \doteq \left\{ \int_{t \in \mathbb{I}} |f(t)|^p dt \right\}^{1/p} \quad \text{for } 1 \leq p < \infty$$

and by

$$\|f\|_\infty \doteq \operatorname{ess\,sup}_{t \in \mathbb{I}} |f(t)| \quad \text{for } p = \infty.$$

A function $f(t)$ belongs to the space $\mathcal{L}^p(\mathbb{I})$ if

$$\|f\|_p < \infty.$$

It can simply be verified by the definition, that the $\mathcal{L}^p(\mathbb{I})$ space is a linear space, and it is also metric space with the distance measure induced by the p -norm:

$$d_p(f, g) = \|f - g\|_p \quad \text{for } f, g \in \mathcal{L}^p(\mathbb{I}).$$

The \mathcal{L}^p spaces defined upon the intervals stated above, i.e. the $\mathcal{L}^p(\mathbb{R})$, $\mathcal{L}^p(\mathbb{R}^*)$, $\mathcal{L}^p(\mathbb{R}^-)$, and $\mathcal{L}^p(a, b)$ are complete normed spaces, hence they can be labelled as Banach-spaces. Practically the cases $p = 1, 2$ and ∞ are used.

Historically the \mathcal{L}^2 norm — by its popular label the *square-norm* — appeared first, its roots can be discovered in the activity of the ancient Greek mathematicians, and has mathematically been formulated by Gauss, who introduced the *least-square* based optimization methods. Least square optimization corresponds to solving extremal value problems in square-norm. The cause of its popularity can be derived from its obvious geometrical interpretation, and the relatively simple mathematical formulation and tractability. Another advantage is originated from the energetical interpretation: the square-norm can be associated with the energy inherent in signals and systems. In the physical reality most systems — the *dissipative* ones, i.e. systems containing no energy sources — represent finite energy. The finite energy of signals — originating from dissipative systems — is equivalent to the boundedness of the \mathcal{L}^2 -norm, hence the \mathcal{L}^2 -spaces are considered equivalent with the class of finite-energy signals. Furthermore, the minimum of the \mathcal{L}^2 -norm, aimed in many optimization tasks, corresponds to the generally used principle of physics, the endeavor of systems for minimal energy.

The simplicity of the mathematical treatment is mainly originated from the property of the normed spaces with square-norm, that they can easily be transformed to inner-product spaces by defining a scalar product as

$$\langle f, g \rangle \doteq \int_{t \in \mathbb{I}} f(t) \overline{g(t)} dt$$

for real or complex values functions f, g with domain \mathbb{I} — overline denotes the complex

conjugation. Equipped with the scalar-product we are able to define *orthogonality* and to apply the principle of the *orthogonal projection*. This scalar product induces a norm by

$$\|f\|^2 = \langle f, f \rangle,$$

which is equivalent with the \mathcal{L}^2 norm. The \mathcal{L}^2 spaces equipped with the scalar product defined above are complete inner-product spaces, hence they form Hilbert-spaces.

Applying the \mathcal{L}^∞ -norm leads us toward the mathematical notion of uniformity, e.g. to uniform continuity, and uniform convergence. By definition the signals belonging to this class are bounded in their values (amplitude), hence if the boundedness is a requirement in the solution of a problem, then the application of \mathcal{L}^∞ norm can be advantageous. The \mathcal{L}^∞ -norm — named popularly *maximum-norm* — involves conservative worst-case and minimax-type optimization methods. These types of considerations became central notions of the post-modern control science, as it introduced *robustness* in the control design and the connecting areas, as e.g. identification, which supersede in many fields the conventional *optimal* methods. Comparing \mathcal{L}^∞ methods to \mathcal{L}^2 ones a lot of difficulties are arisen. One cause of them is the fact, that \mathcal{L}^∞ spaces are not Hilbert-spaces, i.e. the orthogonality cannot be simply defined within them.

The \mathcal{L}^1 spaces has mainly significance in theory, as the Fourier-transform — one of the most fundamental notion in the function-theory — can immediately be defined in them, and they can be used to approximate functions belonging to \mathcal{L}^2 with the purpose to extend Fourier-transform into space \mathcal{L}^2 . Another advantage of the \mathcal{L}^1 spaces are, that some of their characteristics lay near to those of \mathcal{L}^∞ spaces, hence some optimization problems can more simply be solved in the former one. The \mathcal{L}^1 spaces — similarly to \mathcal{L}^∞ has no immediate definition of inner-product, hence in general they are not Hilbert-spaces.

In the following sections the \mathcal{L}^1 , \mathcal{L}^2 , and \mathcal{L}^∞ spaces defined upon several intervals of the real line will be discussed, with the purpose to keep the customary classification of signals,

as it has been outlined in the beginning of this section. Hence

- general or *two-sided* signals are classified into $\mathcal{L}^1(\mathbb{R})$, $\mathcal{L}^2(\mathbb{R})$, $\mathcal{L}^\infty(\mathbb{R})$,
- *causal* signals are classified into $\mathcal{L}^1(\mathbb{R}^*)$, $\mathcal{L}^2(\mathbb{R}^*)$, $\mathcal{L}^\infty(\mathbb{R}^*)$,
- and *periodic* signals are classified into $\mathcal{L}^1(a, b)$, $\mathcal{L}^2(a, b)$, $\mathcal{L}^\infty(a, b)$.

The $\mathcal{L}^p(\mathbb{R}^-)$ spaces for *anti-causal* signals are mentioned only for the completeness of the discussion, they do not show any particular feature in relation with the $\mathcal{L}^p(\mathbb{R}^*)$ -spaces.

It is worth to mention, that the representations discussed in this context are *time-domain representations* of signals. Besides them *frequency-domain representations* are commonly used. These will be introduced on the basis of the Fourier-transform later in this chapter, and will form significant part in the rest of the thesis.

1.3.2 Frequency domain representations

This section is devoted to the frequency domain description of continuous-time signals belonging to space $\mathcal{L}^p(\mathbb{R})$. According to practical reasons the spaces $\mathcal{L}^1(\mathbb{R})$, $\mathcal{L}^2(\mathbb{R})$, and $\mathcal{L}^\infty(\mathbb{R})$ will be considered. A fundamental notion for the signals defined on these spaces is the *Fourier-transform*. For a function f defined on \mathbb{R} is given by

$$(\mathcal{F}f)(\omega) \doteq \hat{f}(\omega) \doteq \int_{-\infty}^{\infty} f(t)e^{-i\omega t} dt$$

It is clear that this is not a precise definition, because we have not taken account the conditions for the existence of the defining integral; the definition gets real meaning in specific classes of functions, where the existence is proved.

The Fourier transform has a physical interpretation, which is fundamental both in the theory and the practice of several disciplines, e.g. in physics, and in technical sciences, such as control theory, and signal processing. The Fourier transform of a time-function is a function of the variable ω according to the above definition. This variable is defined on the

full real line $\omega \in \mathbb{R}$, and is named *circular frequency*. It is related to the notion of *frequency*, denoted by $f \in \mathbb{R}$, by the relation

$$\omega \doteq 2\pi f.$$

The notion of frequency is related to many branches of physics, e.g. periodic motion, vibrations, sounds, waves, etc., as well as many experiences in the real world, e.g. hearing and generating speech and music, broadcasting by radio waves, etc. To simplify our formulae, we will use the *circular frequency* in the course of our discussions.

The notion of *frequency* in the physical sense is undoubtedly older than its inclusion into the mathematical theory, which has been initiated in its earliest form by Gauss, and elaborated by Fourier. Their work was preceded by the experiences of the philosophers of the ancient and the medieval era by describing e.g. the rules of the vibrating chords resulting in the elaboration of musical scales, the motion of the celestial objects, the motion of the pendulum, etc. Later in the history of physics the notion of frequency gained increasing role as more and more phenomena turned out to be related with harmonic vibrations or waves in essence, i.e. the light, the electromagnetic waves, the motion of particles, etc. Besides physics, systems theory and signal processing — arisen to satisfy the demands of different technical fields — have been the main applicer of the frequency notion. Describing the behavior of the systems in the frequency domain has become a fundamental tool to explore the dynamics of systems, since it results in a more direct and perceptible view of the dynamics than that, one can directly obtain from any differential equation describing them. Of course the behavior in frequency is strictly connected to the differential equations describing the system; the first can be derived from the second one — in many cases by simple procedures (i.e. linear time-invariant systems), in other cases by more complicated ones.

The exact definition of the Fourier-transform can be given in the $\mathcal{L}^1(\mathbb{R})$ space, this approach is named the *classical* Fourier-theory.

Definition 1.3.1. The Fourier-transform $\hat{f}(\omega)$ ($\omega \in \mathbb{R}$) of the function $f(t) \in \mathcal{L}^1(\mathbb{R})$ is defined by

$$\hat{f}(\omega) \doteq \int_{-\infty}^{\infty} f(t)e^{-i\omega t} dt.$$

It is obvious, that the defining integral exists, because the integrand $f(t)e^{-i\omega t}$ is also in $\mathcal{L}^1(\mathbb{R})$ if it is true for $f(t)$. However it is not sure, that $\hat{f}(\omega)$ falls within $\mathcal{L}^1(\mathbb{R})$, i.e. the Fourier-transform of $\mathcal{L}^1(\mathbb{R})$ is not an one-to-one map into itself. It can simply be proved, that $\hat{f}(\omega)$ falls into the $\mathcal{L}^\infty(\mathbb{R})$ space (see for a brief introduction and proofs e.g. in [10]).

Further significant properties of the Fourier-transform can be proved within the classical theory, for example

- \hat{f} is uniformly continuous function on \mathbb{R} ;
- $\hat{f}(\omega) \rightarrow 0$ if $\omega \rightarrow \infty$ or $-\infty$;
- if the derivative of f , f' also exists, and $f' \in \mathcal{L}^1(\mathbb{R})$, than $\hat{f}'(\omega) = i\omega\hat{f}(\omega)$;

find proofs in [10].

The existence of the inverse-transform has great significance from the viewpoint of the signal representations: the inverse transform gives the means to reconstruct signal from its Fourier-transform. The inverse Fourier-transform is denoted by $(\mathcal{F}^{-1}\hat{f})(t)$.

Definition 1.3.2. The inverse Fourier-transform of the function $\hat{f}(\omega) \in \mathcal{L}^1(\mathbb{R})$ is defined by

$$(\mathcal{F}^{-1}\hat{f})(t) \doteq \frac{1}{2\pi} \int_{-\infty}^{\infty} \hat{f}(\omega)e^{i\omega t} d\omega.$$

It is clear, that the original signal can be recovered only, if the transform is a function of $\mathcal{L}^1(\mathbb{R})$. The conditions of this are stated in the following theorem:

Theorem 1.3.1. Let $f \in \mathcal{L}^1(\mathbb{R})$ such a function, that its Fourier-transform is also $\hat{f} \in \mathcal{L}^1(\mathbb{R})$. In this case

$$f(t) = (\mathcal{F}^{-1}\hat{f})(t)$$

at every points t where f is continuous.

It is clear, that in this form of the theory the Fourier-transform is not suitable for useful signal representations. First, the space \mathcal{L}^1 is too restrictive, on the other hand there is no guarantee, that any function of the admissible state can be recovered from its transform. An extension of the classical Fourier-theory was given by Plancherel (1910). The Plancherel theory extends the validity of the Fourier-transform into the space $\mathcal{L}^2(\mathbb{R})$, such that constitutes a one-to-one map to itself. That is, every function in $\mathcal{L}^2(\mathbb{R})$ has Fourier-transform in $\mathcal{L}^2(\mathbb{R})$, and the original signal can be recovered in every point by this transform.

In the Plancherel theory of the Fourier-transform the $\mathcal{L}^2(\mathbb{R})$ functions are approximated by sequence of functions in $\mathcal{L}^1(\mathbb{R}) \cap \mathcal{L}^2(\mathbb{R})$, and the transform is expressed by an average limit. The existence of the limit can be proved (this is the Plancherel-theorem) for the entire $\mathcal{L}^2(\mathbb{R})$ space. The Plancherel theory of Fourier-transform is elaborated in many textbooks (see e.g. [46] or [70]; a simplified but clear introduction can be found in [10]).

In accordance with the Plancherel theory the Fourier-transform gives an isomorphism of the $\mathcal{L}^2(\mathbb{R})$ space to itself. Furthermore for every $f \in \mathcal{L}^2(\mathbb{R})$

$$\|f\|_2^2 = \frac{1}{2\pi} \|\hat{f}\|_2^2,$$

i.e. the isomorphism shows an isometry, this is one form of the well-known Parseval identity.

Another form of the Parseval identity is given for the scalar products in the Hilbert-space $\mathcal{L}^2(\mathbb{R})$; for any $f, g \in \mathcal{L}^2(\mathbb{R})$

$$\langle f, g \rangle = \frac{1}{2\pi} \langle \hat{f}, \hat{g} \rangle.$$

An important property of the Fourier-transform is given upon the convolution of two functions in $\mathcal{L}^2(\mathbb{R})$. The continuous-time convolution of f and g in $\mathcal{L}^2(\mathbb{R})$ is denoted and defined as follow:

$$h(t) = (f * g)(t) \doteq \int_{-\infty}^{\infty} f(t - \tau)g(\tau) d\tau.$$

h is also a function in $\mathcal{L}^2(\mathbb{R})$. The convolution property of the Fourier-transform can be expressed as follows:

$$\widehat{(f * g)}(\omega) = \hat{f}(\omega)\hat{g}(\omega).$$

We will show, that through the Fourier-transform a continuous signal representation is obtained in the Hilbert-space $\mathcal{L}^2(\mathbb{R})$. The reconstruction formula of the original signal — i.e. the inverse Fourier-transform — can be written in the form

$$f(t) = \frac{1}{2\pi} \int_{-\infty}^{\infty} \hat{f}(\omega)e^{it\omega} d\omega,$$

which is a continuous representation formula upon the kernel

$$\Phi(\omega, t) = \frac{1}{2\pi}e^{-it\omega},$$

and the weighting function is $\hat{f}(\omega)$. The dual representation formula is given by the Fourier-transform, and the dual kernel is given as

$$\Psi(t, \omega) = e^{-i\omega t}.$$

It can be seen, that the representation is self-dual by disregarding a multiplicative constant.

The representation realized by the Fourier-transform is based upon the set of complex trigonometric functions of frequency distributed on a set of continuum cardinality, which in the current case is the entire real line. The values of the Fourier-transform on a specific frequency point represent the weight of the trigonometric constituent of the given frequency in the signal, hence this representation results in a decomposition of signals into sinusoids. These types of decompositions - based upon the trigonometric system — are called *spectral* representations.

Spectral representations of signals, and in connection with this the behavior of systems on the frequency domain, are widely applied in the technical science and practice. The roots of these types of representations can be found — as those of many other things — in the

ancient Greece: the Pythagorean school of philosophy by observing the rules of sounding a chord, mapped the pitch of sounds on ratios of natural numbers, hence a relative frequency notion has been discovered. Physics of the new era established the contemporary notion of frequency by investigating the periodic motion of celestial and earth objects, vibrations, sounds, waves, and other phenomena. The mathematical interpretation has been given by the French mathematician, physician and philosopher, Fourier in the beginnings of the 19th century. The name "spectrum" has come from optics — on its original form meant the decomposition of the sunlight into constituent colors —, and became generally used notion, as the wave-nature of light had been recognized, and the colors had been identified as frequencies. In the 20th century the spectral view of signals and systems became one of the most important ideas both in physics, and in the technical sciences. Frequency and frequency domain characteristics are widely understood by most of non-professional people e.g. in connection with the radio and TV communication, or in the parameters of a hifi equipment. In the technical sciences spectral view appears in more diversified and complicated forms, as it is used e.g. in electronic or control design, or in failure diagnostics.

In the current section the signal representation in frequency domain is discussed for signals in $\mathcal{L}^2(\mathbb{R})$, i.e. the signals of finite energy — by using the picturesque interpretation of the square-norm. However, spectral methods can be used in a broader class of signals, for example they can be extended toward the ergodic stationary stochastic processes — which do not belong to the class of $\mathcal{L}^2(\mathbb{R})$ —, by introducing the notion of the auto-correlation function. The spectral representation of the auto-correlation results rather in power-density function than the energy-density obtained in \mathcal{L}^2 signals. The spectral theory of stochastic signals can be found in several textbooks.

The space of the Fourier-transforms — a Hilbert-space $\mathcal{L}^2(\mathbb{R})$ of complex-valued functions — can also be interpreted also on the complex plane. The frequency variable ω can be interpreted as a linear parameter of a line running along the imaginary axis, i.e. by

introducing the complex variable s ,

$$s = i\omega,$$

and the Fourier-transform can be interpreted as

$$\hat{f}(s) \doteq \int_{-\infty}^{\infty} f(t)e^{-st} dt.$$

This formula defines the two-sided Laplace-transform. The Fourier-transform is the restriction of the two-sided Laplace-transform on the imaginary axis. Conversely the two-sided Laplace-transform can be considered as the analytic continuation of the Fourier-transform on the complex plane (to be precise — by disregarding countable isolated points).

It can be shown, that the image of the two-sided Laplace-transform forms a linear metric space, with a norm isometric to the $\mathcal{L}^2(\mathbb{R})$ norm, which will be denoted with

$$\mathcal{H}^2(i\mathbb{R})$$

to ensure the analogy with the Hardy spaces that will be discussed later in this chapter. The norm can be expressed as follows:

$$\|\hat{f}\|_2 \doteq \sqrt{\frac{1}{2\pi i} \int_{\mathbb{I}} |\hat{f}(s)|^2 ds},$$

where \mathbb{I} denotes the imaginary axis.

The interpretation on the complex plane has great significance in deriving stability properties of the systems. However, stability can rather be defined for causal systems and the corresponding signals, hence discussion of these aspects is better to do later.

An important question, whether there exist other representations (let us now consider only the continuous ones) in $\mathcal{L}^2(\mathbb{R})$ than that based upon the trigonometric system. The answer is positive, there are many other representations, some examples are enumerates as follow:

- Representations based upon the Walsh-transform.

- Representations based upon the Hilbert-transform.
- Representations based upon the integral wavelet-transform.

In the Walsh-transform the role of the Fourier-transform is substituted by the Walsh-transform, which is based upon a kernel of "square-wave" functions instead of trigonometric ones (a diadic kernel). We won't discuss Walsh-transform within this thesis work, for more information upon this field we refer to the monograph [51].

The kernel and its dual of the Hilbert-transform is for $s = i\omega$

$$\Phi(s, t) := \frac{1}{\pi(s - t)} \quad \Psi(t, s) := \frac{1}{\pi(t - s)}$$

and the transform itself has the following form:

$$(\mathcal{H}f)(s) \doteq \check{f}(s) \doteq \frac{1}{\pi} \int_{-\infty}^{\infty} \frac{f(t)}{s - t} dt.$$

for $s = i\omega$. The representation formula is based upon the inverse transform:

$$f(t) = \frac{1}{\pi} \int_{-\infty}^{\infty} \frac{\check{f}(s)}{t - s} ds$$

It can be proved, that there is a simple relationship between Hilbert and Fourier transforms:

$$(\mathcal{H}f)(\omega) = \text{sign}(\omega)(\mathcal{F}f)(\omega)$$

Indeed, formally the Hilbert-transform can be considered as a convolution of the function with the reciprocal function $1/t$, whose Fourier-transform is $\text{sign}(\omega)$. (The precise proof is more complicated, because the reciprocal function isn't either an \mathcal{L}^1 or \mathcal{L}^2 function, the result comes out only as a limit). It can be seen, that the Hilbert-representation does not tell more about a signal, comparing to the Fourier-representation; but it is useful for other point of view, e.g. in generation an analytic signal (see for details in [12] pp. 30-31).

The integral (or continuous) wavelet-transform is based upon *wavelets* are "small waves", functions in \mathcal{L}^2 with strong decay generated from a "mother wavelet" by dilation and

translation. Let $\psi(t)$ is the mother wavelet, by this the integral wavelet-transform of a function $f(t) \in \mathcal{L}^2(\mathbb{R})$ is a follows:

$$(W_\psi f)(b, a) \doteq \frac{1}{\sqrt{a}} \int_{-\infty}^{\infty} f(t) \overline{\psi\left(\frac{t-a}{b}\right)} dt$$

where a is the dilation (or scaling) parameter, and b is the translation one. There is a reconstruction formula, which results in the wavelet representation of signals:

$$f(t) \doteq \frac{1}{C_\psi} \iint_{\mathbb{R} \times \mathbb{R}} \{(W_\psi f)(b, a)\} \left\{ \frac{1}{\sqrt{a}} \psi\left(\frac{t-a}{b}\right) \right\} \frac{dadb}{a^2},$$

where

$$C_\psi \doteq \int_{-\infty}^{\infty} \frac{|\hat{\psi}(\omega)|^2}{|\omega|} d\omega.$$

The reconstruction formula exists, if the so-called *admissibility condition*

$$C_\psi < \infty$$

is valid for the mother wavelet. That is, not every function of $\mathcal{L}^2(\mathbb{R})$ is admissible to become a mother wavelet. By analyzing the admissibility condition, we can find, that $\psi(t)$ must decay in some measure as $t \rightarrow \infty$ or $t \rightarrow -\infty$, and both limits must be 0. This condition can also be fulfilled with functions with finite support, such types of compactly supported wavelets has been constructed by Ingrid Daubechies, a definitive person in this field [14].

The wavelet representations differ significantly from the Fourier-representation, since the wavelets are objects concentrated in small pieces of the real line, contrary to the trigonometric functions, which — as being periodic ones — fill the whole space. The localization property of wavelets is the characteristic, which makes them suitable for locally temporal representations of signals contrary to the "static" nature of the Fourier-representation. An excellent introduction to the integral wavelet-transform and other wavelet-related fields can be found in [10] and [14].

However wavelet representations for many problems proved to be superior, their usage need some carefulness. For example not all the wavelets give satisfactory spectral representation. Though the dilation (scaling) parameter shows similarity to the frequency variable, they are not identical. There exist wavelet representation, which give a better interpretation to the varying frequency (i.e. give a joint time-frequency representation), this ability is missing from the Fourier representation. Let us refer to the Gabor wavelets (see for it e.g. in [10]), and to other joint time-frequency spectral methods (see [12]).

1.4 Representation of discrete-time signals

Discrete-time signals are considered to be sequences, where the indices the elements are associated with discrete time-instances. Categories of discrete-time signals can be e.g. *sampled* continuous-time signals, *time series*, and *event-driven dataseries*. The last category falls beyond the scope of this thesis work, this is the subject of the field of discrete event systems. Time series and sampled signals are distinguished, though sampled data series can be considered as time series, contrary it is not true in all cases, time series can be produced independently of continuous-time processes, let us mention the economic data series as example. By the mathematical point of view time-series and uniformly sampled continuous signals are equivalent. In the framework of this thesis signals sampled non-uniformly on the time-domain are not considered.

A further principle of classifying the discrete time signals is originated from the norms used and the associated spaces. The usually applied spaces in association with this field are the sequence-space ℓ^2 and the Hardy spaces \mathcal{H}^2 and \mathcal{H}^∞ .

The detailed study of the discrete-time signals is subject of the Chapter 2, as well as selected topics in association with this field are concerned in the subsequent chapters.

Chapter 2

Representation of signals in \mathcal{H}^2

This chapter is devoted to frequency domain representations of discrete-time signals, and the underlying systems, incorporating finite energy. Finite energy principle in the common sense is associated with square-type criteria, and the theory of linear spaces equipped with square norm has proven to be the adequate mathematical formulation to characterize the systems obeying to it. After a brief introduction to frequency domain representations of discrete-time signals and the \mathcal{H}^2 spaces, the problem of constructing basis in the space \mathcal{H}^2 is analyzed. As a generalization of the standard trigonometrical basis, a class of rational bases depending upon the poles associated with the system under consideration will be constructed. Then the characteristics of the representations in these bases will be analyzed, and an algorithm will be given to estimate the representation coefficients based upon measurement data. The results obtained for the space \mathcal{H}^2 are also translated in its orthogonal complement, \mathcal{H}_\perp^2 , since in the "technical" area of systems science this space is preferred in the description of signals and systems.

2.1 Representations of discrete-time signals and systems

In this section the frequency domain representations of *discrete-time* signals, and the underlying systems, incorporating *finite energy* will be studied. Finite energy principle in

the common sense is associated with square-type criteria, and the theory of linear spaces equipped with square norm has proven to be the adequate mathematical formulation to characterize the systems obeying to it. In time domain the finite energy discrete-time signals are considered to be sequences belonging to the ℓ^2 spaces. In most cases the discrete-time signals can be associated with continuous-time ones. The signals originating from systems being subject of macro-physics surely belong to this class, their discrete-time form can be obtained as a result of an abstraction, i.e. by disregarding more subtle view than that given by a discrete time-scale (consider e.g. the discrete-event systems), or by sampling the signal values in discrete time instances. In micro-physics the continuous-time view of the phenomena is not trivial, nonetheless time seems to be continuum, the continuous view is restricted by the uncertainty principle and the quantized nature of the physical quantities. In the present discussion discrete-time signals with instances uniformly spaced on the time scale are considered. If the discrete signal values are obtained by sampling a continuous-time signal, uniform sampling should be performed. In this case sampling must be performed in accordance with the Shannon rule, i.e. the continuous-time signal belonging to the space $\mathcal{L}^2(\mathbb{R})$ should be bound-limited with frequency limit f_B , i.e. for $x \in \mathcal{L}^2(\mathbb{R})$ and its Fourier-transform $\hat{x} \in \mathcal{L}^2(\mathbb{R})$ there exist $f_B > 0$ real number so, that

$$\int_{-f_B}^{f_B} \hat{x}(f)e^{i2\pi ft}df = \int_{-\infty}^{\infty} \hat{x}(f)e^{i2\pi ft}df,$$

as well as the sample-frequency f_S should be at least twice greater than f_B , i.e.

$$f_S \geq 2f_B.$$

Uniform spacing on the discrete frequency scale defines the connection between the instances (sample values) of the signal $x \in \mathcal{L}^2(\mathbb{R})$ and the $\{x_n\} \in \ell^2$ sequences:

$$x_n = x(t_0 + nT) \quad (n \in \mathbb{Z})$$

where $t_0 \in \mathbb{R}$ is an arbitrary reference point on the time-scale, and $T > 0$ is the period of sampling, inverse of the sample frequency ($T = 1/f_S$). The current discussion focuses on

the *causal* signals, i.e. the sequences in ℓ^2 with indices greater or equal to zero, that are related to the continuous-time signal as

$$x_n = x(nT) \quad (n \in \mathbb{N}^*).$$

The frequency-domain representation of the uniformly spaced discrete-time causal signals is given by introducing the z -transform

$$\mathcal{Z}\{x_n\} \doteq X(z) \doteq \sum_{k=0}^{\infty} x_k z^{-k}, \quad (2.1.1)$$

where the X is a complex valued function of the complex variable z . It is easy to show, that z^{-1} represents a positive *shift* operator on the discrete time domain (i.e. on the set of the indices belonging to the sequence):

$$z^{-1} \mathcal{Z}\{x_n\} = \sum_{n=0}^{\infty} x_n z^{-n-1} = \sum_{n=1}^{\infty} x_{n-1} z^{-n} = \mathcal{Z}\{x_{n-1}\} \quad (2.1.2)$$

A positive shift of magnitude one on the indices of the sequence means a positive shift of T on the continuous time scale. A positive shift of T according to the well-known shift property of the Fourier-transform can be expressed on the frequency domain as multiplication with $e^{i\omega T}$, where $\omega \in \mathbb{R}$ denotes the circular frequency ($\omega = 2\pi f$):

$$\mathcal{F}\{x(t - T)\} = e^{-i\omega T} \mathcal{F}\{x(t)\} \quad (2.1.3)$$

By comparing (2.1.3) to (2.1.2), the

$$z = e^{i\omega T} \quad (2.1.4)$$

correspondence can be observed. By extending the $i\omega$ line to the whole complex plane as $s = \sigma + i\omega$ with arbitrary σ , a continuous map $s \mapsto z : \mathbb{C} \mapsto \mathbb{C}$ is given in the form

$$z = e^{sT}. \quad (2.1.5)$$

In the case of continuous-time signals the physically interpretable real frequency (or circular frequency) variable $f \in \mathbb{R}$ ($\omega \in \mathbb{R}$) gets in the whole imaginary axis, while regularity on

the right complex half-plane involves the stability of the system. In the case of sampling with period $T > 0$, according to (2.1.5) the imaginary axis is mapped onto the unit circle, and it can easily be shown, that the left half-plane is mapped on the region inside the unit circle, and the right half-plane on that outside. Furthermore any function of z – called discrete-time or simply discrete frequency-function (spectral function), shows periodicity by T in respect to the circular frequency. By using instead of circular frequency the *normalized circular frequency* variable, denoted by t (confusion with time variable t can be avoided) with definition

$$t \doteq \omega T = 2\pi \frac{f}{f_S}, \quad (2.1.6)$$

where f_S is the sample frequency, periodicity by 2π can be observed. By introducing the normalized circular frequency variable a mapping of the physical frequency scale associated with the sampled system onto the interval $[-\pi, \pi]$ has been given

$$\left[-\frac{f_S}{2}, \frac{f_S}{2} \right] \mapsto [-\pi, \pi].$$

According to the Shannon rule of sampling $f_S/2$ is equal to the maximum of the bound-limit f_B associated with the signal – it is referred a Nyquist-frequency in the literature (denoted by $f_N \doteq f_S/2$). Any spectral function associated with a discrete-time system beyond to the Nyquist-frequency is periodically repeated, however only the "baseband" has physical meaning.

An important class of discrete-time systems comprises stable ones. Here the asymptotical stability is considered: a system is asymptotical stable if the discrete transfer function associated with it contains all its singularities within the unit circle, i.e. the transfer function is regular (analytic) on and outside the unit circle. This stability criterion can be transferred also to the signals, in this case any spectral function plays the role of the transfer function. In our discussion the singularities of a transfer function or spectral function

can be associated with the notion of *poles*. The stability criterion expressed for discrete-time signals and systems is analogous with that given for continuous-time ones, only the interesting region is changed on the complex plane: the left half-plane is replaced by the unit circle in discrete-time.

Since the central idea, the z -transform, is essentially defined as a power series (2.1.1), stability can be associated with the notion of convergence. The convergence region of a power series is given by circular regions with a particular radius. Since (2.1.1) defines an inverse power series the region of convergence is defined of the outer part of a circular region given by the convergence radius. Hence stable systems are associated with convergence radius equal to 1, and the convergence region is found outside the unit circle.

An adequate mathematical tool to analyze functions analytic *within* the unit circle is the theory of Hardy-spaces. This is just contrary to that is needed, analyzing functions analytic outside the unit circle, however as it will be shown, the Hardy-spaces can be applied to this class. In this chapter only the Hardy-space associated with the square-norm, denoted by \mathcal{H}^2 will be considered. A general introduction to the \mathcal{H}^p spaces can be found e.g. in [46, 11], and some aspects of the \mathcal{H}^∞ spaces will be discussed in the succeeding chapter of this thesis.

The Hardy-space \mathcal{H}^2 is a Banach-space of functions $X : \mathbb{C} \mapsto \mathbb{C}$ equipped with the norm (given with a simplified definition, for the full precision one see e.g. [47, 11]):

$$\|X\|_{\mathcal{H}^2} \doteq \sqrt{\frac{1}{2\pi i} \oint_{\mathbb{T}} |X(q)|^2 \frac{dq}{q}} = \sqrt{\frac{1}{2\pi} \int_{-\pi}^{\pi} |X(e^{it})|^2 dt}. \quad (2.1.7)$$

The complex function X belongs to the Hardy space \mathcal{H}^2 , if $\|X\|_{\mathcal{H}^2} < \infty$. It can be shown, that the functions belonging to the space \mathcal{H}^2 are analytic within the unit circle [47]. The notation $\mathcal{H}^2(\mathbb{D})$ is used, if we want to emphasize that the space is related to the unit circle as the regularity region. \mathcal{H}^2 is also a Hilbert-space with the inner product

$$\langle X, Y \rangle \doteq \frac{1}{2\pi i} \oint_{\mathbb{T}} X(q) \overline{Y(q)} \frac{dq}{q} = \frac{1}{2\pi} \int_{-\pi}^{\pi} X(e^{it}) \overline{Y(e^{it})} dt \quad (2.1.8)$$

for functions $X, Y \in \mathcal{H}^2$.

The Hardy-space $\mathcal{H}^2(\mathbb{D})$ can be considered as the space of square-integrable complex functions analytic within the unit circle. Systems theory, nevertheless, prefers to use functions analytic on and outside the unit circle – to assure correspondence with transfer functions (spectral functions) belonging to stable systems (signals). This function space can simply be transformed into a Hardy-space by applying the substitution

$$q = \frac{1}{z}, \quad (2.1.9)$$

i.e. the complex function X of variable $z \in \mathbb{C}$ analytic on and outside the unit circle with the substitution (2.1.9) is transformed into the function $X'(q) = X(1/q)$ of variable q analytic within the unit circle. Since $\mathcal{H}^2(\mathbb{D})$ is a Hilbert-space, it can be shown, that the space of functions analytic on and outside the unit circle is identical to the orthogonal complement of $\mathcal{H}^2(\mathbb{D})$. This space will be denoted by $\mathcal{H}_\perp^2(\mathbb{D})$.

$\mathcal{H}_\perp^2(\mathbb{D})$ is also a Banach-space, the norm belonging to it can be given by the substitution $q = 1/z$ and — since $dq/q = -dz/z$ — reversing the direction of the integration in (2.1.7) as

$$\|X\|_{\mathcal{H}_\perp^2} \doteq \sqrt{\frac{1}{2\pi i} \oint_{\mathbb{T}^\circ} |X(z)|^2 \frac{dz}{z}} = \sqrt{\frac{1}{2\pi} \int_{-\pi}^{\pi} |X(e^{-it})|^2 dt}, \quad (2.1.10)$$

that is technically the same as (2.1.7). In addition $\mathcal{H}_\perp^2(\mathbb{D})$ is a Hilbert-space with the inner product

$$\langle X, Y \rangle \doteq \frac{1}{2\pi i} \oint_{\mathbb{T}^\circ} X(z) \overline{Y(z)} \frac{dz}{z} = \frac{1}{2\pi} \int_{-\pi}^{\pi} X(e^{-it}) \overline{Y(e^{-it})} dt. \quad (2.1.11)$$

As it can be observed, the norms and inner products belonging to the spaces \mathcal{H}^2 and \mathcal{H}_\perp^2 are defined identically, disregarding the direction of the integration path, which is due to the different regions considered (i.e. unit circle containing the zero or the infinite point), and affects only the parameterization.

According to these arguments the description of functions in \mathcal{H}^2 and \mathcal{H}_\perp^2 by using the transform $q = 1/z$ are equivalent. The q -notation — considering the functions analytic

within the unit circle — is more convenient in the mathematical analysis, because the theory of Hardy-spaces can directly be applied. However, z -notation can be considered as the conventional and more natural view at least for the community of technical sciences. Using the concept of functions analytic outside the unit circle provides more direct link to the real-world continuous-time systems, see Figure 2.1, where the connection of the function spaces involved in representing causal signals has been presented. The stable, causal, continuous-

$$\begin{array}{ccc}
 \mathcal{L}^2(\mathbb{R}^*) & \xrightarrow{\text{sampling} / T} & \ell^2(\mathbb{N}^*) \\
 \downarrow \mathcal{F} & & \downarrow \mathcal{Z} \\
 \mathcal{H}_{\perp}^2(i\mathbb{R}) & \xrightarrow[\substack{z = e^{sT} \\ i\omega \mapsto e^{i\omega T}}]{} & \mathcal{H}_{\perp}^2(\mathbb{D})
 \end{array}$$

Figure 2.1: Connection of function spaces

time signals are represented on the frequency domain with complex functions analytic on the right complex half-plane, this function space has been denoted with $\mathcal{H}_{\perp}^2(i\mathbb{R})$. The notation $i\mathbb{R}$ indicates that frequency variable is associated with the imaginary axis. This space is considered to be the orthogonal complement of the space $\mathcal{H}^2(i\mathbb{R})$ of the functions analytic on the left complex half-plane, to ensure full compatibility with the discrete-time case.

Thorough the subsequent discussions both the \mathcal{H}_{\perp}^2 and \mathcal{H}^2 spaces will be used in connection with the discrete-time signal and system representations, by using the distinctive notations z and q respectively for the independent variables. The purely mathematical considerations containing direct reference to the theory of Hardy-spaces are simpler to be done by using the "mathematical" form, i.e. functions of q analytic within the unit circle, otherwise the "technical" form will be used, i.e. functions of z analytic on and outside the unit circle. Assertions and proofs made by using the "mathematical" notation, according to the above considerations, are valid also in the "technical" sense. For the sake of simplicity

instead of \mathcal{H}_\perp^2 space \mathcal{H}^2 will be referred also in the z -notation, if there is no possibility of misunderstanding, in these cases, of course, the assertion $X(z) \in \mathcal{H}^2$, rather means $X(z) \in \mathcal{H}_\perp^2$.

2.2 Standard basis in \mathcal{H}^2

The definition formula of the z -transform (2.1.1) can be interpreted as a representation of the function $X(z)$ in the system of functions

$$1, z^{-1}, z^{-2}, \dots, z^{-n}, \dots$$

with the coefficients

$$x_0, x_1, x_2, \dots, x_n, \dots$$

By using the mathematical notation, with variable $q = 1/z$

$$X(q) = \sum_{n=0}^{\infty} x_n q^n,$$

which can be interpreted as the representation of the function $X(q) \in \mathcal{H}^2$ in the system of functions

$$1, q, q^2, \dots, q^n, \dots \quad (2.2.1)$$

The polynomial system (2.2.1) is linearly independent and complete in the space \mathcal{H}^2 , furthermore it can simply be shown, that it is an orthonormal system, hence it forms orthonormal basis in \mathcal{H}^2 . It is called *standard basis* in \mathcal{H}^2 . Similarly the system

$$1, z^{-1}, z^{-2}, \dots, z^{-n}, \dots$$

forms an orthonormal basis in the space \mathcal{H}_\perp^2 , where it can be considered as the standard basis.

The (2.2.1) system on the unit circle can be expressed as a trigonometrical system

$$1, e^{it}, e^{i2t}, \dots, e^{ikt}, \dots$$

$$1, \cos t + i \sin t, \cos 2t + i \sin 2t, \dots, \cos nt + i \sin nt, \dots$$

hence it is also referred as *trigonometrical basis* in \mathcal{H}^2 .

The classical signal, systems, and control theory concentrate on the representations based upon the standard trigonometric basis. It is well known, that in many cases it is not the best representation, for example the rational functions — being crucial in the systems science — can be represented by infinite power series, and the decay on the coefficients is rather light, or the convergence is rather slow. Finding representation, that results in faster convergence for the functions typically used in system science is a natural intention. However it is unlikely, that there exist a representation, which is universally better than the standard one. More likely particular representations can be found, that are well applicable for particular classes of function characterized with specific properties.

In the 90's the efforts for improving system identification methods for robust control implied representations that can be extended to the \mathcal{H}^∞ space [31, 43, 16, 7]. It is well known fact, that the representations in the standard (trigonometric) basis do not necessarily converge in the space \mathcal{H}^∞ . The use of these representations in the robust control methods raises serious difficulties, hence a valid demand has been to find representations, that can be proved to be convergent also in \mathcal{H}^∞ sense.

2.3 The discrete Laguerre system

2.3.1 Generalization of the standard basis

The definition formula of the z -transform (2.1.1), that can also be interpreted as a representation of the function $X(z)$ in the standard basis of space \mathcal{H}_1^2 , can be regarded as a power

series of negative powers referenced to the origin. There is no reason to restrict ourselves to this reference point, any other point can be selected within the unit circle — this condition is necessary to keep the representation analytic outside the unit circle. Let the reference point be $a \in \mathbb{D}$, with this

$$F(z) = \sum_{n=0}^{\infty} c_n (z - a)^{-n},$$

of course the coefficients differ from the original ones, i.e. the elements of the sequence $\{x_n\}$. It is clear, that the representing system of functions

$$1, \frac{1}{z - a}, \frac{1}{(z - a)^2}, \frac{1}{(z - a)^3}, \dots, \frac{1}{(z - a)^n}, \dots$$

is also a linearly independent and complete system, however it does not form — unlike the trigonometric system — an orthogonal basis. Turning to the "mathematical" form, the representing function set — by applying the substitution $q = 1/z$ — can be given as

$$1, \frac{q}{1 - aq}, \frac{q^2}{(1 - aq)^2}, \frac{q^3}{(1 - aq)^3}, \dots, \frac{q^n}{(1 - aq)^n}, \dots$$

with $a \in \mathbb{D}$. It is obvious, that the elements of the system all belong to the space \mathcal{H}^2 , and the system is linearly independent and the complete \mathcal{H}^2 . This form of functions is not advantageous in representing signals, for this purpose the strictly proper functions are preferred to ensure the uniform asymptotic behavior of all members, hence it is worth the above system to be modified as follows:

$$\frac{1}{1 - aq}, \frac{q}{(1 - aq)^2}, \frac{q^2}{(1 - aq)^3}, \dots, \frac{q^n}{(1 - aq)^{n+1}}, \dots$$

To act on the conventions, that has been formed in this field for the sake of some computational elegance in the manipulations, let the following system rather be used:

$$\frac{1}{1 - \bar{a}q}, \frac{q}{(1 - \bar{a}q)^2}, \frac{q^2}{(1 - \bar{a}q)^3}, \dots, \frac{q^n}{(1 - \bar{a}q)^{n+1}}, \dots \quad (2.3.1)$$

where \bar{a} denotes the complex conjugate of a . The use of the conjugate pole does not affect essentially the representations, in the case of real poles it has no significance, for

the complex case always conjugated complex pair of poles is used in the real, physically existent or realizable systems. The parameter a has been referred above as "pole", however in association with the system (2.3.1) of functions this is not valid. a is rather the inverted pole of the functions, i.e. $\hat{a} = 1/a$ is the pole. Even so, the expression "pole" will henceforth be used for simplicity, because a is really a pole of the "technical" system analyzed.

As it can easily be verified, the system (2.3.1) is remained to be linearly independent and complete in \mathcal{H}^2 . However, the orthogonality does not hold, i.e. the system (2.3.1) do not form an orthogonal system in respect to the inner product belonging to the Hilbert space \mathcal{H}^2 .

Any linearly independent complete system in a Hilbert space can be converted into an orthogonal (and in addition, orthonormal) system by applying the Gram-Schmidt orthogonalization procedure (see e.g. [25] page 157). By applying the orthogonalization procedure to the system (2.3.1), the following system of functions will be obtained:

$$\phi_n(q) = \sqrt{1 - |a|^2} \frac{(q - a)^n}{(1 - \bar{a}q)^{n+1}} \quad n \in \mathbb{N} \quad (2.3.2)$$

The orthogonality can be verified by the following theorem.

Theorem 2.3.1. *The system (2.3.2) forms an orthonormal basis in the \mathcal{H}^2 space.*

Proof. The scalar product of the ϕ_n and ϕ_m elements, for $n, m \in \mathbb{N}$ can be written as

$$\langle \phi_n, \phi_m \rangle = \frac{1}{2\pi} \int_{-\pi}^{\pi} \phi_n(e^{it}) \overline{\phi_m(e^{it})} dt$$

Let definition (2.3.2) be applied with the expression $a = re^{i\varphi}$ for the parameter a :

$$\langle \phi_n, \phi_m \rangle = \frac{(1 - r^2)}{2\pi} \int_{-\pi}^{\pi} \frac{(e^{it} - re^{i\varphi})^n}{(1 - re^{i(t-\varphi)})^{n+1}} \frac{(e^{-it} - re^{-i\varphi})^m}{(1 - re^{-i(t-\varphi)})^{m+1}} dt =$$

by assuming that $n \geq m$

$$= \frac{(1 - r^2)}{2\pi} \int_{-\pi}^{\pi} \frac{[(e^{it} - re^{i\varphi})(1 - re^{i(t-\varphi)})]^m}{[(1 - re^{i(t-\varphi)})(1 - re^{-i(t-\varphi)})]^{m+1}} \frac{(e^{it} - re^{i\varphi})^{n-m}}{(1 - re^{i(t-\varphi)})^{n-m}} dt.$$

Since

$$(e^{it} - re^{i\varphi})(1 - re^{i(t-\varphi)}) = (1 - re^{i(t-\varphi)})(1 - re^{-i(t-\varphi)}) = 1 + 2r \cos(t - \varphi) + r^2,$$

by simplifying in the first factor, we get the form

$$\langle \phi_n, \phi_m \rangle = \frac{1}{2\pi} \int_{-\pi}^{\pi} \frac{1 - r^2}{1 + 2r \cos(t - \varphi) + r^2} \left(\frac{e^{it} - re^{i\varphi}}{1 - re^{i(t-\varphi)}} \right)^{n-m} dt.$$

This is a Poisson-integral applied to the function

$$F(q) = \begin{cases} 1 & \text{for } n = m, \\ \left(\frac{q-a}{1-\bar{a}q} \right)^{n-m} & \text{for } n > m. \end{cases}$$

The Poisson-integral does exist for every $F \in \mathcal{H}^2$ function, and results in the value $F(a)$ (see e.g. in [46] theorems on pages 112 and 332). For the case $n = m$ this results in value 1, for the case $n > m$ the result is 0, since the $F(q)$ function possesses zero for $q = a$ with multiplicity $m - n$. For the case $n < m$ the situation is the same as in case $n > m$, with the exception that the conjugate function appears. Hence

$$\langle \phi_n, \phi_m \rangle = \delta_{nm},$$

which proves the theorem. □

Using the z -notation the system (2.3.2) is transformed to

$$\phi_n(z) = \frac{\sqrt{1 - |a|^2}}{z - a} \left(\frac{1 - az}{z - a} \right)^n \quad n \in \mathbb{N}, \quad (2.3.3)$$

where $a \in \mathbb{D}$ is really the pole of the system (with multiplicity $n + 1$ for the n th element).

The system (2.3.3) forms an orthonormal basis in the space \mathcal{H}_\perp^2 .

The system (2.3.3) with the pole a considered to be real is referred in the literature as the *discrete Laguerre system*. It is called Laguerre according to its analogy with the Laguerre-type orthogonal polynomials and the Laguerre functions built upon them [69].

Laguerre system is called the sequence of continuous-time functions belonging to the space $\mathcal{L}^2(\mathbb{R}^*)$

$$\psi_n(t) = \frac{e^{-\frac{t}{2}}}{n!} L_n(t), \quad (2.3.4)$$

for $n \in \mathbb{N}^*$ and $t \in \mathbb{R}^*$, where

$$L_n(t) = e^t \frac{d^n}{dt^n} (t^n e^{-t}) \quad (n \in \mathbb{N}) \quad (2.3.5)$$

are the so-called Laguerre polynomials. The Laguerre polynomials with different indices are orthogonal to each other with respect to the weight function e^{-t} . The Laguerre functions (2.3.4) can be considered as the weighted and normalized forms of the polynomials (2.3.5), hence they form an orthonormal system in the space $\mathcal{L}^2(\mathbb{R}^*)$. The system (2.3.4) and the scaled forms of it can be considered as the time-domain form of the *continuous Laguerre system*. The analogy with the discrete Laguerre system will be obvious if the frequency domain representations are compared. The simplest way to get the frequency domain representation of the Laguerre functions scaled with the parameter $2p$ is to generate their Laplace-transform (by neglecting the initial values):

$$\mathcal{L}\{\psi_n(2p t)\} = \frac{1}{s+p} \left(\frac{s-p}{s+p} \right)^n$$

Comparing this with the expression (2.3.3) of the discrete Laguerre functions the following important things can be observed: both systems consist of factors *low-pass*

$$\frac{1}{s-a} \quad (\text{continuous}) \quad \frac{1}{z-a} \quad (\text{discrete}),$$

as well as *all-pass*

$$\left(\frac{s-a}{s+a} \right)^n \quad (\text{continuous}) \quad \left(\frac{1-az}{z-a} \right)^n \quad (\text{discrete}).$$

The attributes *low-pass* and *all-pass* has been borrowed from the filtering theory: a low-pass filter passes the lower frequency region of the signals, and attenuates the upper part, the

all-pass filter passes all the frequency regions equally. Really, the absolute values of the all-pass factors — regarding either the continuous and the discrete one — are equal to 1 by running over the imaginary axis on s or the unit circle on z . The stable all-pass function in the mathematical literature is called *inner-function*, and plays a rather important role in the theory of Hardy-spaces, see e.g. pages 336-340 in [46].

The discrete Laguerre system has been introduced into systems science in connection with system identification for robust control in the beginning of the 90's [28, 29, 73, 44], since than it plays significant role in the systems theory [16, 38, 49] by its generalizations, and it has been applied also in the practice [17, 18]. The generalization of the discrete Laguerre system will be discussed later in this thesis. The continuous Laguerre system plays rather theoretical role, however it has been applied on the field of continuous-time systems, see e.g. [31, 9].

2.3.2 The Blaschke-function, and the argument transform

The orthonormal system (2.3.2) can be expressed in a more tractable form by applying the notion of the Blaschke-function, for $n \in \mathbb{N}$ and $\Phi_n(q) \in \mathcal{H}^2(\mathbb{D})$:

$$\Phi_n(q) = \frac{\sqrt{1-|a|^2}}{1-\bar{a}q} b_a^n(q) \quad (2.3.6)$$

where $b_a(q)$ is the Blaschke function

$$b_a(q) = e^{i\delta} \frac{q-a}{1-\bar{a}q} \quad (2.3.7)$$

generated by the parameter $a \in \mathbb{D}$, and δ is an arbitrary constant. The Blaschke-function is an *inner-function*, i.e.

$$|b_a(e^{it})| = 1.$$

This means that the Blaschke function produces only rotation on the unit circle, hence it can be expressed in the form

$$b_a(e^{it}) = e^{i\beta_a(t)}, \quad (2.3.8)$$

where β_a is the so-called *argument-function*.

From the form 2.3.6 can be derived, that in the Laguerre basis the Blaschke function plays the role of the operator q in the standard basis. The consecutive basis functions can be obtained by multiplying with the Blaschke function in the first, and with q in the second one. The Blaschke function — similarly to q — is a *shift* operator in the space $\mathcal{H}^2(\mathbb{D})$. The shift realized by a Blaschke function defined by a single real parameter $0 < a < 1$ is called *Laguerre-shift* operator. The frequency domain characteristics of this operator will be examined in details immediately as follow, however, before doing this, let us discuss briefly its time-domain behavior. The standard shift operator on the time-domain realizes really an exact shift, i.e. the shape of the time-domain function remains unchanged as it has been translated on the time axis. The Laguerre-shift results in a more complicated transform on the time-domain. The impulse-response of the first 16 elements of the Laguerre system has been presented on Figure 2.2. As it can be observed, the impulse is got distorted, and its duration successively increases in the course of the consecutive shifts. Detailed analysis of the time-domain aspects of the Laguerre representations falls beyond the framework of this thesis work, this short discussion has been given just to illustrate the differences of the two representation in this respect.

The argument-function belonging to the Blaschke-function can explicitly be expressed. By considering the parameter a (let us recall that it is the pole in the technical notation) in the form $a = re^{i\varphi}$, with this

$$b_a(e^{it}) = e^{i\delta} \frac{e^{it} - re^{i\varphi}}{1 - re^{-i\varphi}e^{it}} = e^{i(\delta+\varphi)} \frac{e^{it} - re^{i\varphi}}{e^{i\varphi} - re^{it}}.$$

With some manipulation we get

$$\begin{aligned} b_a(e^{it}) &= e^{i(\delta+\varphi)} \frac{(e^{it} - re^{i\varphi})(e^{-i\varphi} - re^{-it})}{(e^{i\varphi} - re^{it})(e^{-i\varphi} - re^{-it})} = e^{i(\delta+\varphi)} \frac{e^{i(t-\varphi)} - 2r + r^2 e^{-i(t-\varphi)}}{1 - r(e^{i(t-\varphi)} + e^{-i(t-\varphi)}) + r^2} = \\ &= e^{i(\delta+\varphi)} \frac{(e^{i\frac{t-\varphi}{2}})^2 - 2r + r^2 (e^{-i\frac{t-\varphi}{2}})^2}{1 - 2r \frac{e^{i(t-\varphi)} + e^{-i(t-\varphi)}}{2} + r^2} = e^{i(\delta+\varphi)} \frac{(e^{i\frac{t-\varphi}{2}} - re^{-i\frac{t-\varphi}{2}})^2}{1 - 2r \cos(t - \varphi) + r^2}. \end{aligned}$$



Figure 2.2: Impulse-response of the Laguerre system (the first 16 elements)

According to the above form the phase of function b_a is given as

$$\arg [b_a(e^{it})] = \delta + \varphi + 2 \arg \left[e^{i \frac{t-\varphi}{2}} - r e^{-i \frac{t-\varphi}{2}} \right],$$

where

$$e^{i \frac{t-\varphi}{2}} - r e^{-i \frac{t-\varphi}{2}} = (1-r) \cos \frac{t-\varphi}{2} + i(1+r) \sin \frac{t-\varphi}{2},$$

hence

$$\arg \left[e^{i \frac{t-\varphi}{2}} - r e^{-i \frac{t-\varphi}{2}} \right] = \arctan \left(\frac{1+r}{1-r} \tan \frac{t-\varphi}{2} \right).$$

Consequently, the argument-function belonging to the Blaschke-function, generated by the parameter $a = re^{i\varphi}$, $\beta_a(t)$, by introducing the notations

$$\mu = \frac{1+r}{1-r} \quad \text{and} \quad \gamma = \delta + \varphi,$$

can be expressed in the following form:

$$\beta(t) = 2 \arctan \left(\mu \tan \frac{t-\varphi}{2} \right) + \gamma \quad (2.3.9)$$

where γ is an arbitrary constant.

The Blaschke-function forms a mapping of the unit circle onto itself. The arbitrary constant γ is conventionally set in such a way that $\beta_a(-\pi) = -\pi$, hence the β_a function realizes a mapping $\beta_a : [-\pi, \pi] \mapsto [-\pi, \pi]$. To derive γ , let us regard

$$-\pi = 2 \arctan \left(\mu \tan \frac{-\pi - \varphi}{2} \right) + \gamma,$$

with some manipulation

$$\tan \frac{\pi + \gamma}{2} = \mu \tan \frac{\pi + \varphi}{2} \quad \Rightarrow \quad \cot \frac{\gamma}{2} = \mu \cot \frac{\varphi}{2}$$

it results in

$$\gamma = 2 \arctan \left(\mu^{-1} \tan \frac{\varphi}{2} \right).$$

It is easy to show, that β is a continuously differentiable function, and it is strictly increasing and invertible function, hence it forms a bijection from the interval $[-\pi, \pi]$ onto itself. The inverse function $t = \beta_a^{-1}(s)$ ($s \in [-\pi, \pi]$) can be obtained as

$$t = 2 \arctan \left(\mu^{-1} \tan \frac{s - \gamma}{2} \right) + \varphi$$

To prove the strictly increasing feature of the β_a function let us differentiate it according to parameter t :

$$\frac{d\beta}{dt} = 2 \frac{1}{1 + \mu^2 \tan^2 \left(\frac{t-\varphi}{2} \right)} \mu \frac{1}{\cos^2 \left(\frac{t-\varphi}{2} \right)} \frac{1}{2} = \frac{\mu}{\cos^2 \left(\frac{t-\varphi}{2} \right) + \mu^2 \sin^2 \left(\frac{t-\varphi}{2} \right)}.$$

It is obvious that the derivative is positive, since $\mu > 0$ in the numerator, and a complete square is found in the denominator, hence β is strictly increasing function. Since the derivative will be used later, let us express it in a more comfortable form: by returning from μ to r ,

$$\begin{aligned} \frac{d\beta}{dt}(t) &= \frac{\frac{1+r}{1-r}}{\cos^2(\frac{t-\varphi}{2}) + (\frac{1+r}{1-r})^2 \sin^2(\frac{t-\varphi}{2})} = \\ &= \frac{(1+r)(1-r)}{(1-r)^2 \cos^2(\frac{t-\varphi}{2}) + (1+r)^2 \sin^2(\frac{t-\varphi}{2})} = \frac{1-r^2}{1-2r \cos(t-\varphi) + r^2}, \end{aligned}$$

which, by using the expression $a = re^{i\varphi}$, results in the form

$$\beta'_a(t) = \frac{1 - |a|^2}{|1 - \bar{a}e^{it}|^2}. \quad (2.3.10)$$

The shape of the argument-functions belonging to some values of parameter a (that correspond to system poles) is presented on Figure 2.3. Real parameter values $a_1 = 0.5$, $a_2 = 0.7$, $a_3 = 0.9$, and $a_4 = 0.99$ are considered.

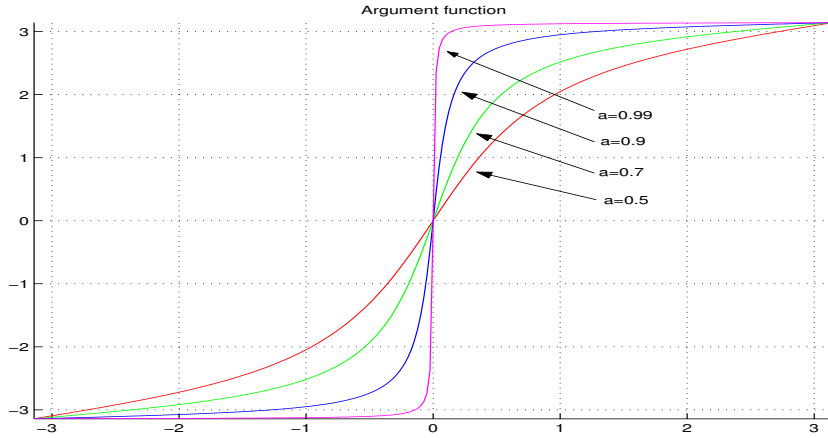


Figure 2.3: Argument-functions belonging to real a values

The representation of functions $F \in \mathcal{H}^2(\mathbb{D})$ in the Laguerre basis can be written as

$$F(q) = \sum_{n=0}^{\infty} l_n \Phi_n(q), \quad (2.3.11)$$

where the numbers $\{l_n\}$ are called *Laguerre coefficients*. Since the system $\{\Phi_n\}$ forms an orthonormal basis in $\mathcal{H}^2(\mathbb{D})$, the Laguerre coefficients can be computed by the scalar products

$$l_n \doteq \langle F, \Phi_n \rangle \quad (n = 0, 1, 2, \dots). \quad (2.3.12)$$

By substituting the expression (2.3.6) of Φ and $a = re^{i\varphi}$ for the parameter a , the scalar product can be written into the form

$$\langle F, \Phi_n \rangle = \frac{\sqrt{1-r^2}}{2\pi} \int_{-\pi}^{\pi} \frac{F(e^{it})}{1-re^{i(t-\varphi)}} b_a^n(e^{-it}) dt.$$

Let the notion of the argument-function belonging to b_a , according to (2.3.8), be used, to get the form

$$\langle F, \Psi_n \rangle = \frac{\sqrt{1-r^2}}{2\pi} \int_{-\pi}^{\pi} \frac{F(e^{it})}{1-re^{i(t-\varphi)}} e^{-in\beta_a(t)} dt.$$

Let the integration variable t be transformed by the argument function $s = \beta_a(t)$ into s , t can be expressed as $t = \beta_a^{-1}(s)$ inverse:

$$\langle F, \Phi_n \rangle = \frac{\sqrt{1-r^2}}{2\pi} \int_{-\pi}^{\pi} \frac{F(e^{i\beta_a^{-1}(s)})}{1-re^{i(\beta_a^{-1}(s)-\varphi)}} e^{-ins} \frac{ds}{\beta'_a(\beta_a^{-1}(s))}.$$

By using the notation $f_a(s)$, and applying the expression (2.3.10) of the derivative of the inverse argument function,

$$f_a(s) \doteq \left[\frac{\sqrt{1-r^2} F(e^{it})}{(1-re^{i(t-\varphi)})\beta'_a(t)} \right]_{t=\beta_a^{-1}(s)} = \left[\sqrt{\frac{1-r}{1+r}} F(e^{it}) (1-re^{-i(t-\varphi)}) \right]_{t=\beta_a^{-1}(s)},$$

the scalar product can be expressed as

$$\langle F, \Phi_n \rangle = \frac{1}{2\pi} \int_{-\pi}^{\pi} f_a(s) e^{-ins} ds. \quad (2.3.13)$$

This is a Fourier-integral belonging to the Fourier-coefficients of the function $f_a(s)$, hence the problem of computing the coefficients of the $\mathcal{H}^2(\mathbb{D})$ representation has been transformed into computing the coefficients of the Fourier-representation of the periodic function f_a belonging to the space $\mathcal{L}^2[-\pi, \pi]$. That is, the derivation of the Laguerre coefficients has

been transferred into the problem of computing the Laguerre Fourier coefficients of the restriction of the $\mathcal{H}^2(\mathbb{T})$ function on the unit circle, that is a function belonging to the space $\mathcal{L}^2[-\pi, \pi]$. The function f_a can exactly be computed in any point of the interval $[-\pi, \pi]$, if the values of the function F are available. Discrete sample values of the function F can be generated by either direct measurements or computations upon measurements by applying signal processing methods. Starting from a set of discrete samples of the function F the Fourier-integral can approximately be computed by applying the Fast Fourier Transform (FFT) algorithm.

The approximate computation can be performed on the basis of an N -point division of the interval $[-\pi, \pi]$. To apply FFT algorithm, this division, considered on the s -domain, should be uniformly spaced. The physically existing frequency scale corresponds to the t -domain, that is given by the inverse of the argument-function β_a . A uniform division on domain s

$$s_0 = -\pi, s_1 = -\pi + \frac{2\pi}{N}, s_2 = -\pi + 2\frac{2\pi}{N}, \dots, s_n = -\pi + n\frac{2\pi}{N}, \dots, s_N = \pi$$

results in a non-uniform division on t

$$t_0 = -\pi, t_1 = \beta_a^{-1}\left(-\pi + \frac{2\pi}{N}\right), t_2 = \beta_a^{-1}\left(-\pi + 2\frac{2\pi}{N}\right), \dots, t_n = \beta_a^{-1}\left(-\pi + n\frac{2\pi}{N}\right), \dots, t_N = \pi.$$

On figure 2.4 a non-uniform division on t (the vertical axis) is presented for 32 sample points generated on a single real pole $a = 0.7$. The transform $\beta_a : t \rightarrow s$ that has been applied on the scales is called *argument-transform* related to the parameter a .

The argument-transform can simply be defined also by using the z -notation. The Blaschke-function in the space $\mathcal{H}_\perp^2(\mathbb{D})$ for the pole $a \in \mathbb{D}$ can be defined as

$$b_a(z) = e^{i\delta} \frac{1 - \bar{a}z}{z - a}$$

where $\delta \in \mathbb{R}$ is an arbitrary constant. If the argument-function for this Blaschke-function is defined as

$$b_a(e^{it}) = e^{-i\beta_a(t)},$$

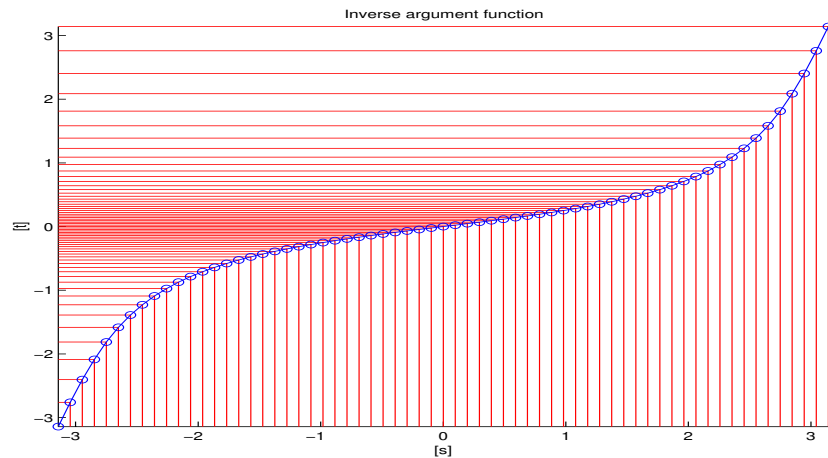


Figure 2.4: Non-uniform division generated by β_a^{-1} function

the basic characteristics of the argument-function remain unchanged, i.e. it is a continuously differentiable strictly increasing function. Hence the argument-transform is formally the same in both the q and z notation, i.e. in both the space \mathcal{H}^2 and \mathcal{H}_\perp^2 .

The cause of the non-uniformly spaced frequency scale produced by the inverse argument-transform is presented on the figure 2.5. The Nyquist diagrams as well Bode-like frequency diagrams containing absolute value and phase belonging to functions possessing a single real pole $a = 0.7$ are presented, by using finite number of uniformly spaced samples on the left-side diagrams, and those given by the argument-transform on the right-side ones. It can be observed, that the Nyquist-plots belonging to the nonuniform scale interpolates better the continuous function, since the nonuniform scale applied on the domain results in uniform spacing of the image. On the frequency-diagrams the observation is different: the nonuniform scale results denser spacing on the sample points in the neighborhood of the peak, and sparser on the places, where "nothing can be observed". This ideas will be elaborated later in this thesis in association with more complex examples.

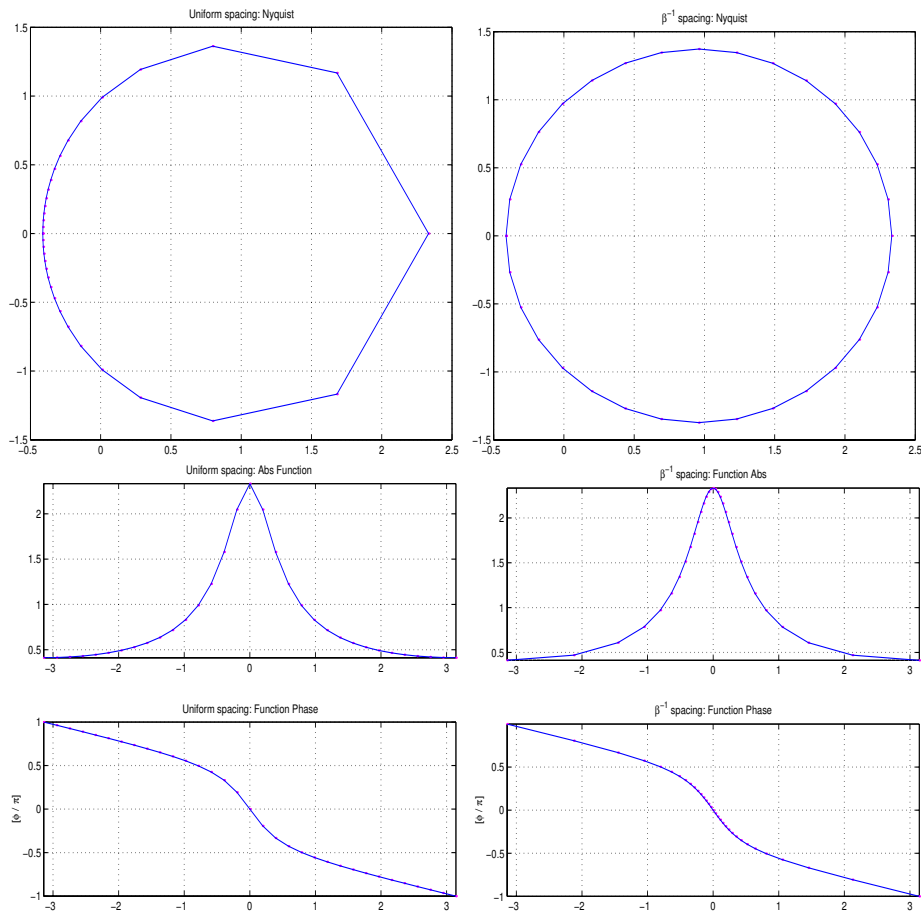


Figure 2.5: Uniform and non-uniform spacing

2.3.3 Identification by Laguerre representation

By using the algorithm described in the section 2.3.2 of estimating the Laguerre coefficients belonging to the system analyzed, an identification problem can be solved:

Problem 2.3.2. *We can measure the transfer function belonging to the system on arbitrary frequency points resulting in a set of measurements $F(e^{it_n})$ ($n = 0, 1, \dots, N$). The task is to find an estimate of the transfer function $F(z)$ in the space \mathcal{H}_\perp^2 with the a priori assumption, that the system possesses a single real pole $a \in \mathbb{D}$, with minimal error in the norm of the*

space.

The problem can be solved by building a discrete Laguerre representation built upon the assumed pole. The procedure can be divided in two major steps:

- Measurement phase: performing transfer function measurements on suitably designed frequency points.
- Representation phase: based upon the set of measurement values computing the representation coefficients.

The suitable non-uniformly spaced frequency scale required for the measurement can be obtained by applying the argument-transform belonging to the a priori assumed pole upon an initial uniform scale of N points. Based upon measurement data spaced non-uniformly on the frequency axis the representation coefficient can be estimated by the approximate evaluation of the Fourier-integral (2.3.13). A more detailed discussion on the realization, will be given later in association with the generalization of the method.

2.4 Generalized orthogonal bases

2.4.1 Generalizing the Laguerre system

It is obvious from the section 2.3, that the Laguerre system represents well the systems possessing one dominant pole, i.e. there exist one pole, which — comparing to the other ones — dominates in forming the dynamics of the system. To express this in more mathematical form, let us consider the partial fraction form of the transfer function belonging to the system. All the rational functions $F \in \mathcal{H}_\perp^2$ can be expressed in the following form:

$$F(z) = \sum_{k=0}^{N-1} \sum_{\ell=1}^{m_k} \frac{A_{k\ell}}{(z - a_k)^\ell}, \quad (2.4.1)$$

where $\{a_k \in \mathbb{D} \mid k = 0, 1, 2, \dots, N - 1\}$ the poles of the system, and $\{m_k \in \mathbb{N} \mid k = 0, 1, 2, \dots, N - 1\}$ are the multiplicities belonging to the them. The coefficients $A_{k\ell}$ weight the role of the particular terms in forming the dynamics of the system. If there exist a pole, that the coefficients belonging to it in the partial fraction representation are far greater than the other ones, this pole is dominant in the system dynamics.

If no dominant pole can be found, or more than one pole is dominating, the Laguerre representation is moreover not advantageous. Similar situation is turned out in the case of complex poles: in physically realizable technical systems the complex poles are considered as conjugated pairs, and there is no reason to select any one of them to use it in the Laguerre representation.

The generalization of the Laguerre system to represent conjugated complex pair of poles is known in the literature as *Kautz system*, named after its inventor [23]. The Kautz system has been investigated by the robust identification community in the 90's [74, 39, 49]. The Kautz system has been generalized, and a general framework has been worked out, where multiple number of real poles and conjugated complex pairs can be included. This system is referred in the literature as *generalized Kautz system*. By reasons that will be clarified soon, the name *generalized orthogonal basis* (GOB) — being also popular — is more advantageous. The more characteristic name is probably the expression *rational orthogonal basis* spreading nowadays.

The generalization does not distinguish real and conjugated complex pairs, the poles are considered to be a the finite set of different numbers residing within the unit circle:

$$a = \{a_n \in \mathbb{D} \mid n = 0, 1, 2, \dots, N - 1\} \quad (2.4.2)$$

$$a_i \neq a_j \quad \text{for } i \neq j, \quad i, j = 0, 1, 2, \dots, N - 1.$$

Of course, physically realizable systems should contain real poles or conjugated complex pairs, and the terms containing the conjugated pairs function as second order blocks, rather

than separated elements. The idea of the generalization is given by the partial fraction representation, let all the terms be considered, belonging to the different poles in all the multiplicities. Let us turn to the mathematical q -notation:

$$\begin{aligned} & \frac{1}{1 - \overline{a_0} q}, \frac{1}{1 - \overline{a_1} q}, \dots, \frac{1}{1 - \overline{a_k} q}, \dots, \frac{1}{1 - \overline{a_{N-1}} q}, \\ & \frac{q}{(1 - \overline{a_0} q)^2}, \frac{q}{(1 - \overline{a_1} q)^2}, \dots, \frac{q}{(1 - \overline{a_k} q)^2}, \dots, \frac{q}{(1 - \overline{a_{N-1}} q)^2}, \\ & \vdots \\ & \frac{q^n}{(1 - \overline{a_0} q)^{n+1}}, \frac{q^n}{(1 - \overline{a_1} q)^{n+1}}, \dots, \frac{q^n}{(1 - \overline{a_k} q)^{n+1}}, \dots, \frac{q^n}{(1 - \overline{a_{N-1}} q)^{n+1}}, \\ & \vdots \end{aligned}$$

for the N -element set of parameters defined by (2.4.2), identical to the poles of the system to be represented. It is clear, that this system is linearly independent, and it can be shown, that it is complete in the space $\mathcal{H}^2(\mathbb{D})$. With the use of the Gram-Schmidt orthogonalization procedure this system can be transformed into an orthonormal system, exactly as it has been done in the Laguerre case.

The generalization advised above seems to be *ad hoc*, and to complete the orthogonalization procedure is rather cumbersome, hence another approach is more advantageous to follow: a more straightforward way for the generalization is given by introducing the so-called *Takenaka-Malmquist* system.

2.4.2 Takenaka-Malmquist system: general considerations

The Takenaka-Malmquist system has been constructed by S. Takenaka [71] and F. Malmquist [34] independently of each other in 1925. It has been introduced into the field of system identification — without mentioning the name of Takenaka or Malmquist — by Ninness and Gustafsson [38, 39, 40].

To introduce the Takenaka-Malmquist system, let us first define the notion of the Blaschke-product.

Definition 2.4.1. For a finite set of parameters $\mathbf{a} = \{a_j \in \mathbb{D}, j = 0, 1, \dots, n-1\}$ the *finite Blaschke-product* of order n is defined as

$$B_{\mathbf{a}|n}(q) \doteq \prod_{j=0}^{n-1} b_{a_j}(q),$$

and for an infinite set of parameters $\mathbf{a} = \{a_j \in \mathbb{D}, j = 0, 1, 2, \dots\}$, the *infinite Blaschke-product* is defined as

$$B_{\mathbf{a}}(q) \doteq \prod_{j=0}^{\infty} b_{a_j}(q),$$

where b_{a_j} for $j = 0, 1, 2, \dots, n$ or ∞ is the Blaschke-function

$$b_{a_j}(q) = e^{i\delta_j} \frac{q - a_j}{1 - \overline{a_j}q}$$

generated by the parameter a_j , (δ_j is an arbitrary constant).

The parameters \mathbf{a} are the zeros of the Blaschke-product in the mathematical notation, i.e. in the case, when $B_{\mathbf{a}|n} \in \mathcal{H}^2(\mathbb{T})$; in the technical sense the parameters \mathbf{a} are identical to the system poles.

Definition 2.4.2. The system of functions

$$\phi_0(q) \doteq \frac{\sqrt{1 - |a_0|^2}}{1 - \overline{a_0}q}, \quad \phi_n(q) \doteq \frac{\sqrt{1 - |a_n|^2}}{1 - \overline{a_n}q} B_{\mathbf{a}|n}(q),$$

for $n = 0, 1, 2, \dots$, where $B_{\mathbf{a}|n}$ is the Blaschke-product of order n associated with the set of parameters $a = \{a_j \in \mathbb{D} \mid j = 0, 1, 2, \dots\}$, is called (infinite) *Takenaka-Malmquist system*.

The following theorem is crucial in respect to the theory to be built:

Theorem 2.4.1. *The infinite Takenaka-Malmquist system associated with the set of parameters $a_n \in \mathbb{D}$ ($n = 0, 1, 2, \dots$) forms an orthonormal basis in \mathcal{H}^2 space iff the series*

$$\sum_{n=0}^{\infty} (1 - |a_n|) = \infty.$$

Proof. The Takenaka-Malmquist system is obviously a linearly independent system, since it consist of strictly proper rationale functions of increasing order.

The orthogonality and the normality can be proved by analyzing the scalar product

$$\langle \phi_n, \phi_m \rangle \doteq \frac{1}{2\pi} \int_{-\pi}^{\pi} \phi_n(e^{it}) \overline{\phi_m(e^{it})} dt, \quad (2.4.3)$$

this can essentially be made in the same way as proving the Theorem 2.3.1.

With $a_m = r_m e^{i\varphi_m}$ and $a_n = r_n e^{i\varphi_n}$ ($m, n \in \mathbb{N}^*$)

$$\begin{aligned} \langle \phi_n, \phi_m \rangle &= \frac{\sqrt{(1-r_n^2)(1-r_m^2)}}{2\pi} \int_{-\pi}^{\pi} \frac{B_{a|n}(e^{it}) \overline{B_{a|m}(e^{it})}}{(1-r_n e^{i(t-\varphi_n)})(1-r_n e^{-i(t-\varphi_m)})} dt = \\ &= \frac{\sqrt{(1-r_n^2)(1-r_m^2)}}{2\pi} \int_{-\pi}^{\pi} \frac{\prod_{j=0}^{n-1} (e^{it} - r_j e^{i\varphi_j}) \prod_{j=0}^{m-1} (e^{-it} - r_j e^{-i\varphi_j})}{\prod_{j=0}^n (1 - r_j e^{i(t-\varphi_j)}) \prod_{j=0}^m (1 - r_j e^{-i(t-\varphi_j)})} dt. \end{aligned}$$

Let us assume that $n > m$, thus the terms

$$\prod_{j=0}^m (1 - r_j e^{i(t-\varphi_j)})(1 - r_j e^{-i(t-\varphi_j)}) = \prod_{j=0}^m (1 - 2r_j \cos(t - \varphi_j) + r_j^2)$$

in the denominator, and

$$\prod_{j=0}^{m-1} (e^{it} - r_j e^{i\varphi_j})(e^{-it} - r_j e^{-i\varphi_j}) = \prod_{j=0}^{m-1} (1 - 2r_j \cos(t - \varphi_j) + r_j^2)$$

in the numerator can be separated. After simplifying with the common terms (which are both positive), the scalar product can be written in the form of a Poisson-integral:

$$\langle \phi_n, \phi_m \rangle = \sqrt{\frac{1-r_n^2}{1-r_m^2}} \frac{1}{2\pi} \int_{-\pi}^{\pi} \frac{1-r_m^2}{1-2r_m \cos(t-\varphi_m) + r_m^2} \frac{\prod_{j=m}^{n-1} (e^{-it} - e^{-i\varphi_j})}{\prod_{j=m+1}^n (1 - e^{-i(t-\varphi_j)})} dt.$$

The Poisson-integral, related to the value $a_m = r_m e^{i\varphi_m}$, has been applied to the function

$$f(q) = \sqrt{\frac{1-r_n^2}{1-r_m^2}} (q - a_m) \prod_{j=m+1}^{n-1} \frac{q - a_j}{1 - \overline{a_j} q}.$$

Since $q = a_m$ is a zero of the function, the Poisson-integral is equal to zero.

For the case of $n < m$ the above discussion can be repeated, except that the conjugate of f will be given in the Poisson-integral.

For the case $m = n$ after simplification the scalar product (2.4.3) gets the form

$$\frac{1}{2\pi} \int_{-\pi}^{\pi} \frac{1 - r_m^2}{1 - 2r_m \cos(t - \varphi_m) + r_m^2} dt = 1.$$

Summarizing the results,

$$\langle \phi_n, \phi_m \rangle = \delta_{nm} \quad \text{for any } m, n \in \mathbb{N}^*,$$

which means that the Takenaka-Malmquist system is orthonormal.

The completeness of the system in \mathcal{H}^2 can be proved by showing, that there does not exist any function $F \in \mathcal{H}^2$ not identical to zero, which is orthogonal to every element of the system. Let us assume that there exists a function $F \neq 0$, that

$$\langle F, \phi_n \rangle = 0 \quad (n \in \mathbb{N}^*).$$

The scalar product can be written as

$$\begin{aligned} \langle F, \phi_n \rangle &= \frac{\sqrt{1 - r_n^2}}{2\pi} \int_{-\pi}^{\pi} \frac{F(e^{it}) \overline{B_{a|n}(e^{it})}}{1 - r_n e^{-i(t - \varphi_n)}} dt = \frac{\sqrt{1 - r_n^2}}{2\pi} \int_{-\pi}^{\pi} \frac{e^{it} F(e^{it}) \overline{B_{a|n}(e^{it})}}{e^{it} - r_n e^{i\varphi_n}} dt = \\ &= \frac{\sqrt{1 - |a_n|^2}}{2\pi i} \oint \frac{F(q) \overline{B_{a|n}(q)}}{q - a_n} dq = \frac{\sqrt{1 - |a_n|^2}}{2\pi i} F(a_n) \overline{B_{a|n}(a_n)}, \end{aligned}$$

according to the Cauchy-formula applied in the last step.

Since the Blaschke-product $B_{a|n}$ has no zero in $q = a_n$, the $F(q)$ function should have zeros in every a_n ($n \in \mathbb{N}^*$). According to the theorem 15.23 in page 305 of [46] for any $F \in \mathcal{H}^2$ with zeros $a_n \in \mathbb{D}$ ($n \in \mathbb{N}^*$), if it is not identically 0 in \mathbb{D} , than

$$\sum_{k=0}^{\infty} (1 - |a_k|) < \infty.$$

This induces that no adequate function F can be found if and only if the

$$\sum_{k=0}^{\infty} (1 - |a_k|) = \infty.$$

condition holds, which proves the completeness. □

The significance of the infinite Takenaka-Malmquist system is mainly theoretical, the special cases followed from it, namely the finite and the periodic case, both are associated with finite number of poles, are used in the praxis of the signal and system representations; the next two sections will be devoted for this topic.

2.4.3 Takenaka-Malmquist system: the finite case

In the case when a finite set of parameters $\mathbf{a} = (a_n | n = 0, 1, \dots, N - 1; N \in \mathbb{N})$ are considered, the Takenaka-Malmquist system consist of finite number of elements:

$$\Psi_0(q) \doteq \frac{\sqrt{1 - |a_0|^2}}{1 - \overline{a_0} q} \quad \Psi_n(q) \doteq \sqrt{1 - |a_n|^2} \frac{\prod_{k=0}^{n-1} (q - a_k)}{\prod_{k=0}^n (1 - \overline{a_k} q)} \quad (2.4.4)$$

The linear combination of the functions (2.4.4) with coefficients $\{c_n\}$, i.e.

$$F(q) = \sum_{n=0}^{N-1} c_n \frac{\sqrt{1 - |a_n|^2} \prod_{k=0}^{N-1} (q - a_k)}{\prod_{k=0}^N (1 - \overline{a_k} q)},$$

spans a subspace of the \mathcal{H}^2 space. To see this, let the expression be brought to the common denominator $\prod_{k=0}^N (1 - \overline{a_k} q)$ as

$$\frac{\sum_{n=0}^{N-1} c_n \sqrt{1 - |a_n|^2} \prod_{k=0}^{n-1} (q - a_k) \prod_{k=n+1}^{N-1} (1 - \overline{a_k} q)}{\prod_{k=0}^N (1 - \overline{a_k} q)}. \quad (2.4.5)$$

Both the numerator and the denominator are polynomials of q , with degree $N - 1$ and N respectively. For the denominator this is trivial; in the numerator every term of the sum contains $N - 1$ factors, for every $0 \leq n < N$ the factor belonging to a_n is missing. Hence the rational function resulted is strictly proper.

If the polynomials of degree $N - 1$ in the numerator are linearly independent, they span the space of every polynomial with degree not greater than $N - 1$. Thus let the following proposition be stated:

Proposition 2.4.2. *The set of polynomials in the numerator of (2.4.5) forms a linearly independent system.*

Proof. A simple indirect proof can be given: let us suppose, that in the numerator of (2.4.5) there exists a c_j coefficient being nonzero, which results in the numerator to be equivalent to zero. In this case the member with index j can be expressed in the form

$$\prod_{k=0}^{j-1} (q - a_k) \prod_{k=j+1}^{N-1} (1 - \bar{a}_k q) = -\frac{1}{c_j} \left(\sum_{\substack{n=0 \\ n \neq j}}^{N-1} c_n \sqrt{1 - |a_n|^2} \prod_{k=0}^{n-1} (q - a_k) \prod_{k=n+1}^{N-1} (1 - \bar{a}_k q) \right). \quad (2.4.6)$$

The left-side polynomial does not contain factors either $(q - a_j)$ or $(1 - \bar{a}_j q)$. Instead all the members of the right-side sum contain a common factor either $(q - a_j)$ or $(1 - \bar{a}_j q)$, depending upon whether $j < n$ or $j > n$ respectively. This is a contradiction, hence the linear independence has been proved. \square

This means, that the finite Takenaka-Malmquist system based upon the set of parameters $\mathbf{a} = (a_n \in \mathbb{D}, n = 0, 1, \dots, N-1, N \in \mathbb{N})$ spans the space of the strictly proper rational functions with poles

$$(1/\bar{a}_n, n = 0, 1, \dots, N-1, N \in \mathbb{N})$$

falling outside the unit circle, which is a subspace of \mathcal{H}^2 . Because of its significant role in the theory to be built, let this subspace be denoted by $\mathcal{B}_{a|N} \mathcal{H}^2$, and $\mathcal{B}_{a|N} \mathcal{H}^2 \subset \mathcal{H}^2$.

The numerator can be written in the form

$$\sum_{n=0}^{N-1} d_n q^n$$

where the d_n coefficients are linear functions of c_n -s. These coefficient can be done equal to the numerator coefficients of the rational to be represented, hence the c_n coefficients of the finite Takenaka-Malmquist representation can be computed by solving a linear equation

$$\sum_{j=0}^{N-1} c_j e_{nj} = d_n \quad (n = 0, 1, 2, \dots, N-1)$$

where the $\{e_n\}$ and $\{d_n\}$ parameters are the coefficients of the numerator polynomials belonging to the powers n of q in the numerator of the rational function (2.4.5), and the

function to be represented, respectively. To give a general formula of computing the matrix of parameters $\{e_{ij}\}$ is quite difficult, however for given orders it is easy to compute them iteratively, as it has been realized in *MATLAB*[®] by function `tmcoefrq`. The unambiguous solution of the linear equation is guaranteed by the linear independence of the numerator polynomials.

Let us see some simple examples to demonstrate the method.

Example 2.4.3. *Let us derive the finite Takenaka-Malmquist representation of the rational functions*

$$F_1(q) = \frac{0.125}{q^2 - 6q + 8} \quad \text{and} \quad F_2(q) = \frac{0.125(q-1)}{q^2 - 6q + 8}.$$

These rationals are equivalent with

$$F_1(q) = \frac{1}{(1-0.25q)(1-0.5q)} \quad \text{and} \quad F_2(q) = \frac{q-1}{(1-0.25q)(1-0.5q)}.$$

The Takenaka-Malmquist representations based upon parameters $a = (0.25, 0.5)$ are as follows:

$$F_1(q) = \frac{1.1803378}{(1-0.25q)} + \frac{0.6598289(q-0.25)}{(1-0.25q)(1-0.5q)},$$

$$F_2(q) = \frac{-0.8852533}{(1-0.25q)} - \frac{0.6598289(q-0.25)}{(1-0.25q)(1-0.5q)}.$$

The coefficients has been computed with the function `tmcoefrq`.

It is not difficult to compute the coefficients by hand in this case. The general form of the Takenaka-Malmquist representation for $N = 2$ and parameters (a_0, a_1) by introducing the notations $p_0 = \sqrt{1 - |a_0|^2}$ and $p_1 = \sqrt{1 - |a_1|^2}$ is as follows:

$$c_0 p_0 \frac{1}{(1 - \overline{a_0} q)} + c_1 p_1 \frac{(q - a_0)}{(1 - \overline{a_0} q)(1 - \overline{a_1} q)},$$

which is equal to

$$\frac{c_0 p_0 (1 - \overline{a_1} q) + c_1 p_1 (q - a_0)}{(1 - \overline{a_0} q)(1 - \overline{a_1} q)} = \frac{(c_1 p_1 - c_0 p_0 \overline{a_1}) q + (c_0 p_0 - c_1 p_1 a_0)}{(1 - \overline{a_0} q)(1 - \overline{a_1} q)}.$$

A common model for F_1 and F_2 , as well as for any strictly proper rational with the given denominator can be

$$F(q) = \frac{d_0 + d_1q}{(1 - 0.25q)(1 - 0.5q)}.$$

By comparing the coefficients belonging to the powers 0 and 1 of q , we get the set of linear equations

$$\begin{aligned} p_0 c_0 - p_1 a_0 c_1 &= d_0 \\ -p_0 \bar{a}_1 c_0 - p_1 c_1 &= d_1. \end{aligned}$$

The solution for c_0 and c_1 is

$$\begin{aligned} c_0 &= \frac{d_0 + d_1 a_0}{p_1 (1 - a_0 \bar{a}_1)} \\ c_1 &= \frac{d_0 \bar{a}_1 + d_1}{p_0 (1 - a_0 \bar{a}_1)}. \end{aligned}$$

It can be verified that by using the values for the parameters and the polynomial coefficients given above, these formulas result in the coefficient values computed by `tmcoefrq`.

A more complex example with one real pole and a conjugated complex pair is given:

Example 2.4.4. *Let us derive the finite Takenaka-Malmquist representation of the rational function*

$$F(q) = \frac{0.25(q^2 - 4q + 3)}{q^3 - 6q^2 + 10q - 8}.$$

The poles and zeros of the function are $(1+i, 1-i, 4)$, and $(1, 3)$ respectively. More familiar form for is

$$F(q) = \frac{(q-1)(q-3)}{(1 - \frac{1+i}{2}q)(1 - \frac{1-i}{2}q)(1 - \frac{1}{4}q)}.$$

The Takenaka-Malmquist representation based upon the parameters $(\frac{1}{4}, \frac{1-i}{2}, \frac{1+i}{2})$ is as follows:

$$F(q) = 2.726580 \frac{1}{1 - \frac{1}{4}q} +$$

$$(-1.719684 + 1.086116i) \frac{q - \frac{1}{4}}{(1 - \frac{1}{4}q)(1 - \frac{1+i}{2}q)} +$$

$$(0.226274 + 1.583919i) \frac{(q - \frac{1}{4})(q - \frac{1+i}{2})}{(1 - \frac{1}{4}q)(1 - \frac{1+i}{2}q)(1 - \frac{1-i}{2}q)}$$

The coefficients has been computed with the function `tmcoefrq`. It can be observed, that the coefficients depend – as it is obvious from the representation – on the application order of the parameters \mathbf{a} .

The *MATLAB*[®] procedure for computing the Takenaka-Malmquist representation coefficients of rational functions has been realized both in q and z notation under names `tmcoefrq` (that has been used above) and `tmcoefrz`, respectively.

2.4.4 Takenaka-Malmquist system: the periodic case

In the case when a finite set of parameters is available, an orthonormal basis can be obtained by periodically repeating them, that is if N number of different parameters are given, the infinite sequence of parameters associated with the infinite Takenaka-Malmquist system is

$$a_0, a_1, a_2, \dots, a_{N-1}, a_0, a_1, a_2, \dots, a_{N-1}, a_0, a_1, \dots$$

Let the N -element blocks be indexed by ℓ , thus the k -th parameter in the ℓ -th block can be expressed as

$$a_n = a_{\ell N+k}.$$

The Blaschke-product $B_{a|n}$ can be grouped into repeating blocks of size N , except the last one, which contain less than N elements, i.e

$$B_{a|n}(q) = B_{a|N}^\ell(q) B_{a|k}(q).$$

Hence the system Φ_n for $n > 0$ will be

$$\Phi_n(q) = \frac{\sqrt{1 - |a_k|^2}}{1 - \overline{a_k}q} B_{a|k}(q) B_{a|N}^\ell(q).$$

The above manipulation does not affect either the linear independence or the orthogonality of the Takenaka-Malmquist system, as the periodically repeated members act on successively increasing powers in the rational functions. The necessary and sufficient condition of the completeness is automatically fulfilled as

$$\sum_{k=0}^{N-1} (1 - |a_k|) = C \quad (C > 0)$$

result in the same constant C for every N -member block of parameters, thus for infinite number of blocks the sum is infinite. Hence the following theorem is considered to be proved:

Theorem 2.4.5. *The system Φ_n for $n = \ell N + k$ ($\ell \in \mathbb{N}, N \in \mathbb{N}^*$) defined on the set of parameters $a = \{a_k \in \mathbb{D} \mid k = 0, 1, \dots, N - 1\}$*

$$\Phi_0(q) \doteq \frac{\sqrt{1 - |a_0|^2}}{1 - \overline{a_0}q}, \quad \Phi_n(q) \doteq \frac{\sqrt{1 - |a_k|^2}}{1 - \overline{a_k}q} B_{a|k}(q) B_{a|N}^\ell(q), \quad (2.4.7)$$

where $B_{a|k}$ and $B_{a|N}$ are finite Blaschke-products of order k and N respectively, forms an orthonormal basis in the space $\mathcal{H}^2(\mathbb{D})$.

The system (2.4.7), obtained as the Takenaka-Malmquist system constructed by the periodic repetition of finite number of parameters (system poles) is called *generalized orthogonal (orthonormal) basis*, and abbreviated as *GOB*.

In Tables 2.1 and 2.2 the sequence of the generalized orthogonal basis functions expressed with the Blaschke functions and directly by rational functions, respectively. In the rational forms the normalizing factors belonging to the particular basis functions have been notated by $\{d_{k\ell}\}$ for simplification. The constants are

$$d_{k\ell} = \sqrt{1 - |a_k|^2} e^{i\ell\Delta_N} \prod_{j=0}^{k-1} e^{i\delta_j} \quad \text{and} \quad \Delta_N = \prod_{j=0}^{N-1} e^{i\delta_j},$$

ℓ	k	$\Phi_{\ell N+k}(q)$
0	0	$\frac{\sqrt{1- a_0 ^2}}{1-\bar{a}_0 q}$
0	1	$\frac{\sqrt{1- a_1 ^2}}{1-\bar{a}_0 q} b_{a_0}(q)$
0	2	$\frac{\sqrt{1- a_2 ^2}}{1-\bar{a}_0 q} b_{a_0}(q)b_{a_1}(q)$
\vdots	\vdots	\vdots
0	$N-1$	$\frac{\sqrt{1- a_{N-1} ^2}}{1-\bar{a}_{N-1} q} b_{a_0}(q)b_{a_1}(q) \dots b_{a_{N-2}}(q)$
1	0	$\frac{\sqrt{1- a_0 ^2}}{1-\bar{a}_0 q} b_{a_0}(q)b_{a_1}(q) \dots b_{a_{N-2}}(q)b_{a_{N-1}}(q)$
1	1	$\frac{\sqrt{1- a_1 ^2}}{1-\bar{a}_1 q} b_{a_0}^2(q)b_{a_1}(q) \dots b_{a_{N-2}}(q)b_{a_{N-1}}(q)$
1	2	$\frac{\sqrt{1- a_2 ^2}}{1-\bar{a}_2 q} b_{a_0}^2(q)b_{a_1}^2(q)b_{a_2}(q) \dots b_{a_{N-2}}(q)b_{a_{N-1}}(q)$
\vdots	\vdots	\vdots
1	$N-1$	$\frac{\sqrt{1- a_{N-1} ^2}}{1-\bar{a}_{N-1} q} b_{a_0}^2(q)b_{a_1}^2(q) \dots b_{a_{N-2}}^2(q)b_{a_{N-1}}(q)$
2	0	$\frac{\sqrt{1- a_0 ^2}}{1-\bar{a}_0 q} b_{a_0}^2(q)b_{a_1}^2(q) \dots b_{a_{N-2}}^2(q)b_{a_{N-1}}^2(q)$
2	1	$\frac{\sqrt{1- a_1 ^2}}{1-\bar{a}_1 q} b_{a_0}^3(q)b_{a_1}^2(q) \dots b_{a_{N-2}}^2(q)b_{a_{N-1}}^2(q)$
2	2	$\frac{\sqrt{1- a_2 ^2}}{1-\bar{a}_2 q} b_{a_0}^3(q)b_{a_1}^3(q)b_{a_2}^2(q) \dots b_{a_{N-2}}^2(q)b_{a_{N-1}}^2(q)$
\vdots	\vdots	\vdots
2	$N-1$	$\frac{\sqrt{1- a_{N-1} ^2}}{1-\bar{a}_{N-1} q} b_{a_0}^3(q)b_{a_1}^3(q) \dots b_{a_{N-2}}^3(q)b_{a_{N-1}}^2(q)$
\vdots	\vdots	\vdots
ℓ	k	$\frac{\sqrt{1- a_k ^2}}{1-\bar{a}_k q} b_{a_0}^{\ell+1}(q)b_{a_1}^{\ell+1}(q) \dots b_{a_k}^{\ell+1}(q)b_{a_{k+1}}^{\ell}(q) \dots b_{a_{N-1}}^{\ell}(q)$
\vdots	\vdots	\vdots

Table 2.1: The elements of the generalized orthogonal basis (Blaschke form)

where the δ_k ($k = 0, 1, \dots, N-1$) are arbitrary constants belonging to the Blaschke functions according to (2.3.7), which are conventionally selected in such a way, that the Blaschke functions map the unit circle onto itself without phase shift (see in Section 2.3.2). As it can easily be verified, the generalized orthogonal basis results in the Laguerre system if a single (real) system pole, and in the Kautz system if a conjugated complex pair is assumed.

Comparing the system (2.4.7) with finite system (2.4.4), it can be observed, that in the system (2.4.7) the finite Takenaka-Malmquist system is repeated infinitely by multiplying

ℓ	k	$\Phi_{\ell N+k}(q)$
0	0	$d_{00} \frac{1}{1-\bar{a}_0 q}$
0	1	$d_{10} \frac{q-a_0}{(1-\bar{a}_0 q)(1-\bar{a}_1 q)}$
0	2	$d_{20} \frac{(q-a_0)(q-a_1)}{(1-\bar{a}_0 q)(1-\bar{a}_1 q)(1-\bar{a}_2 q)}$
\vdots	\vdots	\vdots
0	$N-1$	$d_{(N-1)0} \frac{(q-a_0)(q-a_1)\dots(q-a_{N-2})}{(1-\bar{a}_0 q)(1-\bar{a}_1 q)\dots(1-\bar{a}_{N-2} q)(1-\bar{a}_{N-1} q)}$
1	0	$d_{01} \frac{(q-a_0)(q-a_1)(q-a_2)\dots(q-a_{N-2})(q-a_{N-1})}{(1-\bar{a}_0 q)^2(1-\bar{a}_1 q)(1-\bar{a}_2 q)\dots(1-\bar{a}_{N-2} q)(1-\bar{a}_{N-1} q)}$
1	1	$d_{11} \frac{(q-a_0)^2(q-a_1)(q-a_2)\dots(q-a_{N-2})(q-a_{N-1})}{(1-\bar{a}_0 q)^2(1-\bar{a}_1 q)^2(1-\bar{a}_2 q)\dots(1-\bar{a}_{N-2} q)(1-\bar{a}_{N-1} q)}$
1	2	$d_{21} \frac{(q-a_0)^2(q-a_1)^2(q-a_2)\dots(q-a_{N-2})(q-a_{N-1})}{(1-\bar{a}_0 q)^2(1-\bar{a}_1 q)^2(1-\bar{a}_2 q)^2(1-\bar{a}_3 q)\dots(1-\bar{a}_{N-2} q)(1-\bar{a}_{N-1} q)}$
\vdots	\vdots	\vdots
1	$N-1$	$d_{(N-1)1} \frac{(q-a_0)^2(q-a_1)^2(q-a_2)^2\dots(q-a_{N-2})^2(q-a_{N-1})}{(1-\bar{a}_0 q)^2(1-\bar{a}_1 q)^2(1-\bar{a}_2 q)^2\dots(1-\bar{a}_{N-2} q)^2(1-\bar{a}_{N-1} q)^2}$
2	0	$d_{02} \frac{(q-a_0)^2(q-a_1)^2(q-a_2)^2\dots(q-a_{N-2})^2(q-a_{N-1})^2}{(1-\bar{a}_0 q)^3(1-\bar{a}_1 q)^2(1-\bar{a}_2 q)^2\dots(1-\bar{a}_{N-2} q)^2(1-\bar{a}_{N-1} q)^2}$
2	1	$d_{12} \frac{(q-a_0)^3(q-a_1)^2(q-a_2)^2\dots(q-a_{N-2})^2(q-a_{N-1})^2}{(1-\bar{a}_0 q)^3(1-\bar{a}_1 q)^3(1-\bar{a}_2 q)^2\dots(1-\bar{a}_{N-2} q)^2(1-\bar{a}_{N-1} q)^2}$
2	2	$d_{22} \frac{(q-a_0)^3(q-a_1)^3(q-a_2)^2\dots(q-a_{N-2})^2(q-a_{N-1})^2}{(1-\bar{a}_0 q)^3(1-\bar{a}_1 q)^3(1-\bar{a}_2 q)^3(1-\bar{a}_3 q)^2\dots(1-\bar{a}_{N-2} q)^2(1-\bar{a}_{N-1} q)^2}$
\vdots	\vdots	\vdots
2	$N-1$	$d_{(N-1)2} \frac{(q-a_0)^3(q-a_1)^3(q-a_2)^3\dots(q-a_{N-2})^3(q-a_{N-1})^2}{(1-\bar{a}_0 q)^3(1-\bar{a}_1 q)^3(1-\bar{a}_2 q)^3\dots(1-\bar{a}_{N-2} q)^3(1-\bar{a}_{N-1} q)^3}$
\vdots	\vdots	\vdots
ℓ	k	$d_{k\ell} \frac{(q-a_0)^{\ell+1}(q-a_1)^{\ell+1}\dots(q-a_{k-1})^{\ell+1}(q-a_k)^\ell\dots(q-a_{N-1})^\ell}{(q-\bar{a}_0 q)^{\ell+1}(1-\bar{a}_1 q)^{\ell+1}\dots(1-\bar{a}_k q)^{\ell+1}(1-\bar{a}_{k+1} q)^\ell\dots(1-\bar{a}_{N-1} q)^\ell}$
\vdots	\vdots	\vdots

Table 2.2: The elements of the generalized orthogonal basis

it with the powers of the Blaschke-product belonging to \mathbf{a} . The system (2.4.7) spans the subspace $\mathcal{B}_{a|N} \mathcal{H}^2 \subset \mathcal{H}^2$. Multiplication with the powers $\ell \in \mathbb{N}$ of $B_{a|N}$ completes the space $\mathcal{B}_{a|N} \mathcal{H}^2$ into the whole \mathcal{H}^2 , i.e. $B_{a|N}^\ell \mathcal{B}_{a|N} \mathcal{H}^2$ ($\ell \in \mathbb{N}$) spans the orthogonal complement of $\mathcal{B}_{a|N} \mathcal{H}^2$.

The role of the Blaschke product playing in forming an orthogonal basis in \mathcal{H}^2 suggests that the Blaschke product $B_{a|N}$ can be considered as a shift operator in the space \mathcal{H}^2 . As the stable Blaschke product is an inner-function in \mathcal{H}^2 , it is suitable to play the role of a shift operator, however, since it is applied in a block of basis functions (containing N elements) rather than particular functions, the notion of the shift operation should be

extended. Studying this topic falls beyond the scope of this thesis work, however we refer to the literature: a successful attempt to extend the idea of the shift operator, and the z -transform like constructions is the so-called *Hambo*-transform, that has been introduced by P.S.C. Heuberger and P.M.J. Van den Hof [45, 22], and elaborated in cooperation with J. Bokor, Z. Szabó, et al. [15, 67].

The representation of any function $F \in \mathcal{H}^2$ can be given as

$$F(q) = \sum_{n=0}^{\infty} c_n \Phi_n(q) = \sum_{n=0}^{\infty} \langle F, \Phi_n \rangle \Phi_n(q)$$

we will refer to it as the representation in the generalized orthogonal basis (GOB representation) belonging to the parameters (system poles) \mathbf{a} . The coefficients c_n ($n \in \mathbb{N}$) of the representation can effectively be computed by applying the argument-transform introduced in Section 2.3.2, and will be generalized for multiple poles in the next section.

2.4.5 Argument-transform for the generalized orthogonal basis

An adequate extension of the notion of argument function to a N -element set of parameters $\mathbf{a} = \{a_0, a_1, \dots, a_{N-1}\}$ $a_k \in \mathbb{D}$ ($k = 0, 1, \dots, N-1$) is given by taking the arithmetic mean of the argument functions with the definition (2.3.8), belonging to the particular parameters:

$$\beta_{\mathbf{a}}(t) = \frac{\beta_{a_0}(t) + \beta_{a_1}(t) + \dots + \beta_{a_{N-1}}(t)}{N}$$

The main characteristics are inherited: the $\beta(t)$ function is a bijection from $[-\pi, \pi]$ onto itself, it is strictly increasing function, it is continuously differentiable, invertible, and its inverse is also differentiable. The derivative of its inverse can be obtained from the rule of differentiating the inverse function, i.e.

$$\rho_{\mathbf{a}}(s) \doteq \frac{d}{ds} \beta_{\mathbf{a}}(s) = \frac{N}{\beta'_{a_0}(\beta_{\mathbf{a}}^{-1}(s)) + \beta'_{a_1}(\beta_{\mathbf{a}}^{-1}(s)) + \dots + \beta'_{a_{N-1}}(\beta_{\mathbf{a}}^{-1}(s))}$$

where the derivative of the β functions belonging to the single poles can be computed by

$$\beta'_k(t) = \frac{1 - |a_k|}{|1 - \overline{a_k} e^{it}|^2} \quad (k = 0, 1, \dots, N-1)$$

An example for the argument function and its derivative belonging to the set of parameters $(0.9, 0.99e^{0.5i}, 0.99e^{-0.5i}, 0.95e^{0.8i}, 0.95e^{-0.8i})$ can be seen on Figure 2.6.

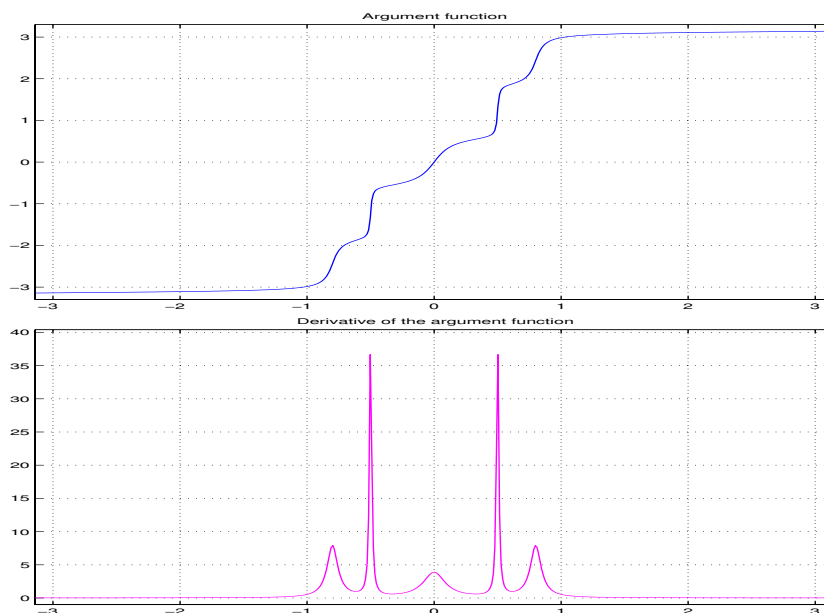


Figure 2.6: Argument-functions and its derivative of 5 poles

The representation of a function $F(q) \in \mathcal{H}^2$ in the generalized orthogonal basis is given with coefficients $\{c_n\}$ ($n \in \mathbb{N}^*$ by

$$F(q) = \sum_{n=0}^{\infty} c_n \Phi_n(q).$$

The coefficients can be computed with the indexing $n = \ell N + k$, where $k = 0, 1, \dots, N - 1$ and $\ell \in \mathbb{N}^*$ by

$$c_{\ell N+k} \doteq \langle F, \Phi_{\ell N+k} \rangle = \frac{1}{2\pi} \int_{-\pi}^{\pi} F(e^{it}) \overline{\Phi_{\ell N+k}(e^{it})} dt.$$

By expressing the ℓ -th power of the Blaschke product with the argument-function

$$B_a^\ell(e^{it}) = e^{i\ell N \beta_a(t)},$$

it can be written as

$$\langle F, \Phi_{\ell N+k} \rangle = \frac{1}{2\pi} \int_{-\pi}^{\pi} F(e^{it}) \overline{\Phi_k(e^{it})} e^{-i\ell N \beta_a(t)} dt. \quad (2.4.8)$$

Let the variable t be substituted with $t = \beta_a^{-1}(s)$, by applying the expression of the derivative of inverse β (2.4.5) to transform the integral,

$$\langle F, \Phi_{\ell N+k} \rangle = \frac{1}{2\pi} \int_{-\pi}^{\pi} F(e^{i\beta_a^{-1}(s)}) \overline{\Phi_k(e^{i\beta_a^{-1}(s)})} \rho_a(s) e^{-i\ell N s} ds.$$

By using the notation

$$f_k(s) = F(e^{i\beta_a^{-1}(s)}) \overline{\Phi_k(e^{i\beta_a^{-1}(s)})} \rho_a(s), \quad (2.4.9)$$

the scalar product can be expressed in the form

$$\langle F, \Phi_{\ell N+k} \rangle = \frac{1}{2\pi} \int_{-\pi}^{\pi} f_k(s) e^{-i\ell N s} ds. \quad (2.4.10)$$

This is a Fourier-integral belonging to the Fourier-coefficients of the function f_k , hence similarly as it has been done in the Laguerre case (see Section 2.3.2), the problem of computing the coefficients of the $\mathcal{H}^2(\mathbb{D})$ representation has been transformed into computing the coefficients of the Fourier-representation of periodic functions f_k ($k = 0, 1, \dots, N-1$) belonging to the space $\mathcal{L}^2[-\pi, \pi]$. The factor N in the exponent in the Fourier transform 2.4.10 means that the sequence of the Fourier coefficients of f_k is N times denser, hence the GOB coefficients can be obtained from it by decimation by N . The scalar product (2.4.10) can be computed approximately by applying an FFT algorithm as it will be presented as follows.

The approximate computation of the coefficients can be performed by the discretization of the Fourier-integral in (2.4.10). Let $\{s_m\}$ be an equidistant division of the interval $[-\pi, \pi]$ containing M points, i.e. with $\Delta s = 2\pi/M$ (let M be even)

$$s_m = m\Delta s \quad m = -M/2, \dots, -1, 0, 1, \dots, M/2 - 1.$$

The Fourier-integral can be approximated by the finite sum

$$c_{\ell N+k} \doteq \frac{1}{2\pi} \int_{-\pi}^{\pi} f_k(s) e^{-i\ell N s} ds \cong \frac{\Delta s}{2\pi} \sum_{m=-M/2}^{M/2-1} f_k(s_m) e^{-i\ell N m \Delta s}.$$

By applying $\Delta s = 2\pi/M$ we get for the approximated coefficients denoted with $\tilde{c}_{\ell N+k}$ as

$$\tilde{c}_{\ell N+k} = \frac{1}{M} \sum_{m=-M/2}^{M/2} f_k(s_m) e^{-i2\pi N \frac{\ell m}{M}}.$$

By considering $\ell N = j$, the form

$$\tilde{c}_{\ell N+k} = \frac{1}{M} \sum_{m=-M/2}^{M/2} f_k(s_m) e^{-i2\pi \frac{j m}{M}}. \quad (2.4.11)$$

is the expression of a finite discrete Fourier-transform, which can efficiently be computed with the Fast Fourier Transform (FFT) algorithm.

In order to compute the discrete Fourier-transform (2.4.11) the values of f_k functions are needed in the uniformly spaced scale $\{s_m\}$. The components of f_k can by this viewpoint be characterized as follow:

- The values of the function F to be represented on discrete points of the unit circle are needed, i.e. $F(e^{it_m})$. These values can in the practice be associated with sample points on several frequencies in the interval $[0, f_N]$, where f_N is the Nyquist frequency. The sample values can usually be obtained by direct measurements, or estimations based upon time-domain data. The discrete scale $\{t_m\}$ can be obtained by the transform $t = \beta_a^{-1}(s)$, i.e. starting from a uniformly spaced scale $\{s_m\}$, it results in a non-uniform scale $\{t_m\}$.
- The values of the first N basis functions on discrete points of the unit circle are needed, i.e. $\Phi_k(e^{it_m})$ ($k = 0, 1, \dots, N-1$). These values can directly be computed according to the definition (2.4.7). The computation should be performed on the non-uniform scale $\{t_m\}$ obtained by the transform $t = \beta_a^{-1}(s)$ starting from the uniform scale $\{s_m\}$.

- The values of the derivative of the inverse argument function belonging to \mathbf{a} , $\rho_a(s)$ can directly be computed according to the definition (2.4.5) on the uniformly spaced scale $\{s_m\}$.

The mapping $\beta_a : [-\pi, \pi] \mapsto [-\pi, \pi]$, $s = \beta_a(s)$, is called *argument transform*, hence the non-uniform scale $\{t_m\}$ that is needed in the algorithm to compute the representation coefficients is obtained by the *inverse argument transform* generated by the parameters \mathbf{a} .

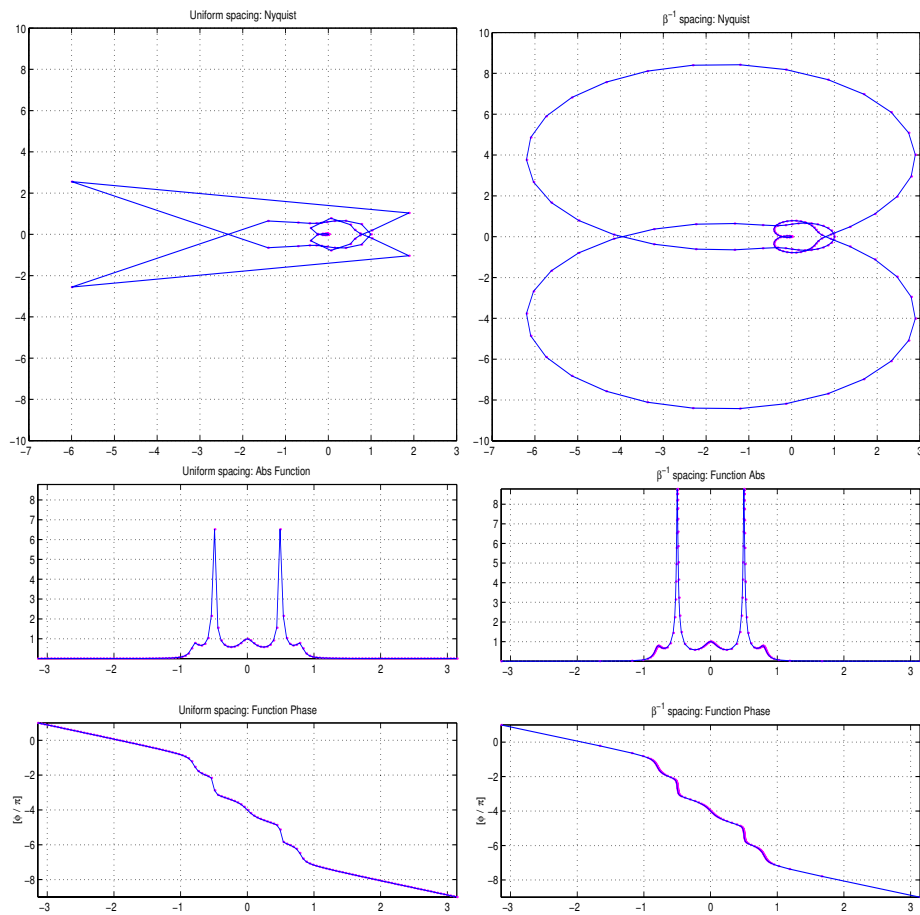


Figure 2.7: Nyquist and Bode diagrams for uniform/non-uniform spacing

A qualitative characterization of the nonuniform scale generated by the inverse argument

transform is given on Figure 2.7, where the Nyquist and Bode-type plots of the frequency function belonging to a system with poles

$$[0.9, 0.99e^{0.5i}, 0.99e^{-0.5i}, 0.95e^{0.8i}, 0.95e^{-0.8i}]$$

are presented. The left-side and right-side diagrams present the functions on 128 sample points by using uniform and nonuniform spacing, respectively.

It can be observed, that the nonuniform spacing produced by the inverse argument function results in an arrangement of points, which reconstruct (or interpolate) better the shape of the diagrams even in the use of coarse scales. The Nyquist diagram reconstructed by linear interpolation of the neighboring sample points show smaller distortion by using the nonuniform scale. On the Bode diagrams the sample points are arranged denser in the regions where the changes are more dramatic, e.g. in the locations of peaks, i.e. there the distortion of the reconstruction becomes smaller. This example suggests, that the nonuniform spacing of sample points generated according to knowledge upon the system poles can lead to better approximations of the system characteristics even in low number of samples. This topic will be elaborated in details in the next chapter.

The algorithm of approximately computing the coefficients of the representation of function F in the generalized orthogonal basis generated by assumed system poles a can be formulated as follows:

- Deriving a uniformly spaced scale on the interval $[-\pi, \pi]$ of M points on s , i.e. $\{s_m\}$.
- Transforming the uniform scale $\{s_m\}$ into the nonuniform $\{t_m\}$ scale by using the inverse argument function β_a^{-1} .
- Deriving the function values $f_k(s_m)$ $k = 0, 1, \dots, N - 1$ by using the measured or computed values of the function F and the computed values of the basis functions Φ_k on the unit circle on sample points $\{t_m\}$ for the M number of sample points.

- Performing N number of M -point FFTs resulting in $\{d_{kj}\}$ finite sequences of Fourier coefficients according to (2.4.11), where $k = 0, 1, \dots, N - 1$ and $j = 0, 1, \dots, M - 1$.
- Decimating the sequences of the coefficients by N , and ordering the elements of the N number of sequences into a single sequence of the GOB coefficients by applying $\ell = j/N$, $c_{\ell N+k} = d_{k,\ell N}$ for $k = 0, 1, \dots, N - 1$ and $\ell = 0, 1, \dots, M/N - 1$.

The above description can only be considered as an outline, the algorithm will in details be specified and characterized in the next chapter.

2.4.6 General orthogonal basis in the z -domain

In this section the definitions, theorems and characteristics of the generalized orthogonal bases belonging to the space \mathcal{H}^2 will be translated into the space \mathcal{H}_\perp^2 , i.e. the z -notation will be used. This will be useful in the applications, since in the technical field the z -notation is preferred. As it has been discussed in the Section 2.1, the connection between the q and z notation is essentially given by the transform $z = 1/q$. However, satisfying some types of requirements, e.g. the strictly properness of the rational functions, can result in some modifications, e.g. extra forward or backward shift, i.e. multiplication or division by z . Nevertheless, the parameters \mathbf{a} can directly be associated with the *poles* of both the system under consideration, and the associated Blaschke product, and basis functions.

First the definition of the Blaschke function and the Blaschke product is given:

Definition 2.4.3. For a finite set of poles $\mathbf{a} = \{a_k \in \mathbb{D} \mid k = 0, 1, \dots, N - 1\}$, the *finite Blaschke-product* of order n is defined as

$$B_{a|n}(z) \doteq \prod_{k=0}^{n-1} b_{a_k}(z),$$

and for an infinite set of $\mathbf{a} = \{a_k \in \mathbb{D} \mid k \in \mathbb{N}^*\}$, the *infinite Blaschke-product* is defined as

$$B_a(z) \doteq \prod_{k=0}^{\infty} b_{a_k}(z),$$

where b_{a_k} for $k = 0, 1, 2, \dots, N - 1$ or $k \in \mathbb{N}^*$ is the Blaschke-function

$$b_{a_k}(z) = e^{i\delta_k} \frac{1 - \overline{a_k} z}{z - a_k}$$

generated by the pole a_k , (δ_k is an arbitrary constant).

The generalized orthogonal basis is defined by the analogous form of Theorem 2.4.5 stated for \mathcal{H}^2 :

Theorem 2.4.6. *The system Φ_n for $n = \ell N + k$ ($N \in \mathbb{N}$ and $\ell \in \mathbb{N}^*$) defined on the set of poles $\mathbf{a} = \{a_k \in \mathbb{D} \mid k = 0, 1, \dots, N - 1\}$*

$$\Phi_0(z) \doteq \frac{\sqrt{1 - |a_0|^2}}{z - a_0}, \quad \Phi_n(z) \doteq \frac{\sqrt{1 - |a_k|^2}}{z - a_k} B_{a|k}(z) B_{a|N}^\ell(z), \quad (2.4.12)$$

where $B_{a|k}$ and $B_{a|N}$ are finite Blaschke-products of order k and N respectively, forms an orthonormal basis in the space $\mathcal{H}_\perp^2(\mathbb{D})$.

The elements of the basis can be seen in the Blaschke form on Table 2.3, and in rational form on Table 2.4. The normalization constants $d_{k\ell}$ in the latter one are defined as

$$d_{k\ell} = \sqrt{1 - |a_k|^2} e^{i\ell\Delta_N} \prod_{j=0}^{k-1} e^{i\delta_j} \quad \text{and} \quad \Delta_N = \prod_{j=0}^{N-1} e^{i\delta_j},$$

where δ_j for $j = 0, 1, \dots, N - 1$ are the phase constants belonging to the Blaschke-functions b_{a_j} respectively, and $\Delta_{\mathbf{a}}$ is the same belonging to the Blaschke-product $B_{\mathbf{a}}$.

The first N basis functions $\Phi_k(z)$ according to (2.4.12) can be considered as a Takenaka-Malmquist system in $\mathcal{H}_\perp^2(\mathbb{D})$, which spans the space of the strictly proper rational functions of variable z of maximal degree N with poles exactly \mathbf{a} , denoted as $\mathcal{B}_{\mathbf{a}}^N \mathcal{H}_\perp^2(\mathbb{D})$, a subspace of $\mathcal{H}_\perp^2(\mathbb{D})$.

The representation of function $F \in \mathcal{H}_\perp^2(\mathbb{D})$ can be expressed as

$$F(z) = \sum_{n=0}^{\infty} c_n \Phi_n(z),$$

ℓ	k	$\Phi_{\ell N+k}(z)$
0	0	$\frac{\sqrt{1- a_0 ^2}}{z-a_0}$
0	1	$\frac{\sqrt{1- a_1 ^2}}{z-a_0} b_{a_0}(z)$
0	2	$\frac{\sqrt{1- a_2 ^2}}{z-a_0} b_{a_0}(z)b_{a_1}(z)$
\vdots	\vdots	\vdots
0	$N-1$	$\frac{\sqrt{1- a_{N-1} ^2}}{z-a_{N-1}} b_{a_0}(z)b_{a_1}(z)\dots b_{a_{N-2}}(z)$
1	0	$\frac{\sqrt{1- a_0 ^2}}{z-a_0} b_{a_0}(z)b_{a_1}(z)\dots b_{a_{N-2}}(z)b_{a_{N-1}}(z)$
1	1	$\frac{\sqrt{1- a_1 ^2}}{z-a_1} b_{a_0}^2(z)b_{a_1}(z)\dots b_{a_{N-2}}(z)b_{a_{N-1}}(z)$
1	2	$\frac{\sqrt{1- a_2 ^2}}{z-a_2} b_{a_0}^2(z)b_{a_1}^2(z)b_{a_2}(z)\dots b_{a_{N-2}}(z)b_{a_{N-1}}(z)$
\vdots	\vdots	\vdots
1	$N-1$	$\frac{\sqrt{1- a_{N-1} ^2}}{z-a_{N-1}} b_{a_0}^2(z)b_{a_1}^2(z)\dots b_{a_{N-2}}^2(z)b_{a_{N-1}}(z)$
2	0	$\frac{\sqrt{1- a_0 ^2}}{z-a_0} b_{a_0}^2(z)b_{a_1}^2(z)\dots b_{a_{N-2}}^2(z)b_{a_{N-1}}^2(z)$
2	1	$\frac{\sqrt{1- a_1 ^2}}{z-a_1} b_{a_0}^3(z)b_{a_1}^2(z)\dots b_{a_{N-2}}^2(z)b_{a_{N-1}}^2(z)$
2	2	$\frac{\sqrt{1- a_2 ^2}}{z-a_2} b_{a_0}^3(z)b_{a_1}^3(z)b_{a_2}^2(z)\dots b_{a_{N-2}}^2(z)b_{a_{N-1}}^2(z)$
\vdots	\vdots	\vdots
2	$N-1$	$\frac{\sqrt{1- a_{N-1} ^2}}{z-a_{N-1}} b_{a_0}^3(z)b_{a_1}^3(z)\dots b_{a_{N-2}}^3(z)b_{a_{N-1}}^2(z)$
\vdots	\vdots	\vdots
ℓ	k	$\frac{\sqrt{1- a_k ^2}}{z-a_k} b_{a_0}^{\ell+1}(z)b_{a_1}^{\ell+1}(z)\dots b_{a_k}^{\ell+1}(z)b_{a_{k+1}}^\ell(z)\dots b_{a_{N-1}}^\ell(z)$
\vdots	\vdots	\vdots

Table 2.3: The elements of the generalized orthogonal basis (Blaschke form)

where the coefficients can be computed by the scalar product belonging to the space $\mathcal{H}_\perp^2(\mathbb{D})$

$$c_n = \langle F, \Phi_n \rangle.$$

The scalar product can be written in the form

$$\langle F, \Phi_n \rangle \doteq \frac{1}{2\pi} \int_{-\pi}^{\pi} F(e^{it}) \overline{\Phi_n(e^{it})} dt, \quad (2.4.13)$$

which is advantageous because, on the one hand, the values of a frequency function can be measured on the unit circle; on the other hand, the elements of the generalized orthogonal basis can be expressed on the unit circle by the *argument function*.

ℓ	k	$\Phi_{\ell N+k}(z)$
0	0	$d_{00} \frac{1}{z-a_0}$
0	1	$d_{10} \frac{1-\bar{a}_0 z}{(z-a_0)(z-a_1)}$
0	2	$d_{20} \frac{(1-\bar{a}_0 z)(1-\bar{a}_1 z)}{(z-a_0)(z-a_1)(z-a_2)}$
\vdots	\vdots	\vdots
0	$N-1$	$d_{(N-1)0} \frac{(1-\bar{a}_0 z)(1-\bar{a}_1 z)\dots(1-\bar{a}_{N-2} z)}{(z-a_0)(z-a_1)\dots(z-a_{N-2})(z-a_{N-1})}$
1	0	$d_{01} \frac{(1-\bar{a}_0 z)(1-\bar{a}_1 z)(1-\bar{a}_2 z)\dots(1-\bar{a}_{N-2} z)(1-\bar{a}_{N-1} z)}{(z-a_0)^2(z-a_1)(z-a_2)\dots(z-a_{N-2})(z-a_{N-1})}$
1	1	$d_{11} \frac{(1-\bar{a}_0 z)^2(1-\bar{a}_1 z)(1-\bar{a}_2 z)\dots(1-\bar{a}_{N-2} z)(1-\bar{a}_{N-1} z)}{(z-a_0)^2(z-a_1)^2(z-a_2)\dots(z-a_{N-2})(z-a_{N-1})}$
1	2	$d_{21} \frac{(1-\bar{a}_0 z)^2(1-\bar{a}_1 z)^2(1-\bar{a}_2 z)\dots(1-\bar{a}_{N-2} z)(1-\bar{a}_{N-1} z)}{(z-a_0)^2(z-a_1)^2(z-a_2)^2(z-a_3)\dots(z-a_{N-2})(z-a_{N-1})}$
\vdots	\vdots	\vdots
1	$N-1$	$d_{(N-1)1} \frac{(1-\bar{a}_0 z)^2(1-\bar{a}_1 z)^2(1-\bar{a}_2 z)^2\dots(1-\bar{a}_{N-2} z)^2(1-\bar{a}_{N-1} z)}{(z-a_0)^2(z-a_1)^2(z-a_2)^2\dots(z-a_{N-2})^2(z-a_{N-1})^2}$
2	0	$d_{02} \frac{(1-\bar{a}_0 z)^2(1-\bar{a}_1 z)^2(1-\bar{a}_2 z)^2\dots(1-\bar{a}_{N-2} z)^2(1-\bar{a}_{N-1} z)^2}{(z-a_0)^3(z-a_1)^2(z-a_2)^2\dots(z-a_{N-2})^2(z-a_{N-1})^2}$
2	1	$d_{12} \frac{(1-\bar{a}_0 z)^3(1-\bar{a}_1 z)^2(1-\bar{a}_2 z)^2\dots(1-\bar{a}_{N-2} z)^2(1-\bar{a}_{N-1} z)^2}{(z-a_0)^3(z-a_1)^3(z-a_2)^2\dots(z-a_{N-2})^2(z-a_{N-1})^2}$
2	2	$d_{22} \frac{(1-\bar{a}_0 z)^3(1-\bar{a}_1 z)^3(1-\bar{a}_2 z)^2\dots(1-\bar{a}_{N-2} z)^2(1-\bar{a}_{N-1} z)^2}{(z-a_0)^3(z-a_1)^3(z-a_2)^3(z-a_3)^2\dots(z-a_{N-2})^2(z-a_{N-1})^2}$
\vdots	\vdots	\vdots
2	$N-1$	$d_{(N-1)2} \frac{(1-\bar{a}_0 z)^3(1-\bar{a}_1 z)^3(1-\bar{a}_2 z)^3\dots(1-\bar{a}_{N-2} z)^3(1-\bar{a}_{N-1} z)^2}{(z-a_0)^3(z-a_1)^3(z-a_2)^3\dots(z-a_{N-2})^3(z-a_{N-1})^3}$
\vdots	\vdots	\vdots
ℓ	k	$d_{k\ell} \frac{(1-\bar{a}_0 z)^{\ell+1}(1-\bar{a}_1 z)^{\ell+1}\dots(1-\bar{a}_{k-1} z)^{\ell+1}(1-\bar{a}_k z)^\ell\dots(1-\bar{a}_{N-1} z)^\ell}{(z-a_0)^{\ell+1}(z-a_1)^{\ell+1}\dots(z-a_k)^{\ell+1}(z-a_{k+1})^\ell\dots(z-a_{N-1})^\ell}$
\vdots	\vdots	\vdots

Table 2.4: The elements of the generalized orthogonal basis

The argument function associated with the Blaschke-function $b_a(z) \in \mathcal{H}_\perp^2$ belonging to a single pole $a \in \mathbb{D}$ will be defined in such a way, that formally be identical to the \mathcal{H}^2 form. This can be obtained by defining the argument function $\beta_a(t)$ with the formula

$$b_a(e^{it}) = e^{-i\beta_a(t)}. \quad (2.4.14)$$

Hence the argument function remains to be a strictly increasing, continuously differentiable, invertible function $\beta : [-\pi, \pi] \mapsto [-\pi, \pi]$.

Let the pole a be given in the form $a = re^{i\varphi}$ and the Blaschke-function be expressed on

the unit circle in the form

$$\begin{aligned} b_a(e^{it}) &= e^{i\delta} \frac{1 - re^{i(t-\varphi)}}{e^{it} - re^{i\varphi}} = e^{i(\delta-\varphi)} \frac{e^{i\varphi} - re^{it}}{e^{it} - re^{i\varphi}} = \\ &= e^{i(\delta-\varphi)} \frac{(1-r) \cos\left(\frac{t-\varphi}{2}\right) - i(1+r) \sin\left(\frac{t-\varphi}{2}\right)}{1 - 2r \cos(t-\varphi) + r^2} \end{aligned}$$

with similar consideration as it has been done in Section 2.3.2. The argument of the resulted expression can be obtained as

$$\arg [b_a(e^{it})] = \delta - \varphi - 2 \arctan\left(\frac{1-r}{1+r} \tan \frac{t-\varphi}{2}\right),$$

hence the argument function belonging to the pole $a = re^{i\varphi}$ can be expressed as

$$\beta_a(t) = \varphi - \delta + 2 \arctan\left(\frac{1-r}{1+r} \tan \frac{t-\varphi}{2}\right).$$

Since δ is an arbitrary constant, the argument function of the Blaschke-function belonging to $\mathcal{H}_\perp^2(\mathbb{D})$ has the same form as that belonging to $\mathcal{H}^2(\mathbb{D})$. It is usual to select the constant δ such, that $\beta_a(t)$ map the interval $[-\pi, \pi]$ exactly to oneself, i.e. to make

$$b_a(e^{-i\pi}) = -1. \tag{2.4.15}$$

Since $e^{-i\pi} = -1$,

$$b_a(e^{-i\pi}) = -e^{i\delta} \frac{1 + re^{-i\varphi}}{1 + re^{i\varphi}} = e^{i(\delta-\pi)} \frac{1 + r \cos \varphi - ir \sin \varphi}{1 + r \cos \varphi + ir \sin \varphi},$$

and

$$\arg [b_a(e^{-i\pi})] = \delta - \pi - 2 \arctan\left(\frac{r \sin \varphi}{1 + r \cos \varphi}\right),$$

hence δ should be selected as

$$\delta = 2 \arctan\left(\frac{r \sin \varphi}{1 + r \cos \varphi}\right)$$

to satisfy condition (2.4.15).

The argument function $\beta_{\mathbf{a}}(t)$ belonging to the N -element set of poles \mathbf{a} can be expressed by the arithmetical mean of the β_{a_k} functions belonging to the individual poles ($k = 0, 1, \dots, N - 1$)

$$\beta_{\mathbf{a}}(t) \doteq \frac{\beta_{a_0}(t) + \beta_{a_1}(t) + \dots + \beta_{a_{N-1}}(t)}{N},$$

hence the Blaschke-product can be expressed on the unit circle

$$B_{\mathbf{a}}(e^{it}) = e^{-iN\beta_{\mathbf{a}}(t)},$$

and the elements of the generalized orthogonal basis can be expressed as

$$\Phi_{N\ell+k}(e^{it}) = \Phi_k(e^{it}) e^{-iN\ell\beta_{\mathbf{a}}(t)}.$$

Hence the coefficient of index $n = N\ell + k$ of the GOB representation belonging to function $F \in \mathcal{H}_{\perp}^2(\mathbb{D})$ will be given as

$$c_n \doteq \langle F, \Phi_{N\ell+k} \rangle = \frac{1}{2\pi} \int_{-\pi}^{\pi} F(e^{it}) \overline{\Phi_k(e^{it})} e^{iN\ell\beta_{\mathbf{a}}(t)} dt. \quad (2.4.16)$$

This formula corresponds to the formula (2.4.8) belonging to the \mathcal{H}^2 case, a significant difference is, that (2.4.16) describes an inverse Fourier-transform instead of Fourier-transform, that is given by (2.4.8).

Similarly as it has been presented in Section 2.4.5, the Fourier-integral (2.4.16) can approximately be evaluated in discretized form, by using a nonuniform scale on parameter t obtained by using the inverse argument transform belonging to the pole-set \mathbf{a} assumed. The evaluation can be performed by using inverse Fast Fourier Transform (iFFT), hence an efficient method is given to approximately compute the coefficients of a GOB representation belonging to a function $F(z) \in \mathcal{H}_{\perp}^2$. The exact algorithm will in details be discussed in the next chapter.

Chapter 3

Realizing the GOB representation

In this chapter the problems of realizing signal representations in generalized orthogonal bases are discussed. The algorithm established theoretically in Chapter 2 is elaborated until realization. Furthermore the characteristics of the argument transform are analyzed, focusing on the interpolation/approximation properties if finite number of samples are used. These properties make these methods suitable to describe systems in general sense, beyond the GOB representations; a measurement scheme will be proposed to support these efforts.

3.1 Computing the GOB coefficients in z -domain

In Chapter 2 an algorithm of approximately computing the coefficients of a GOB representation belonging to a function $F(q) \in \mathcal{H}^2$ and $F(z) \in \mathcal{H}_1^2$ has — at least theoretically — been established in Section 2.4.5 and in 2.4.6, respectively. The algorithms realize the evaluation of the scalar products defining the coefficients by applying a discretization based upon a non-uniform frequency scale obtained by inverse argument transform, and the FFT and inverse FFT algorithms, respectively, for computing. The practically realizable form of the algorithm will be presented in this chapter. The algorithm has been realized both in q , and z forms, however the z -r will here be described in details, because that form can be realized on physical data, hence its practical significance is superior. The q -form is rather

significant in the theory, and can mainly be used in numeric testing the algorithms built upon GOB representations.

Let us start from the expression (2.4.16) of the scalar product with the substitution $t = \beta_{\mathbf{a}}^{-1}(s)$:

$$\langle F, \Phi_{N\ell+k} \rangle = \frac{1}{2\pi} \int_{-\pi}^{\pi} F(e^{i\beta_{\mathbf{a}}^{-1}(s)}) \overline{\phi_k(e^{i\beta_{\mathbf{a}}^{-1}(s)})} e^{iN\ell s} \beta'_{\mathbf{a}}(s) ds.$$

The derivative of the inverse argument function occurs as a consequence of transforming the integration variable, as it has been shown in Section 2.4.5. By introducing the function

$$f_k(s) \doteq F(e^{i\beta_{\mathbf{a}}^{-1}(s)}) \overline{\phi_k(e^{i\beta_{\mathbf{a}}^{-1}(s)})} \beta'_{\mathbf{a}}(s) \quad (k = 0, 1, \dots, N-1),$$

it can be expressed in the form of a special — N -times ”dilated” — Fourier integral:

$$\langle F, \Phi_{N\ell+k} \rangle = \frac{1}{2\pi} \int_{-\pi}^{\pi} f_k(s) e^{iN\ell s} ds.$$

The Fourier-integral can be computed approximately by using a discrete scale by dividing the interval $[-\pi, \pi]$ into M equal parts (let M be even), i.e.

$$\Delta s = \frac{2\pi}{M} \quad s_m = -\pi + m\Delta s \quad (m = 0, 1, \dots, M-1).$$

The integral can be approximated with the sum (let be $j = N\ell$)

$$\begin{aligned} \hat{c}_{j+k} &= \frac{\Delta s}{2\pi} \sum_{m=0}^{M-1} f_k(s_m) e^{ij(-\pi+m\Delta s)} = \\ &= \frac{1}{M} \sum_{m=0}^{M-1} f_k(s_m) e^{i2\pi \frac{j(m-M/2)}{M}} = \left(\frac{1}{M} \sum_{m=0}^{M-1} f_k(s_m) e^{i2\pi \frac{jm}{M}} \right) e^{-i2\pi \frac{j(M/2)}{M}}. \end{aligned} \quad (3.1.1)$$

The expression in the parenthesis is a standard discrete inverse Fourier-transform, which can effectively be evaluated by the Fast Fourier Transform (FFT) algorithm (more exactly the inverse Fast Fourier Transform (FFT) — iFFT — algorithm, that does not essentially differ from the FFT). The multiplicative term

$$e^{-i2\pi \frac{j(M/2)}{M}}$$

applied on the Fourier-transform corresponds to a translation of $M/2$ points on the discrete form of the function to be transformed, and π translation on the continuous scale. Hence the algorithm to obtain approximately the coefficients is given by

$$\hat{c}_{j+k} = \frac{1}{M} \sum_{m=0}^{N-1} f_k(s_{m+N/2}) e^{i2\pi \frac{jm}{M}} \quad (3.1.2)$$

To prove it let $m' = m + M/2$ be substituted

$$\hat{c}_{j+k} = \frac{1}{M} \sum_{m'=\frac{M}{2}}^{\frac{3M}{2}-1} f_k(s_{m'}) e^{i2\pi \frac{j(m'-M/2)}{M}}. \quad (3.1.3)$$

The sum through the whole period of any periodic sequence is invariant to any translation, i.e. for any $\{a_m\}$ where $a_{m+M} = a_m$, and any $|p| \leq M$ integer

$$\sum_{m=p}^{p+M-1} a_m = \sum_{m=0}^{M-1} a_m$$

The proof is simple: since the translation-invariance by the period M is trivial,

$$\sum_{m=0}^{M-1} a_m = \sum_{m=0}^{p-1} a_m + \sum_{m=p}^{M-1} a_m = \sum_{m=p}^{M-1} a_m + \sum_{m=M}^{p+M-1} a_m = \sum_{m=p}^{p+M-1} a_m.$$

According to the translation invariance (3.1.3) can be write in the form

$$\hat{c}_{j+k} = \frac{1}{M} \sum_{m=0}^{M-1} f_k(s_m) e^{i2\pi \frac{j(m-M/2)}{M}},$$

that is identical to (3.1.1), which proves the formula (3.1.2).

Since f_k functions are periodic by 2π , the translation of π is equivalent to swapping the positive and negative halves of the function. Swapping is a frequently used action in the FFT analysis, usually is used a posteriori to shape the spectrum in the customary layout with zero frequency on the centrum; here swapping can be used before the transform is performed.

The algorithm represented by (3.1.2) needs the values of the function f_k by using a displacement of π on the variable s ($M/2$ on the indices), that, because of its periodicity

— is equivalent with swapping the left and right half of the function in the interval $[-\pi, \pi]$ before executing the transform (swapping is a frequently used action in the FFT techniques).

The transform (3.1.2) results in N number of redundant sequences $\hat{c}_j^{(k)}$ ($k = 0, 1, \dots, N-1$) — each belonging to a particular ϕ_k function — N -times denser than the sequence of the coefficients. Hence the coefficients can be obtained by decimating the sequences by N :

$$\begin{array}{llll} \hat{c}_0 = \hat{c}_0^{(0)} & \hat{c}_1 = \hat{c}_0^{(1)} & \dots & \hat{c}_{N-1} = \hat{c}_0^{(N-1)} \\ \hat{c}_N = \hat{c}_N^{(0)} & \hat{c}_{N+1} = \hat{c}_N^{(1)} & \dots & \hat{c}_{2N-1} = \hat{c}_N^{(N-1)} \\ \hat{c}_{2N} = \hat{c}_{2N}^{(0)} & \hat{c}_{2N+1} = \hat{c}_{2N}^{(1)} & \dots & \hat{c}_{3N-1} = \hat{c}_{2N}^{(N-1)} \\ \vdots & \vdots & & \vdots \\ \hat{c}_{\ell N} = \hat{c}_{\ell N}^{(0)} & \hat{c}_{\ell N+1} = \hat{c}_{\ell N}^{(1)} & \dots & \hat{c}_{(\ell+1)N-1} = \hat{c}_{\ell N}^{(N-1)} \\ \vdots & \vdots & & \vdots \end{array}$$

The values of the functions f_k ($k = 0, 1, \dots, N-1$) applied in the transform (3.1.2) can be computed on the basis of measurement values belonging to the function F to be represented, as well as sample values of the elements of the generalized orthonormal basis. The sample points are determined by the inverse of the argument function $\beta_{\mathbf{a}}$ belonging to the basis:

$$f_k(s_j) = F(e^{i\beta_{\mathbf{a}}^{-1}(s_j)}) \overline{\phi_k(e^{i\beta_{\mathbf{a}}^{-1}(s_j)})} \beta'_{\mathbf{a}}(s_j) \quad (k = 0, 1, \dots, N-1),$$

i.e. the sample points can be determined by the transform

$$t_j = \beta_{\mathbf{a}}^{-1}(s_j) \quad (j = 0, 1, \dots, M-1), \quad (3.1.4)$$

where $\{s_j\}$ is a uniformly spaced division of the interval $[-\pi, \pi]$. Since The inverse argument function is nonlinear, the resulting $\{t_j\}$ scale is non-uniformly spaced division of the same interval. The transform (3.1.4) is referred as *inverse argument-transform* belonging to the generalized orthonormal basis generated upon the poles \mathbf{a} .

The sample values of the basis elements $\phi_k(e^{it_j})$ can be obtained by computations, hence they can be evaluated in any point within the interval $[-\pi, \pi]$. However, the sample points

of the function F can be obtained by observations — physically realizable measurements or computations — performed on the system to be analyzed. Only the interval $[0, \pi]$ has physical meaning: the parameter t can be considered as *normalized circular frequency*, and the interval $[0, \pi]$ is related to the frequency interval $[0, f_N]$, where f_N is the Nyquist-frequency connected to the applied time-domain sampling rule. The mapping between the sample points t_j and f_j is given by

$$t_j = \frac{f_j}{f_N} \pi \quad \text{i.e.} \quad f_j = \frac{f_N}{\pi} t_j.$$

The points of F corresponding to the negative half of the interval can be generated by the rule

$$F(e^{-it}) = \overline{F(e^{it})} \quad (3.1.5)$$

that is valid for all the existing or physically realizable real systems, that possess only real poles or conjugated complex pole-pairs.

Hence the sample points of function F that are suitable to use in the GOB representation can be obtained by applying the procedure as follow:

1. Determining a non-uniformly spaced $\{t_j\}_{j=0}^{M-1}$ scale in the interval $[-\pi, \pi]$ by using the inverse argument transform belonging to the GOB starting from a uniformly spaced scale $\{s_j\}_{j=0}^{M-1}$ in the same interval.
2. Measuring or computing the values of the frequency function in frequencies corresponding to the parameter values $t_j \geq 0$ ($j = 0, 1, \dots, M/2 - 1$).
3. Completing the function by adding its negative half by applying

$$F(e^{-it-j}) = \overline{F(e^{it_j})} \quad (j = 1, 2, \dots, M/2 - 1)$$

according to the rule (3.1.5).

The values of the frequency function can be generated directly as transfer functions measurements, or by using spectral estimation methods on the basis of time-domain measurements.

The algorithm described above has been realized in the *MATLAB*[®] environment both in the z and q forms (procedures `gobcoefz` and `gobcoefq`, applying the sub-procedures `gobbfnz` and `gobbfq` to compute the basis functions, respectively). Furthermore, reconstruction procedures has also been realized for testing purposes, i.e. to compare the function reconstructed from the representation to the original one (procedures `gobrecz` and `gobrecq`).

A crucial point in the algorithm of computing the coefficients is the derivation of the inverse argument function on a discrete scale. Since the inverse argument function cannot explicitly be expressed for the case of multiple poles, a numeric approximation can be advantageous. Since the argument function is a strictly increasing function, successive approximation methods well converge. The algorithm for approximating the value t that corresponds to the point s according to $t = \beta_a^{-1}(s)$ can be performed by repeating the following iteration ($\nu = 0, 1, 2, \dots$):

Initialization: Let $[t_\ell^{(0)}, t_u^{(0)}] \subset [-\pi, \pi]$ be an interval selected such that with the values

$$s_\ell^{(0)} = \beta_a(t_\ell^{(0)}) \text{ and } s_u^{(0)} = \beta_a(t_u^{(0)}) \text{ the value } s \text{ } s_\ell^{(0)} \leq s < s_u^{(0)}.$$

The ν -th step: Let the interval $[t_\ell^{(\nu)}, t_u^{(\nu)}]$ be halved by assigning the point $t_m^{(\nu)}$ as

$$t_m^{(\nu)} = \frac{t_u^{(\nu)} - t_\ell^{(\nu)}}{2},$$

and let the corresponding s -value be computed by the argument function:

$$s_m^{(\nu)} = \beta_a(t_m^{(\nu)}).$$

If the point s falls in the interval $[s_\ell^{(\nu)}, s_m^{(\nu)}]$, this will be the new interval to continue

the iteration, otherwise this interval will be the $[s_m^{(\nu)}, s_u^{(\nu)}]$, i.e.

$$\begin{aligned} \text{if } s_\ell^{(\nu)} \leq s < s_m^{(\nu)} \quad \text{then } t_\ell^{(\nu+1)} &= t_\ell^{(\nu)} \quad t_u^{(\nu+1)} = t_m^{(\nu)}, \\ \text{if } s_m^{(\nu)} < s \leq s_u^{(\nu)} \quad \text{then } t_\ell^{(\nu+1)} &= t_m^{(\nu)} \quad t_u^{(\nu+1)} = t_u^{(\nu)}. \end{aligned}$$

Termination: The iteration can be stopped if $|s - s_m^{(\nu)}| < \varepsilon$, where $\varepsilon > 0$ is a predefined threshold value.

Since $\beta_a(t)$ is strictly increasing function in the interval $[-\pi, \pi]$, finding a unique solution is guaranteed.

The generation of the complete scale on the interval $[-\pi, \pi]$ of variable t can be performed by repeating the above iteration for every point of the uniformly spaced s_k scale. The iterations are advantageous to start from a system of subintervals of $[-\pi, \pi]$ on the variable t , which correspond to subintervals on the domain s containing exactly one point of the scale $\{s_k\}$. This can be produced from an arbitrary system of disjoint subintervals covering completely the interval $[-\pi, \pi]$ (e.g. generated by an uniformly spaced point-set) by successively dividing the subintervals containing more than one point of s_k on domain s until only one point remain within them.

In the procedures `gobcoefz` and `gobcoefq` the above algorithm has been implemented. In *MATLAB*[®] the accuracy 10^{-12} on the iteration can simply be achieved in acceptable run-time conditions.

3.2 Computing the GOB coefficients: examples

Now, some examples will be presented to illustrate the power of the GOB representation algorithm. A simulated collision signal is considered as it can be measured by an accelerometer or microphone operating in the audible frequency band of the sounds. These type of signals can be measured in the Loose Part Monitoring Systems (LPMS) that are applied in

pressurized water nuclear reactors with the purpose to detect unwanted (loosen by cavity or fatigue of materials, or unintentionally inserted) parts circulating in the pipes with the water, and colliding on the walls.

Example 3.2.1. A continuous-time signal is considered for $t \in \mathbb{R}^*$ as follows:

$$x(t) = Ae^{-\delta t} \sin(2\pi f_0 t)$$

where $\delta, f_0 \in \mathbb{R} > 0$ constants. The signal is discretized with sample frequency $f_s > f_0$ at least twice, i.e.

$$x_k = x(k\Delta t) \quad (k = 0, 1, 2, \dots) \quad \Delta t = \frac{1}{f_s}$$

Hence the signal is represented by the sequence

$$x_k = Ae^{-\delta k\Delta t} \sin(2\pi f_0 k\Delta t).$$

An example with parameters

$$f_s = 20kHz \quad N = 4096 \quad A = 1 \quad f_0 = 440Hz \quad \delta = 20$$

can be seen on Figure 3.1.

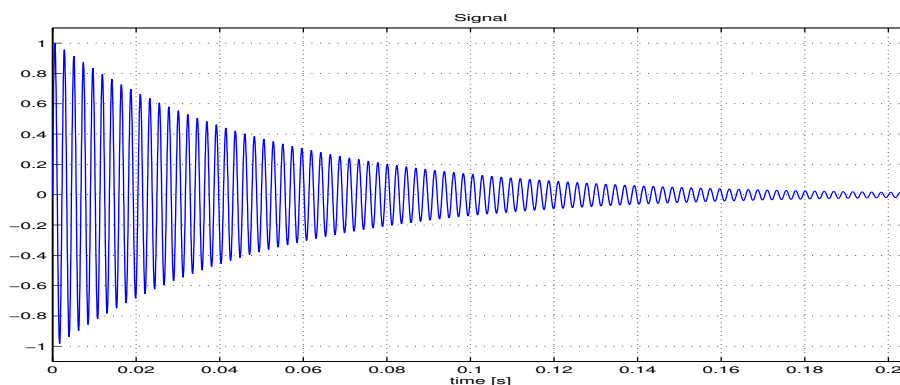


Figure 3.1: Example 3.2.1. — the pure signal

The z -transform of the sequence can be expressed as follow:

$$X(z) \doteq \sum_{k=0}^{\infty} x_k z^{-k} = \frac{Ae^{-\delta\Delta t} \sin(2\pi f_0\Delta t)z}{z^2 - 2e^{-\delta\Delta t} \cos(2\pi f_0\Delta t)z + e^{-2\delta\Delta t}}.$$

By introducing $a = e^{-\delta\Delta t}e^{i\omega_0\Delta t}$, where $\omega_0 = 2\pi f_0$ is the circular frequency, the z -transform gets the form

$$X(z) = A\Im(a) \frac{z}{(z-a)(z-\bar{a})},$$

that is, (a, \bar{a}) are the poles (a conjugated complex pair) associated with signal. The absolute value of the poles depends on the decay rate or damp factor δ , and their angle on the frequency of the periodic component f_0 , i.e.

$$|a| = e^{-\delta\Delta t} \quad \text{and} \quad \arg(a) = 2\pi f_0\Delta t = \omega_0\Delta t$$

respectively.

The poles in the given example are $0.98947 \pm 0.13765i$, the absolute value is 0.99900, the poles reside quite near to the unit circle, i.e. the associated system is lightly damped.

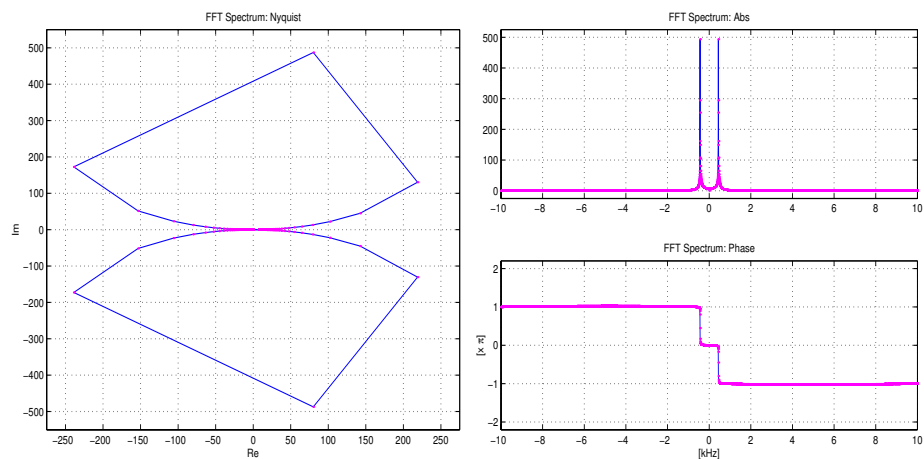


Figure 3.2: Example 3.2.1. — classical discrete Fourier-transform

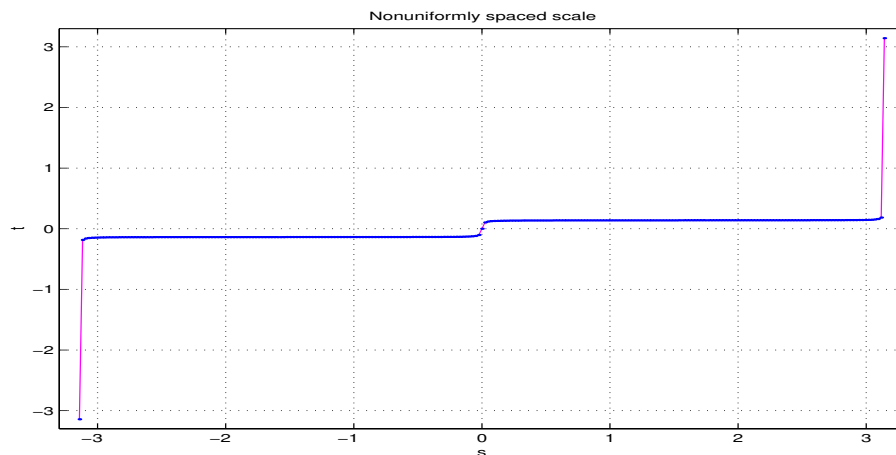


Figure 3.3: Example 3.2.1. — The inverse argument function (256 sample points)

The results of classical Fourier-analysis — based upon uniform spacing on sample points on the frequency domain — can be seen on Figure 3.2, in the form of Nyquist as well as linearly scaled absolute value - phase diagrams, with the sample points indicated by circles. It can be seen, that in spite of the dense sampling (4096 points per period) the shape reconstructed on the basis of the sample points is quite distorted in significant parts of the diagrams (see Nyquist diagram), and the sampling is unnecessarily dense in regions, where no any interesting is happens on the spectrum (see the absolute values or phase diagram).

As a first step to apply a generalized orthogonal basis, let a non-uniformly spaced frequency scale be derived on the basis of the inverse argument function, based upon the poles (a, \bar{a}) , by using the procedure `argifnq` written in *MATLAB*[®]. A scale consisting 256 points is presented on Figure 3.3. The sample-points has been marked with circles drawn on the top of the FFT spectrum for comparison on Figure 3.4. The function values on the selected sample points has been computed by using a nonuniform discrete Fourier-transform scheme based upon a Horner-type polynomial evaluation algorithm. This algorithm is far slower than fast Fourier-transform (FFT), however it is applied to significantly smaller

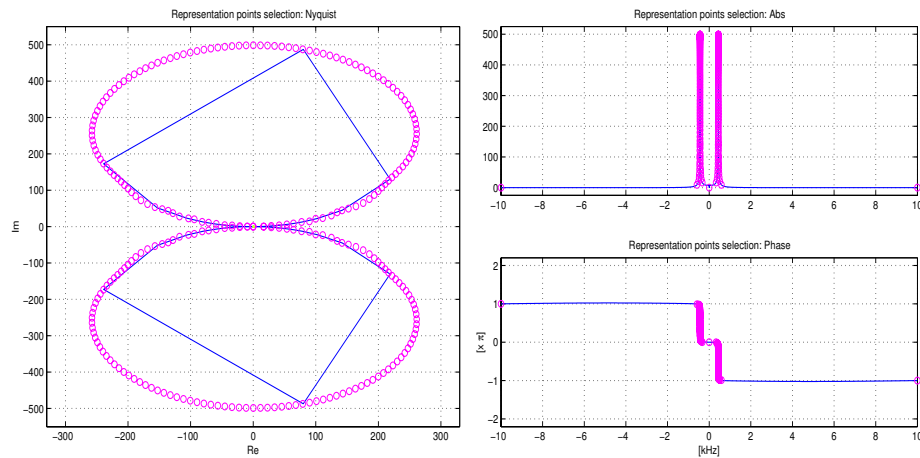


Figure 3.4: Example 3.2.1. — Sample point selection by non-uniform scale

number of points, in the given case 256 in contrast to the number of data points 4096. The faster way, to apply FFT to the whole set of data, and then select the values falling the nearest to the non-uniformly spaced frequencies cannot be used here: the resolution of the 4096-point FFT is $1.5 \cdot 10^{-3}$, and the required resolution in the densest part of the nonuniform scale is $2.4546 \cdot 10^{-5}$ relative to the interval $[-\pi, \pi]$.

The representation coefficients has been computed with the *MATLAB*[®] procedure `gobcoefz`. The coefficients are presented in graphical form on Figure 3.5: the real and imaginary parts has been given in Nyquist form as well as on separated diagrams. The point-order on the Nyquist-diagram is coded by colors: from the starting point the order is red, green, cyan, etc. It can be observed, that the number of the significant coefficients is 2, i.e. it is exactly equal to the number of the poles.

On Figure 3.6 the function reconstructed by using 2 coefficients (red line) can be compared to the functions obtained by linearly interpolating the uniformly spaced (blue line) and the non-uniformly spaced (green line) sample values. The coefficient values compared to the theoretical ones can be seen on the following table. The theoretical values has been

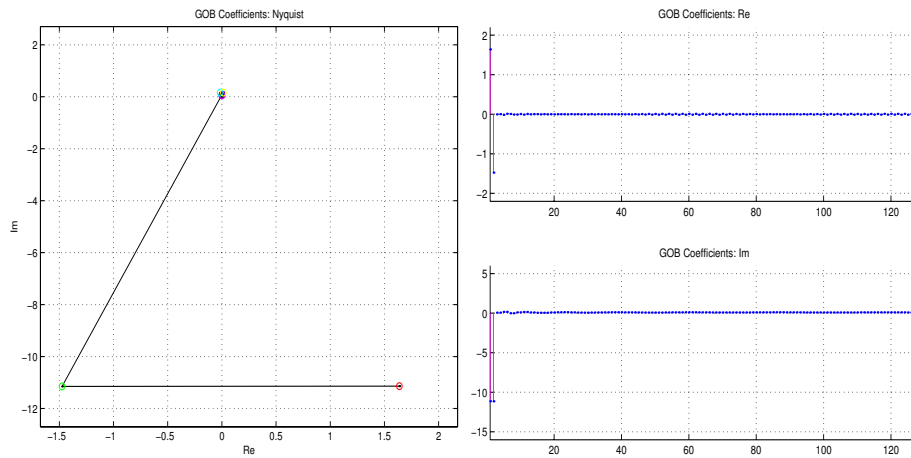


Figure 3.5: Example 3.2.1. — the GOB coefficients

computed by using the theoretical Fourier-transform formula of the signal, otherwise the same algorithm has been used.

	c_0	c_1
<i>Theoretical</i>	$1.6192 - 11.057i$	$-1.4579 - 11.068i$
<i>Computed</i>	$1.6375 - 11.137i$	$-1.4749 - 11.148i$

As it can be observed: there is a small error on the coefficients originating from the estimation of the discrete Fourier-transform.

Example 3.2.2. *The Example 3.2.1 is modified such that noise is added to the collision signal. The signal-to-noise ratio (SNR) is equal to 10, the additive noise is normally distributed with zero mean. The time-function can be seen on Figure 3.7.*

The coefficients and the result of the reconstruction can be seen on Figure 3.8. It can be observed, that there is a small noise on the coefficients, however this level of the signal-to-noise ratio do not significantly affect the dominance of the first two coefficients. The reconstruction can be performed by using the dominant coefficients, in the example all

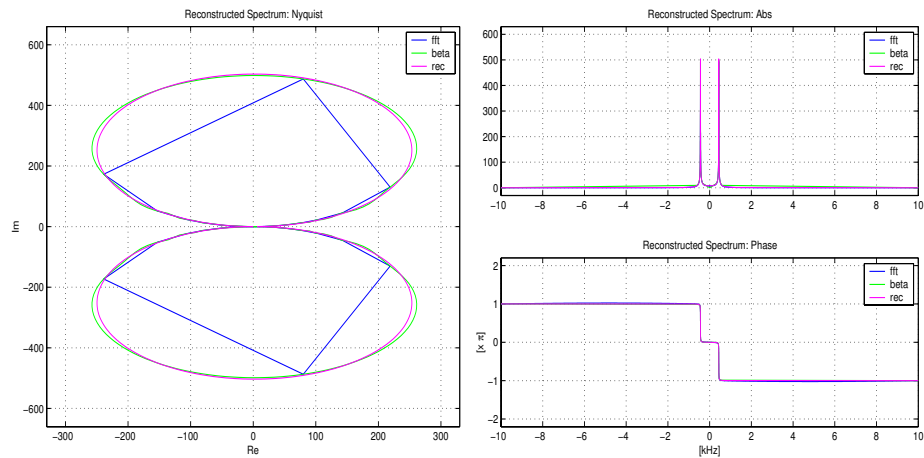


Figure 3.6: Example 3.2.1. — reconstruction in GOB by using 2 coefficients

the computed coefficients has been used.

Example 3.2.3. *The Example 3.2.1 is modified such that the damping factor δ applied for deriving the reference poles selected to be the half of the original one. This means, that the assumed poles used to build the orthogonal basis are less damped as the real ones.*

The coefficients and the result of the reconstruction can be seen on Figure 3.8. The coefficients show an exponentially decreasing character, however the decay is rather fast. More than two dominant coefficients can be found, the reconstruction cannot be performed by using only the first two ones, in the example all the computed coefficients has been used.

Example 3.2.4. *The Example 3.2.1 is modified such that the frequency f_0 applied for deriving the reference poles selected to be 5% greater than in the original case. This means, that the assumed poles used to build the orthogonal basis are radially displaced on the complex plane by keeping their distance from the origin.*

Figure 3.10 presents the results. A great number of coefficients is required to reconstruct the function, i.e. no dominant ones that can be selected. Hence it can be stated, that the system to be analyzed significantly differs from that a priori assumed.

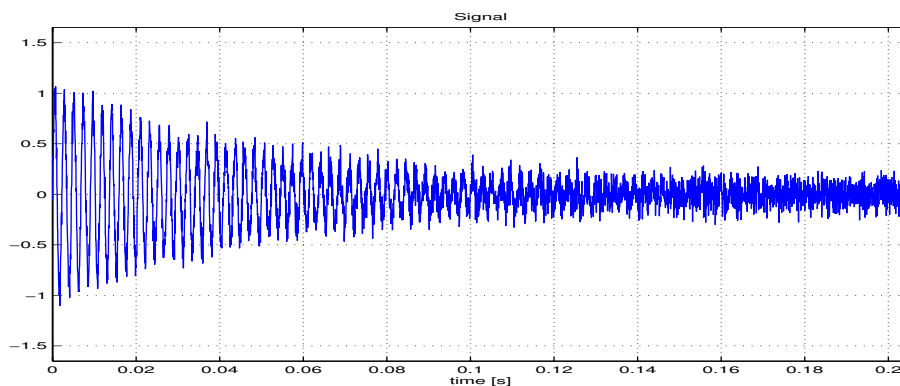


Figure 3.7: Example 3.2.2. — signal with noise

Finally an example based upon real measured data will be presented:

Example 3.2.5. *The signal of a hammer beat on a stainless steel piece of pipe with diameter 1" has been measured by using a broad band Brüel&Kjaer accelerometer. The signal was sampled with frequency 41 kHz after applying an anti-aliasing filter with corner frequency set to 18 kHz. The time-function of the signal can be seen on Figure 3.11, and its auto-spectral density function computed by using FFT algorithm can be seen on Figure 3.12. One dominant peak can be observed on the spectrum, hence one reference pole will be selected. By estimation the frequency and damp parameters have been given as $f_0 = 6546$ Hz and $\delta = 200$ 1/s.*

The GOB representation verified the assumption concerning the dominant pole, since two dominant coefficients has found. However, the remaining coefficients are not fully eligible, hence the reconstruction of the function by two coefficients is not accurate. The GOB representation lets the spectral peaks other than found in the neighborhood of the f_0 frequency out of consideration, since no sample values arranged outside this region. The width of the "sampled" region depends upon δ , i.e. the distance of the pole from the unit circle. Reference poles residing very close to the unit circle results in quite narrow sampling

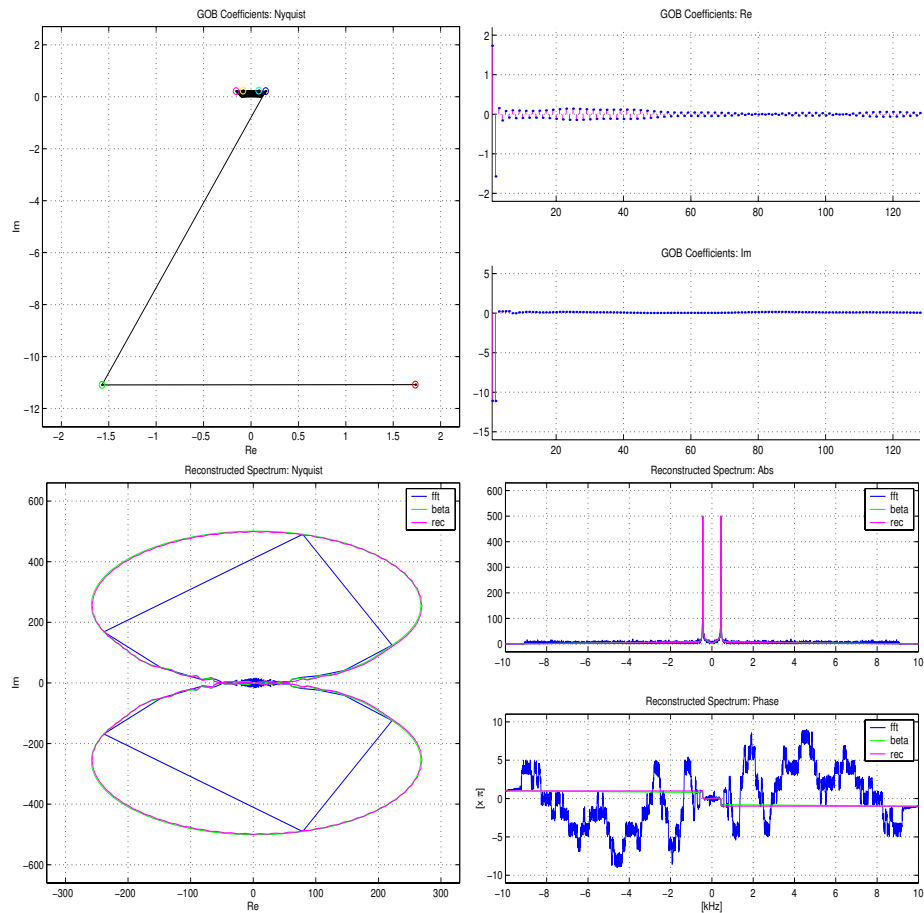


Figure 3.8: Example 3.2.2. — adding noise

region.

3.3 Obtaining frequency domain data

Obtaining frequency domain data, due to the digital signal processing methods that have become definitive in our times, usually means applying the Fast Fourier Transform (FFT) algorithm on uniformly sampled time domain data. The FFT algorithm is an extremely effective algorithm, using $N \log N$ computational steps, if N is the number of data points.

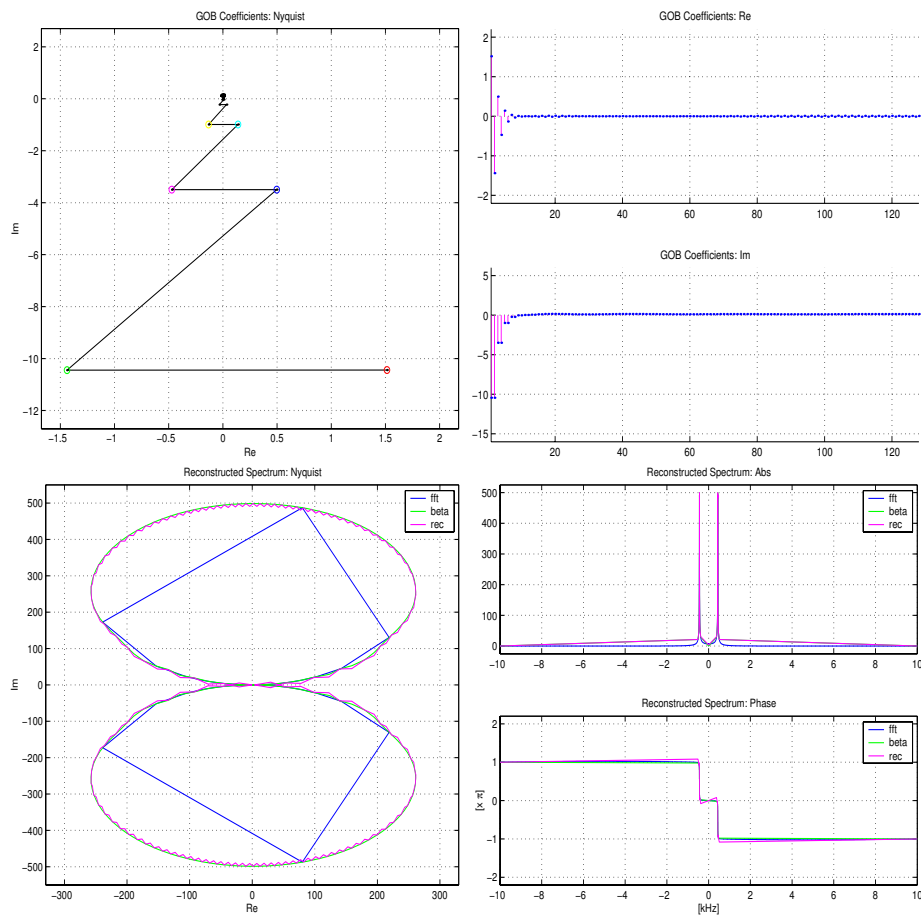


Figure 3.9: Example 3.2.3. — perturbation on damping

The FFT algorithms assume uniformly spaced data also on the frequency domain, which has not been considered as drawback until the classical spectral analysis methods are used. However GOB representation algorithms require non-uniformly spaced frequency domain data, hence this feature of the FFT becomes really a drawback. This section is devoted to find other alternatives for obtaining frequency domain data either from time domain data or directly from frequency domain measurements. The alternatives that have emerged are as follow:

- Using FFT to transform time domain data, and selecting the demanded frequencies

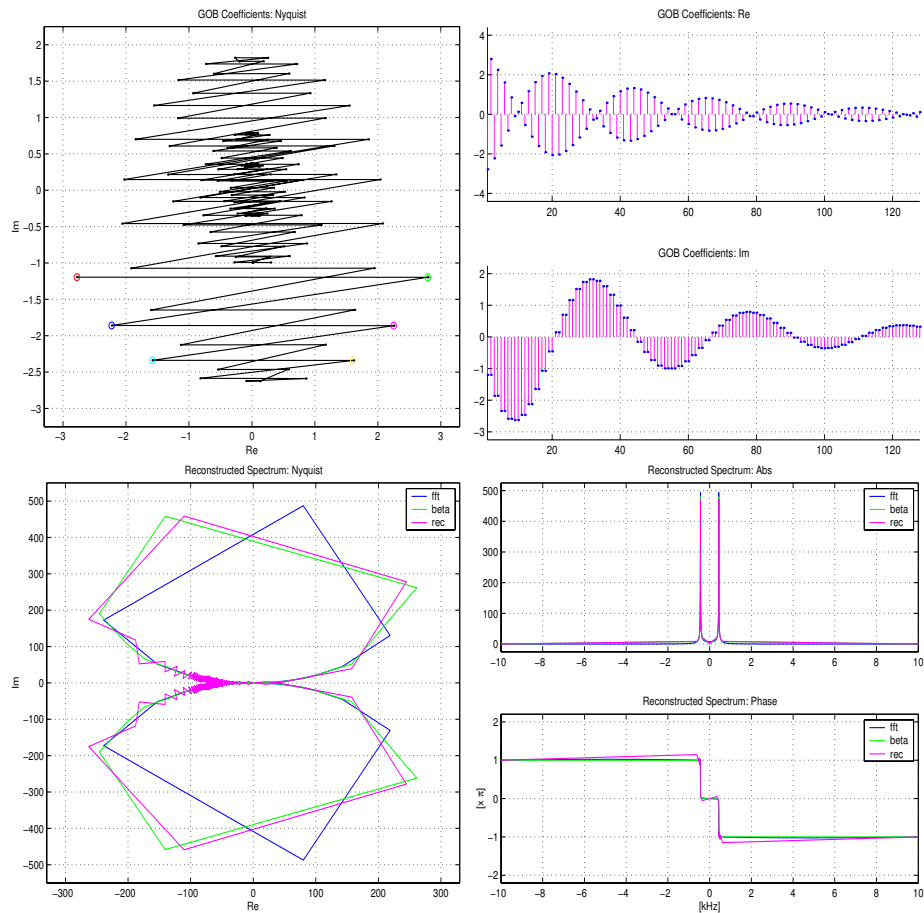


Figure 3.10: Example 3.2.4. — perturbation on frequency

from the uniformly spaced frequency domain data.

- Using discrete Fourier transform (DFT) on non-uniformly spaced frequency values.
- Direct frequency domain transfer function measurement.

The first two approaches can be applied on signals, however the third one can be realized only on systems, that should be excited with external, arbitrary signals, which is not tolerable by all of them.

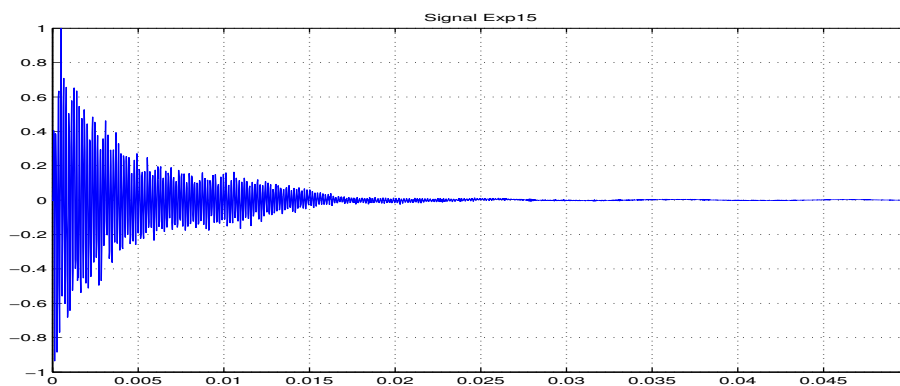


Figure 3.11: Example 3.2.5. — hammer beat on a pipe

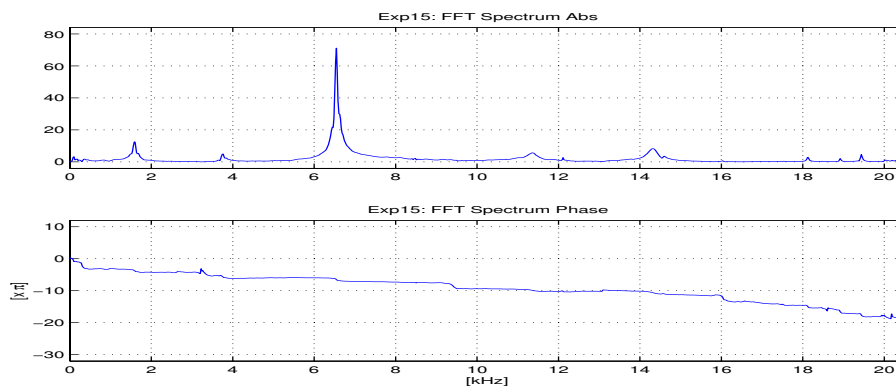


Figure 3.12: Example 3.2.5. — classical APSD spectrum

If the FFT algorithm is used to compute frequency domain data, an approximated non-uniformly spaced scale can be generated by selecting the data with frequencies close enough to the frequency values in the demanding scale. The conditions of doing this is, the resolution of the uniformly spaced scale obtained by FFT to be far better than the maximal resolution in the non-uniform scale. That is, with the common notations, by considering N sample points on the uniformly spaced s , and M points on the non-uniform t scale,

$$\frac{2\pi}{N} \ll \min_{j=1 \dots (M-1)} (t_j - t_{j-1}),$$

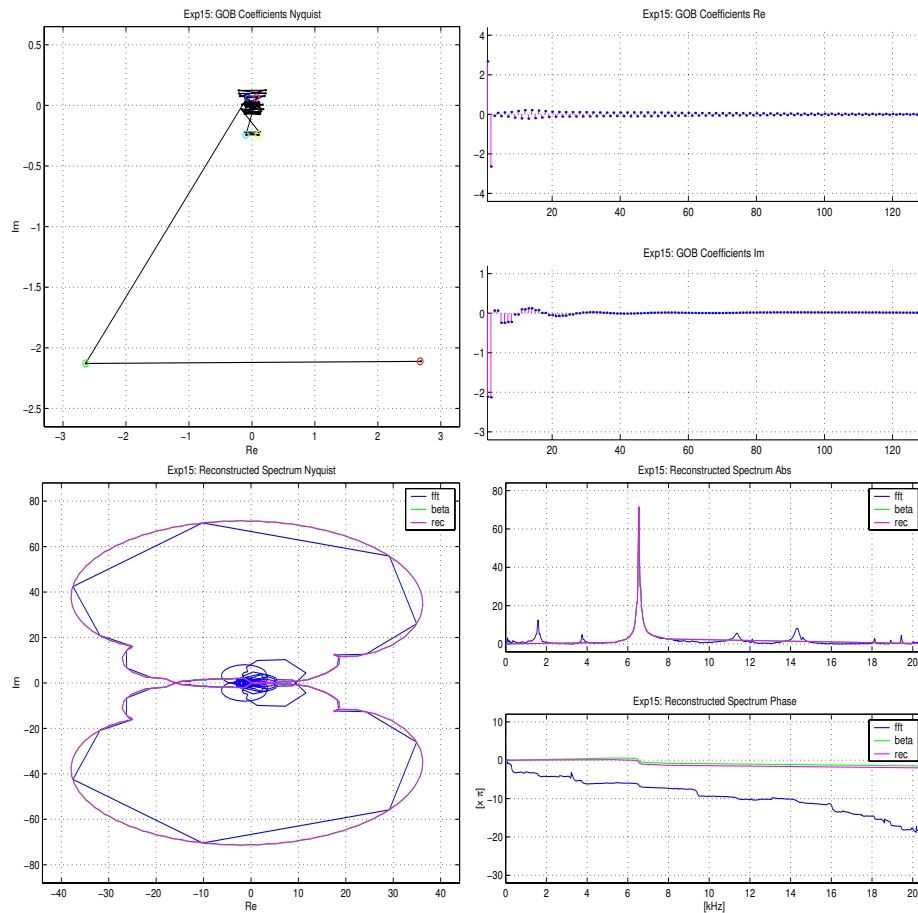


Figure 3.13: Example 3.2.5. — hammer beat on pipe

since the resolution on the uniform scale is constant $2\pi/N$. This requirement can be fulfilled if

- the number of samples in the uniform scale are far greater than those in the nonuniform one, i.e. $N \gg M$, and
- the nonuniform scale does not contain extremely dense regions, that is true if the system poles does not reside too close to the unit circle, i.e. the system is damped enough.

The first conditions is usually hold in practical cases, data numbers of 1024, 2048, 4096, 8192 are not considered high for the FFT algorithms regarding the computational efficiency of the computers today, on the other hand the GOB algorithms use at most 256, 512 number of samples. However, the second condition should be checked in the particular cases, e.g. in the examples presented in Section 3.2 it has not been satisfied.

The general form of the discrete Fourier transform (DFT) algorithm does not prescribe uniform scale on the frequency domain, however in this case it cannot be evaluated by the FFT algorithm. Let x_k ($k = 0, 1, \dots, N - 1$) be the time-domain data values, f_s the sample frequency, $X(f)$ the value of the Fourier-transform on a specific frequency, and f_n ($n = 0, 1, \dots, M - 1$), arbitrarily spaced points on the interval $[-f_s/2, f_s/2]$, $N, M \in \mathbb{N}$:

$$X(f_n) = \sum_{k=0}^{N-1} x_k e^{-i2\pi k \frac{f_n}{f_s}}$$

Computing the values of $X(f_n)$ on the set of $\{f_0, f_1, \dots, f_{M-1}\}$ is equivalent with the evaluation of a polynomial of degree $N - 1$ on a set of M different values. Using the Horner scheme in the evaluation, computing the value on one point requires N computational steps, hence the total number of the computational steps required is NM (see for more exhaustive analysis on this topic e.g. in Section 32 of [13]). For $M = N$ this is N^2 , which is far greater than $N \log N$ given for the FFT algorithm. However, the polynomial evaluation can be efficiently used, if the number of points to be computed is far smaller than the degree, i.e. $M \ll N$.

In principle there exist polynomial evaluation algorithm, that can be performed with $N \log N$ steps, e.g. one has been described in [27] pp. 118-119, however this algorithm raises serious numerical problems (similar ones as occurring in the Lagrange interpolation applied for large number of points), hence — until now — successfully usable algorithm has not been given.

The systems being subject of identification actions, e.g. industrial plants and their parts, transportation equipments, vehicles, etc., — according to their operating mode and handling restrictions — can be classified to several classes:

- The system cannot be subject of any arbitrary excitation, it can only be observed under ordinary operational conditions. For example, it is obvious, that because of safety requirements no any experiment in the operation is allowed on a plane on the air, or a nuclear reactor filled with nuclear fuel.
- External excitations are allowed, however there are limitations on the input signals that are allowed or reasonable to apply. Some examples:
 - Excitation over the absolute maximum ratings of an electronic, electromechanical, or mechanical object can cause damages, e.g. excessive load, power, frequency, etc.
 - Excitation over a specific range results in risk or even danger on the human operators and the environment, causes excessive noise, vibration, emission of harmful materials, etc.
 - Excitation over a specific range increases the costs, e.g. it requires high energy, fuel, raw materials, etc.
 - Excitation of an integrating type system, e.g. a motor drive, or a servo mechanism in open loop, with some types of signals results in overflow and overload.
 - Making experiments for identification purpose results in outage in the regular operation, which can cause financial loss at the owners.

This is the most frequent category of the systems.

- As an extremum: any type of external excitation is tolerable by the system — that is practically impossible. It is more plausible to add: within reasonable limits.

Hence, the two cases must be considered by the viewpoint of acquiring information of the system for identification purpose:

- The inputs cannot be affected, only observation of the inputs and outputs is allowed.
- The inputs of the system can be affected, i.e. test with excitation is allowed.

In the first case the observation of inputs and outputs in essence means recording the signals in the time domain, hence the frequency domain data can be obtained by some type of the Fourier-transform. The obvious drawback of this case, that there is no evidence upon whether the full dynamics of the system is represented in the signals.

In the case when the input signals can be defined arbitrarily, they can be selected such that the full dynamics be represented. The notion of "full dynamics" should exactly be defined: here a definition restricted to the spectral functions is sufficient. In the case of discrete time signals with a sample frequency satisfying the Shannon-rule, the full dynamics can be associated with the frequency band $[0, f_N]$ (f_N is the Nyquist frequency). A satisfactory test signal would be one that has a constant spectrum in the full band from zero until the Nyquist frequency. However finite duration test signal, that produces this spectrum does not exist, this is the spectrum of an infinite duration stochastic signal, the band-limited white-noise.

The digital identification algorithms usually use only finite number of discrete frequency points, hence the input test signal should only be prescribed in these points. A signal, which fulfill this requirement is a *multi-sine* with components of the desired frequencies. A disadvantage of this signal is, that it is also a signal of infinite duration, but it can well be approximated with its sufficiently long finite records.

Instead of the multi-sine signal, which contain all the components simultaneously, the components can be applied in sequence, every one in duration, which is large enough to approximate well the periodic signal. At least 3 to 5 complete period is usually enough,

hence the sufficient duration of a component depends upon its frequency, lower frequencies require longer duration. The frequency of the sine signal given on the input of the system can be changed step by step (this procedure is more precise), or continuously, this is the so-called *chirp* function. Using linear chirp (i.e. sine with linearly increasing frequency) is more frequent in the practice, however it is not optimal — the accuracy is cut off on the lower frequencies if the speed of frequency change is fixed.

In the case of multi-sine or chirp type methods the gain and the phase-shift on the predefined frequencies should be measured. Some alternatives for doing this:

- If the sine signals of different frequencies are given sequentially on the input, the gain and the phase-shift between the input and output sines can be measured by using simple time-domain algorithms. The time-domain gain and phase measurement can become quite difficult and inaccurate, if noise or nonlinear distortion occur on the output signal.
- Spectral analysis methods are used on the signals, i.e. Fourier-transform is performed or some type of spectral density function is estimated. The amplitude and the phase of the components can be estimated by the function values of the amplitude and phase spectrum on the predefined frequencies. The advantage of this method is, that works also in the case of heavy noises, since the sines occur on the spectrum as narrow peaks, usually much higher than the noise level. The spectrum estimation can be improved by windowing and averaging methods, well known in the spectral analysis field.

In the case, when components with frequencies spaced too closely to each other, the sequential application is more advantageous, to avoid the distortions originating from the finite resolution of the spectral estimation (for details see any elementary signal processing textbook, e.g. [8]).

The argument functions belonging to real physical systems are odd, i.e.

$$\beta_{\mathbf{a}}(-t) = -\beta_{\mathbf{a}}(t) \quad (3.3.1)$$

since the complex poles are included together with their conjugated pairs. Hence the positive half, i.e. the values $t \geq 0$, are sufficient to consider, and the negative half can be reconstructed by (3.3.1), if needed in the algorithms. Since the values of parameter $t \geq 0$ have direct physical meaning according to its connection with the frequency variable as

$$f = \frac{f_S}{2\pi} t,$$

introduced in Section 2.1, only this part is originated from physical measurements.

3.4 Applying the inverse argument transform

The frequency values belonging to the non-uniformly spaced scales on the frequency domain constructed by the inverse argument transform based upon a predefined set of poles are used to determine the measurement data, that serves as input for the discrete algorithm of representing signals in the generalized orthogonal bases generated upon these poles. Besides this "regular" use of this scale, based upon these frequency points an advantageous spectral description can be achieved for systems, that correspond to the concerned pole structure. The required correspondence is obvious according to the discussions of Chapter 2: a system is completely correspondent with a pole structure, if it belongs to the subspace generated by the finite Takenaka-Malmquist system defined upon this pole-set, i.e. concerning the poles \mathbf{a} , it belongs to $\mathcal{B}_{\mathbf{a}}^N \mathcal{H}_{\perp}^2$. In the practice in many cases approximate correspondence is enough to obtain advantageous descriptions, i.e. the system is enough to fall near to the space $\mathcal{B}_{\mathbf{a}}^N \mathcal{H}_{\perp}^2$.

The examples of Chapter 2 and those presented in the current chapter have shown the advantages referred above: the discrete form of the frequency functions based upon finite

number of sample points result in better representation of the original function, if the representation points are selected according to the inverse argument function, compared to that resulted from uniformly spaced data. This phenomenon has been examined experimentally for numerous systems with different pole and zero layouts by the means of the procedures written *MATLAB*[®], as well by an interactive computer application written in a C language environment. As an illustrative example a system is considered with the following set of poles:

$$[0.9, 0.99e^{0.5i}, 0.99e^{-0.5i}, 0.98e^{0.8i}, 0.98e^{-0.8i}]$$

Two cases are presented:

Exact representation: the poles associated with the GOB are exactly the same as those belonging to the system, the frequency functions belonging to this case can be seen on Figure 3.14.

Approximate representation: the poles associated with the GOB differ on one of the conjugated complex pairs: that associated with parameter $t = 0.5$ is shifted to value $t = 0.4$, i.e. the poles applied to realize the non-uniform frequency scale are

$$[0.9, 0.99e^{0.4i}, 0.99e^{-0.4i}, 0.98e^{0.8i}, 0.98e^{-0.8i}].$$

The frequency functions belonging to this case are presented on Figure 3.15.

The organization of the figures is the same: left-side diagrams are associated with the uniform, the right-side ones with the non-uniform scale. From the top downward first the Nyquist diagram of the frequency function can be seen, than the absolute value and the phase of the functions is presented in "lin-lin" as well as in "log-log" style (Bode-like diagrams).

Some important facts can directly be observed on the diagrams:

Exact representation: The Nyquist diagram belonging to the exactly realized non-uniform frequency scale realize the expected shape with higher fidelity. The sample points are arranged uniformly on the curve resulting in the relative its "smoothness", comparing to the classical Nyquist plot. On the Bode-type diagrams belonging to the non-uniform case the sample points are concentrated on the neighborhood of the spectral peaks, while are arranged rather sparsely on the other regions. The peaks are characterized with greater number of samples, resulting in more exact representation of the function shape.

Approximate representation: Both the Nyquist and the Bode plots are partially distorted. The distortion occurs on the regions that can be associated with the pole displaced, i.e. on the external circle of the Nyquist diagram, and on the neighborhood of the lower frequency peak in association with the Bode diagrams. It can also be observed on the latter ones, that the denser arrangement of the samples associated with the lower frequency pole falls on a region, where no significant change can be seen, on the other hand the existent peak is missed. Otherwise, the representation is better than that given by the uniform spacing.

According to these observations as well as the experiments referred above, the experiences can be summarized as follow:

- In the Nyquist-type graphic representation:
 - The uniformly spaced points are placed with high non-uniformity along the Nyquist-curve, resulting in difficulties in some places to reconstruct the expected shape, if a not a dense enough scale has been used.
 - An exact non-uniform spacing according to the inverse argument function of the samples results in a highly uniform layout of the points along the Nyquist-curve,

resulting in good reconstructing properties even in the case when small number of data has been used.

- In the case of an approximate matching of the system concerned with the predefined poles, non-uniform spacing results in more uniform arrangement of the function points along the Nyquist-curve, while the difference is not excessively high.
- In the Bode-like graphic representation:
 - The uniformly spaced points are placed uniformly along the horizontal axis, independently from the actual shape of the function, resulting in the same resolution both around the peaks and the constant or slowly varying portions. Hence the reconstruction ability of the diagram can be poor on the neighborhood of the peaks, if no sufficient number of sample points has been used.
 - An exact non-uniform spacing according to the inverse argument function of the samples results in denser point arrangement in the neighborhood of peaks and abrupt changes on the curve, comparing to the constant or slowly changing portions. Hence this spacing represents the function with high fidelity just there, where interesting things are shown in respect to the system dynamics.
 - In the case of an approximate matching of the signal concerned with the predefined poles, non-uniform spacing provides more accurate description of spectral peaks, if the difference is not excessively high.

Hence, the use of non-uniform spacing of frequency values, according to the inverse argument function associated with a predefined set of poles, is advantageous in representing spectral properties of systems, that — at least approximately — conform to the *a priori* assumption, i.e. its poles are — at least partly and approximately — identical with those belonging to the predefined set. The use of the non-uniformly spaced frequency scale, generated

in such way, has great significance not only in GOB representations, but also in classical nonparametric spectral function based methods (being common e.g. in the fields of detection and identification) applied on systems, if some *a priori* knowledge is available in association with their pole structure.

The exact mathematical discussion of the observations summarized above is not easy, because neither the goodness of the representation of a function by its discrete values is uniquely defined, nor the characteristics used for classifying the result. Analyzing multiple approaches resulting from several mathematical definitions exceeds the framework of the current thesis work. Representing a function on the basis of its sample values belongs to the field of interpolations. This field has been concerned in connection with the reproducing kernel of the subspace generated upon a finite pole set in the Section 4.3.2 of Chapter 4. An interpolation operator has been defined in the subspace $\mathcal{B}_a^N \mathcal{H}^2(\mathbb{D})$

$$(L_{\mathcal{H}})F(t) \doteq \sum_{k=0}^{N-1} \frac{K(e^{it}, e^{it_k})}{K(e^{it_k}, e^{it_k})} F(t_k),$$

where $\{t_k | (k = 0, 1, \dots, N - 1)\}$ is a non-uniformly spaced scale in the interval $[-\pi, \pi]$ based upon the inverse argument function $\beta_{a|N}(t)$ defined in $\mathcal{B}_a^N \mathcal{H}^2(\mathbb{D})$. This fact explains and supports the central role of this scale in the interpolation of functions belonging — and residing close — to the subspace $\mathcal{B}_a^N \mathcal{H}^2(\mathbb{D})$. Precise discussion and proofs of these ideas is subject of further research in this field.

Nevertheless, the idea of applying a non-uniformly spaced frequency scale on the basis of the inverse argument function associated with a predefined set of poles can be expressed as a method of designing measurement scheme or constructing a experiment plan. This method is advantageous in the cases, when there exist *a priori knowledge* upon the *pole locations*, that can be associated with the system to be analyzed. The method establishes the scheme of selecting a scale containing finite number of frequency values, that represent in best way the system in respect to an a priori fixed set of poles associated with the system.

The frequency scale can be applied in direct frequency-domain measurements, in designing input signals for systems tests with external excitation, or can be used in computing spectral function values on the basis of time-domain measurements. The method will be referred with the logo *ARGFUN* in the following parts of the thesis.

The structure of the *ARGFUN* method is summarized as follow:

Pesumptions: The reference pole set containing N different poles, real ones or conjugated complex pairs, as $\mathbf{a} = \{a_k \in \mathbb{D} \mid k = 0, 1, \dots, N - 1\}$, is fixed. It is assumed, that the system to be analyzed at least approximately conforms to this set of poles in the respect of the subspace $\mathcal{B}_{\mathbf{a}}^N \mathcal{H}_{\perp}^2 \subset \mathcal{H}_{\perp}^2$ generated by the N -dimensional Takenaka-Malmquist system built upon \mathbf{a} . Moreover it is assumed, that the sample frequency associated with the system, and the signals belonging to it, is f_S , and it conforms to the Shannon rules of sampling.

Step 1: A uniformly spaced scale consisting of M points (M is assumed to be even) is generated on the interval $[-\pi, \pi]$ of the variable s :

$$s_j = -\pi + j \frac{2\pi}{M} \quad (j = 0, 1, 2, \dots, M - 1)$$

Step 2: A non-uniformly spaced scale is generated according to the inverse of the argument function $\beta_{\mathbf{a}}$ associated with the poles \mathbf{a} by

$$t_j = \beta_{\mathbf{a}}^{-1}(s_j) \quad (j = 0, 1, 2, \dots, M - 1)$$

Step 3: The physically realizable frequency scale containing $M/2$ points is derived from the values of the scale $\{t_j \geq 0\}$, as

$$f_j = \frac{f_S}{2\pi} t_j \quad (j = M/2, M/2 + 1, \dots, M - 1)$$

Remark: in the algorithmic realizations the generation of the negative part of the scale can be avoided.

A crucial point in applying the method in practical cases is how to find the appropriate reference pole set. This topic belongs to the field of the system identification, and will be discussed in the Chapter 5. As an illustration here some examples are given to present the cause of particular reference pole selections. A system with one conjugated complex pole pair $[0.99e^{0.5i}, 0.99e^{-0.5i}]$ is considered, and the reference poles are selected as

Example (i): $[0.95e^{0.5i}, 0.95e^{-0.5i}]$ — overdamped poles,

Example (ii): $[0.96e^{0.5i}, 0.96e^{-0.5i}]$ — overdamped poles,

Example (iii): $[0.99e^{0.5i}, 0.99e^{-0.5i}]$ — the exact case,

Example (iv): $[0.995e^{0.5i}, 0.995e^{-0.5i}]$ — underdamped poles,

Example (v): $[0.98e^{0.55i}, 0.98e^{-0.55i}]$ — overtuned poles,

Example (vi): $[0.98e^{0.65i}, 0.98e^{-0.65i}]$ — overtuned poles.

The frequency functions of the examples are presented on the Figure 3.16 on the order as enumerated above. The sample point are marked with circles on the diagrams. It can be observed, that

- The dampedness of the reference pole affects the width of the region, that is covered by sample points with greater density.
- The tuning of the reference pole affects the location the sampled region on the frequency scale.

These type of considerations can serve as useful "rules of thumb", that complement the exact identification methods.

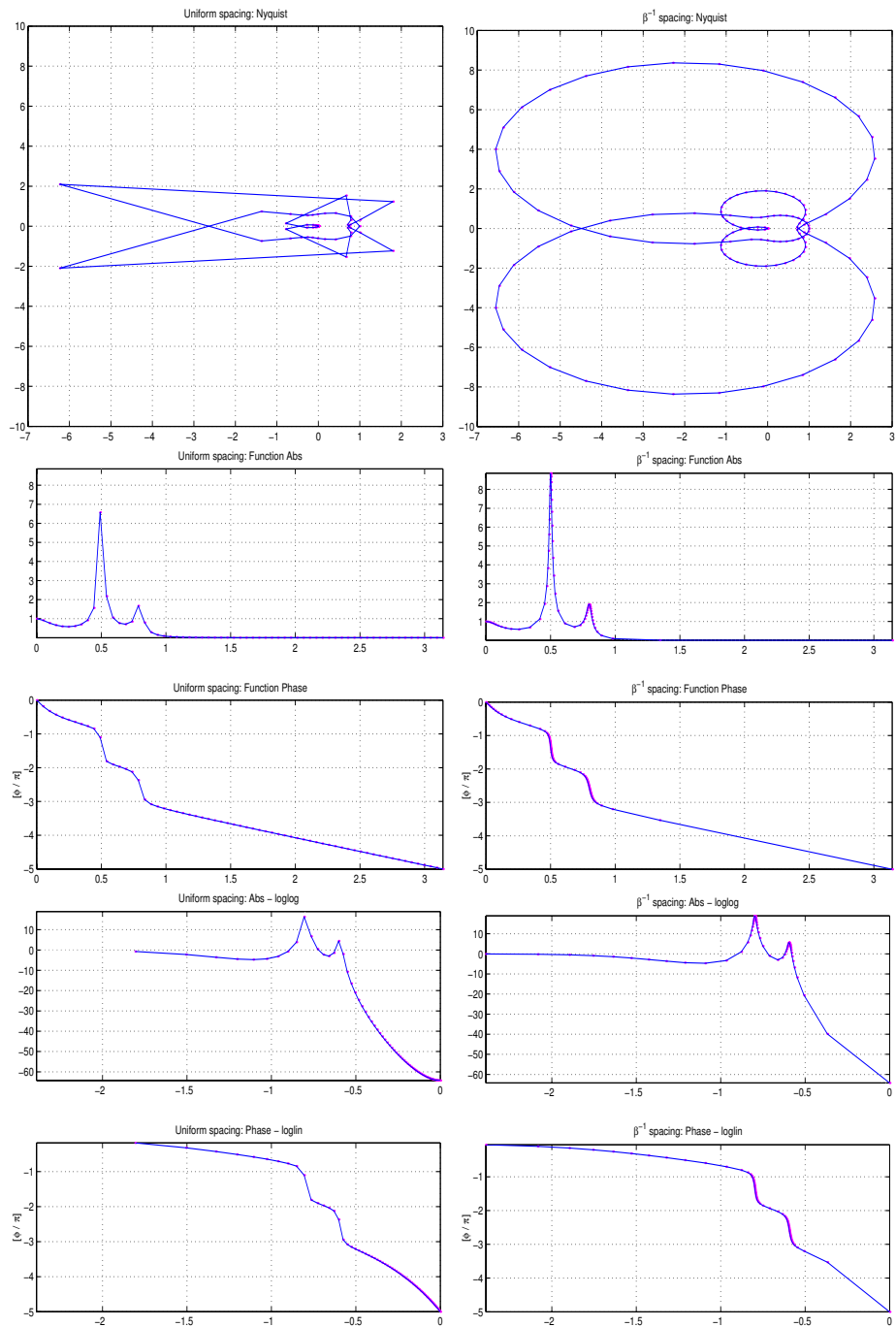


Figure 3.14: Exact representation: uniform (left) / non-uniform (right)

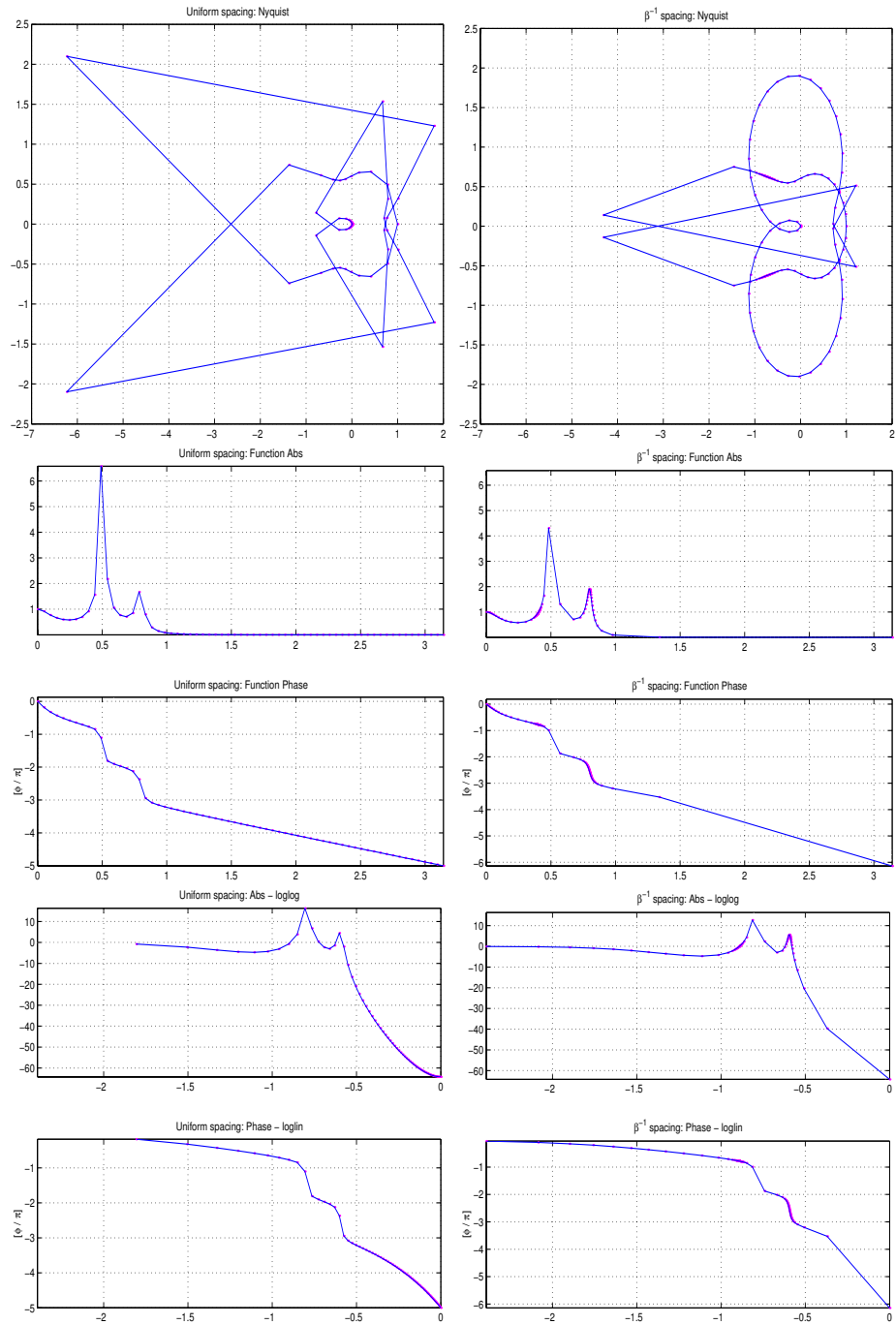


Figure 3.15: Approximate representation: uniform (left) / non-uniform (right)

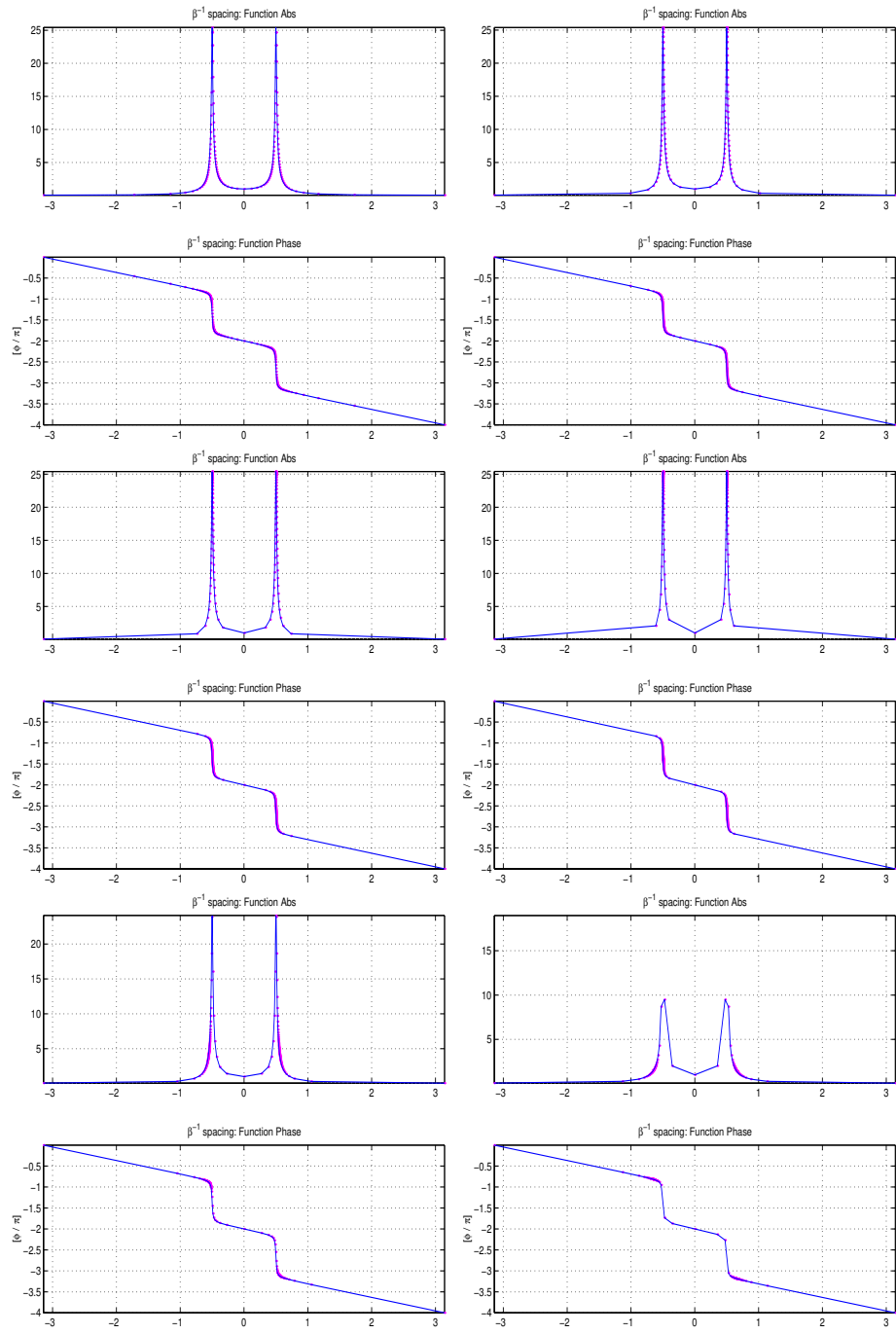


Figure 3.16: The cause of selecting reference poles

Chapter 4

Applying GOB representations: detection

In this chapter an application area of the signal representations in generalized orthogonal bases will be presented: the application of GOB representations in detection, feature enhancement, noise suppression and related problems will be discussed.

4.1 Detection, feature enhancement and noise suppression

This section is devoted to the applications of signal representations in the detection area of signal processing, as well as in related areas such as feature enhancement and noise suppression. Detection of particular objects or phenomena in signals corrupted by noise and disturbing effects is a classical and thoroughly studied field both in signal processing and in other areas of systems science. The detection problem can be static or dynamic (or temporal). In the static case detection aims to recognize a permanently existent feature in the signal; in the dynamic one the goal is to recognize the occurrence of the investigated feature in the course of time, this problem has been widely studied by the scientific community within the framework of the so-called change-detection field (see [4], [5]). Due to the applications in numerous areas in industry a significant subfield within change-detection is the detection of *failures*, see a recently published survey [35] as a reference on this field.

Detection is a decision problem, its goal is usually to give an answer YES or NO to the question whether or not the investigated object, feature, or phenomenon is present in the signal (of course multi-objective decision problems can also be formed). Feature enhancement and noise suppression are similar problems, with the difference, that their results are not binary decisions, rather are quantitative forms comprising information of the significant — useful for particular purposes — part of the signal, by treating the remaining parts as noise, disturbance or unwanted effects. Feature enhancement (and more or less noise suppression) serves in most cases as the first step toward the solution of the detection problem, a decision procedure — either on deterministic or statistical framework — is only needed to be performed upon its result. Feature enhancement and noise suppression differ from each other basically in their goal: feature enhancement — as it is expressed in its name — aims to enhance the useful part in the signal, on the other hand the goal of noise suppression is to eliminate the unwanted content.

Detection is a rather significant problem in many areas of the real life. Some classical examples: detection of objects on the radar screen, recognition of fingertips in criminology, recognition of failures by the sounds and vibrations of machineries (e.g. in nuclear or fossil power plants). Today, automated test, failure detection, and diagnostics are important constituents of the safety of systems that represent potential risk to their environment, such as industrial or power production plants, land, marine, and air vehicles. Transportation engineering can profit in several areas from the detection field: detection of lane borders, or obstacles on the road in front of a vehicle, recognition of abnormalities in the movement of vehicle, detection of failures in the operation of the engine, brakes, and other on-board equipment are characteristic examples to stress its significance.

In the case of human recognition the basic assumption in applying detection methods is rather simple: the object or effect to be found cannot immediately be seen, it is entirely or partially hidden in noises and disturbing effects. Automated recognition — in

the absence of the delicate human perception — requires detection methods also in more obvious situations, when noise and disturbances are not so heavy. Detection methods are also significant in the cases, when the effects to be recognized are expressed in higher level than the common sense, i.e. by using abstract mathematical definitions. For example: frequency domain (spectral) detection methods spread far beyond the possibilities offered by the natural frequency notion originated mainly from the acoustic perception of humans. Furthermore machine recognition can extend the boundaries of the human perception both in variety, range, and sensitivity.

Sensitivity and selectivity of detection methods is a rudimentary question. Sensitivity roughly means the ability of the method to detect even the weak presence of the effect; selectivity mirrors the distinction capability between the demanded effect and any disturbing one.

Within the framework of this thesis an approach to generate *sensitive* and *selective* methods for the detection of specific effects in signals — based upon *signal representations* built upon the characteristics of the demanded effects themselves — will be presented. The main idea is to build the demanded characteristics into the representing function set. In this case the representation coefficients belonging to the analyzed signal will mirror the weights of the presence of representing functions in the signal. Qualitatively, a small number of dominant coefficients of lower order can sign a significant presence of the demanded effect — this assertion will be enhanced later for the cases studied within the thesis work.

Feature enhancement and noise reduction can also easily presented within this framework: the reconstruction of the signal from the representation by keeping the dominant coefficients, and discarding the ones falling bellow a limit will result in a signal free of noises and disturbances. Furthermore the set of the dominant coefficients contains the information of the demanded features in a condensed form — and can suit as basis for decision procedures to realize detection. Of course, these ideas can at this point be considered as

qualitative assumptions, their purification will be given in the subsequent part of the thesis for some specific cases.

A common procedure to perform a detection problem on this base consist of the steps as follow:

- The representing function space is derived on the basis of the characteristics to be detected.
- The signal representation is performed, i.e. the signal is transformed into the coefficient space of the representation. This results in a countable set of coefficients for discrete representations, and a function-space for continuous ones. The coefficient space is expected to enhance the characteristics decided a priori to investigate.
- The criteria of the existence of the feature to be detected is expressed on the basis of the coefficient space. In most cases this means the selection of the lowest order dominant coefficients.
- A decision procedure is performed by applying the detection criteria.

A large variety of decision methods are available either on deterministic or statistical framework.

A common procedure to perform feature enhancement or noise suppression can similarly be constructed, here a reconstruction step is used in the decision procedure:

- Fixing the representing function space.
- Performing the signal representation.
- The significant representation coefficients (the dominant ones as excepted)are kept, and the remaining ones are discarded.
- The signal is reconstructed by using the significant coefficients only.

The reconstructed function can be used for further investigation, e.g. for human or automated decision making.

As examples, some conventional detection methods are based on signal representations. For example any spectral detection method is based upon the signal representation in the standard trigonometric basis, i.e. decision making upon spectral features (e.g. spectral peaks) conforms to the method described above. In this case the demanded feature is the harmonic periodicity in several frequencies of the signal. However, the selected feature fixes a rather broad class of signals, the goal of the thesis work is to establish some narrower classes, which correspond to practical application areas.

In the subsequent sections special representation based detection methods will be presented, which are constructed by using a priori knowledge available of the system and the related signals. First a priori knowledge, that can be used in broader sense, will be defined, then a specific detection scheme will be presented, which is based upon the generalized orthogonal bases introduced in the previous chapter.

4.2 Using a priori knowledge in representations

Detection methods — even the classical ones — assume some amount and type of a priori knowledge: e.g. the Fourier-based spectral methods apply the fact, that almost every signal can be decomposed into sinusoids of several frequencies (i.e. harmonic components); or the Walsh-type methods assume the same fact by using square-functions instead of sinusoids. It can simply be seen, that the assumptions fitting better to a particular signal result in a "better" representation — the representation is more characteristic, i.e. more interesting objects can be recognized, the objects can more sharply be distinguished, the objects are well localized, etc. For example most industrial structures, consisting of elastic vibrating parts, produce spectral "peaks" in several frequencies, which can well be distinguished

by using Fourier-based analysis methods. On the other hand, Walsh-type methods are certainly be advantageous in detection of objects in a pixelized image, where the "atomic" objects are rectangular, and they are especially powerful in detection of rectangular objects. However, the a priori assumptions used in the Fourier and Walsh type representations can be considered as "weak" ones, as they fit more or less to almost all types of signals. In the followings the goal is to find more distinctive a priori assumptions, that can result in the characterization of narrower classes of signals, to obtain more sensitive detection methods for the particular class.

The idea used here is rather simple: let the function space used as the basis of the representation be selected according to a priori assumptions upon the objects desired to be detected, i.e. let the knowledge built in a signal representation be embodied in the representing function set. The characteristics of the constituents of the signal space will be inherited in the representation in a weighted form, hence the representation offers information upon the measure of the presence of these characteristics on the analyzed signal.

The knowledge built into the representation is considered to be "*a priori*" to stress the fact, that it is assumed before any analysis has been made. *A priori* assumptions are rather frequent both in the scientific analysis and the everyday practice. In many cases the a priori assumptions are being failed, they are proved to be invalid, which also includes information i.e. a *negative* decision, the absence of the characteristics investigated; however on the other hand they frequently result in *positive* decisions, and can be confident source of information.

There are many possibilities to build a priori knowledge into the representing functions, however no general purpose scheme can be given on how to perform this. Instead, some examples will be given, and one of them — that is connected to the generalized bases studied in the previous chapter — will be investigated in details. Let be seen the examples in the following paragraphs.

In the Fourier-based spectral representations the representing function set is consisting of sine and cosine functions parameterized by the frequency, realizing a scaling (or contraction/dilation) of the prototype function on the time-scale. The weights given in a representation can be considered as amplitudes of the constituent sinusoids of different frequencies. It is well known, that if the signal to be analyzed contains a single sine of a particular frequency, this will result in a well distinguished object, a sharp "spectral peak" on the parameter space, i.e. on the frequency domain. In the case of multiple sinusoids, of course, multiple peaks occur in the spectra. This happens if any periodic component is present in the signal. Non-periodic content (e.g. transients, noises) does not result in sharp peaks, that cases are characterized by spread spectra.

Another possibility to build a priori knowledge into the representing function can be given by using the function shape in time-domain. A contemporary approach to realize this idea is given by applying wavelets. The function shape is fixed by selecting the mother wavelet, and the representing function set will be given by the dilated and translated forms of it. The weights belonging to the representation of a particular signal can be considered as amplitude of the component of a given dilation (scaling), and translation (time offset). That is, the representation is able to realize multiple occurrences of the dilated and amplified forms of the demanded shape, that can be characterized by the two-dimensional coefficient space — function of scale and translation. Decision upon the existence of components similar to the demanded shape can be based upon localized maxima on the coefficient space. An enhancement of the demanded components and a suppression of the unwanted parts (e.g. noises) can be given by nullifying the coefficients falling under a limit of significance. There is no possibility to elaborate the concept of applying wavelets in detection and the related areas in the current thesis work, this can be subject of the further research.

The methods proposed in this thesis can be considered as an extension of the frequency-domain approach, and are based on the concept of *generalized orthogonal bases*, introduced

in Chapter 2. The establishment of a particular generalized orthogonal basis is performed by *a priori* assumed *poles* of the system to be analyzed. An *a priori* knowledge upon the poles of the system under consideration (i.e. poles of the transfer function associated with the system) can be given by an estimation (as the result of an identification process) or by a speculative model constructed upon physical, structural, and behavioral considerations.

The poles of a dynamical system are rudimental in determining the dynamics, i.e. the answer of the system to several input effects, its transient behavior, its speed of taking a new state or absorbing the disturbances, its reaction to high frequency inputs, etc. Hence any change on the pole-structure e.g.

- displacement of one or more poles,
- disappearing of one or more poles,
- occurring new poles,

can be associated with changes on the system dynamics. Some examples:

- Fatigue, wear, and moisture of mechanical parts causes slow changes in the elasticity, mass, dampness, and friction resulting changes in the vibration modes of the system — associated with small changes of the existent poles.
- A break in the structural parts can cause an abrupt change in the vibration modes, resulting in a larger change in the poles.
- A break can also produce a new vibration mode in the system, which can be associated with a new pole.
- A loosed structural part (in a loose part monitoring system) can lead to the disappearance of an existent vibration mode associated with a pole.

The association of operation modes with the pole structure can be done upon the basis of the system model, and additional information of the structure and the physics of the system behavior.

However, the use of the pole information in detection does not restrict the effects to be detected on the changes in the poles itself. It will be shown, that — by using the concept of the representation in generalized orthogonal bases — changes on the zero structure, e.g. changes on the full transfer function, are also detectable. The application of a presumed pole structure is suite as a parameterization of the systems, and intends to restrict the class of systems to be included in the analysis – which is rather broad in the case of using Fourier-based methods, i.e. the standard trigonometric bases — resulting in greater sensitivity and selectivity.

The use of pole-information is not new in the detection area. The well known linear parametric change detection methods assume linear models (e.g. AR, ARMA, state-space, and matrix fraction representations), which — directly or indirectly — must include information upon the system's pole structure. Change detection filters generated upon this basis can effectively be used to detect several presumed changes with high sensitivity and selectivity (see e.g. [1], [2], and [3]).

The method proposed in this thesis work shows numerous advantages over the parametric detection methods. First of all: it does not require a complete model of the system, just the location of the poles, not included their multiplicity; that will be given by the representation itself. Hence the representation based upon a presumed pole structure covers a broader class of the systems, with the freedom of concerning several multiplicities of poles and — within an admissible region — arbitrary zero structure. Furthermore the method works also in the case of applying approximately known pole structure. These advantages among other characteristics of the method will be clarified in details in the course of the following sections.

4.3 Detection scheme by using generalized orthogonal bases

A method intended to recognize objects and phenomena in signals belonging to dynamic systems will be proposed:

- By assuming a set of poles belonging to the dynamic system a frequency domain representation scheme is built applying the concept of the generalized orthonormal basis (GOB).
- A decision scheme is established based upon the connection of the physical object or phenomenon to be detected and the representation coefficients.
- A signal belonging to the system is represented in the established basis, i.e. the representation coefficients are computed (estimated).
- The decision scheme is applied for the actual set of representation coefficients.

In this form of method the representation coefficients are directly be used in the decision process. However computing of coefficients is not necessary in all cases, numerically simpler methods can be obtained by introducing some new — easy to compute — quantities derived upon the coefficients; a discrete scalar product based upon the concept of reproducing kernel, will be presented in one of the following sections.

The use of generalized orthogonal bases offers the promise of obtaining detection method, which is sensitive to the object or phenomenon intended to be detected, and is selective in detecting multiple ones of them. In the current case the "object" or "phenomenon" — which of them is taken, it depends upon the specific viewpoint of the investigation — can be considered the matching of the analyzed signal with the a priori assumed set of poles. To understand what this matching means in details, let us recall the finite Takenaka-Malmquist system introduced in Section 2.4.3.

The finite Takenaka-Malmquist system is based upon a finite set of $N \in \mathbb{N}$ poles, and as it has been shown, it represents a subspace of \mathcal{H}^2 containing the strictly proper rational functions of \mathcal{H}^2 with order not greater than N . Let this subspace be denoted by $\mathcal{B}_a^N \mathcal{H}^2$.

Any function $F(z) \in \mathcal{H}_\perp^2$ belonging also to $\mathcal{B}_a^N \mathcal{H}^2$ can exactly be represented in the Takenaka-Malmquist system defined upon the set of poles $\{a_n\}_{n=0}^{N-1}$, as it has been shown in Section 2.4.3. Since the generalized orthogonal basis can be interpreted as a periodically repeated finite Takenaka-Malmquist system, $F(z)$ can be represented by finite number of coefficients in the generalized orthonormal basis from indices 0 to $N - 1$. This fact can be used to detect whether the signal to be analyzed belongs to the subspace $\mathcal{B}_a^N \mathcal{H}^2$ or not; a positive decision can be made, if at most the first N representation coefficients differ significantly from zero. Beyond this, more detailed analysis can be performed based upon the exact number and the actual values of the coefficients; this will be discussed in the next section.

If the function analyzed does not belong to the subspace $\mathcal{B}_a^N \mathcal{H}^2$, it can belong to a broader, nevertheless finite dimensional subspace of \mathcal{H}^2 , if it contains poles with multiplicity greater than one, strictly from the set $\{a_n\}_{n=0}^{N-1}$. This case can be detected, if finite — however greater than N — number of significant coefficients has been found.

Otherwise, if the analyzed function does not belong even to this extended subspace, the representation will become infinite. To understand the mechanism of this, let us consider some simple cases.

Let $\{\Phi_n\}$ be the generalized orthonormal basis defined upon the single pole $a \in \mathbb{D}$ (which is essentially a Laguerre system with the exception, that complex pole is considered)

$$\Phi_n(z) \doteq \sqrt{1 - |a|^2} \frac{(1 - \bar{a}z)^n}{(z - a)^{n+1}} \quad (n = 0, 1, 2, \dots),$$

and assume that function $F(z) \in \mathcal{H}_1^2$ contains a single pole with multiplicity one. Let the pole be different than a with difference Δa , such that

$$F(z) = \frac{1}{z - (a + \Delta a)} \quad a + \Delta a \in \mathbb{D}.$$

$F(z)$ can be expressed in series form related to a as

$$F(z) = \frac{1}{z - a} + \frac{\Delta a}{(z - a)^2} + \frac{(\Delta a)^2}{(z - a)^3} + \cdots = \sum_{k=0}^{\infty} \frac{(\Delta a)^k}{(z - a)^{k+1}}.$$

The coefficients of the representation can be computed by evaluating the scalar products $\langle F, \Phi_n \rangle$ for $n = 0, 1, 2, \dots$. To do this, let us return to the mathematical form with $q = 1/z$:

$$\Phi_n(q) \doteq \sqrt{1 - |a|^2} \frac{(q - a)^n}{(1 - \bar{a}q)^{n+1}} \quad (n = 0, 1, 2, \dots),$$

and

$$F(q) = \frac{1}{1 - \bar{a}q} + \frac{q\Delta\bar{a}}{(1 - \bar{a}q)^2} + \frac{(q\Delta\bar{a})^2}{(1 - \bar{a}q)^3} + \cdots = \sum_{k=0}^{\infty} \frac{(q\Delta\bar{a})^k}{(1 - \bar{a}q)^{k+1}}. \quad (4.3.1)$$

The coefficients c_n ($n=0,1,2,\dots$) are given as

$$c_n \doteq \langle F, \Phi_n \rangle = \frac{\sqrt{1 - |a|^2}}{2\pi} \int_{-\pi}^{\pi} \sum_{k=0}^{\infty} (\Delta\bar{a})^k \frac{e^{ikt}}{(1 - \bar{a}e^{it})^{k+1}} \frac{(e^{-it} - \bar{a})^n}{(1 - ae^{-it})^{n+1}} dt.$$

After simple transformations a Poisson kernel can be separated within the integrand:

$$c_n = \frac{1}{\sqrt{1 - |a|^2}} \sum_{k=0}^{\infty} (\Delta\bar{a})^k \frac{1}{2\pi} \int_{-\pi}^{\pi} \frac{1 - |a|^2}{(1 - \bar{a}e^{it})(1 - ae^{-it})} \frac{e^{ikt}(e^{-it} - \bar{a})^n}{(1 - \bar{a}e^{it})^k(1 - ae^{-it})^n} dt,$$

since $(1 - \bar{a}e^{it})(1 - ae^{-it}) = 1 - 2|a|\cos(t - \varphi) + |a|^2$ with $a = |a|e^{i\varphi}$. For $k \leq n$ after simplification of terms $(1 - \bar{a}e^{it})^k$, the Poisson integral can be expressed as

$$\frac{1}{2\pi} \int_{-\pi}^{\pi} \frac{1 - |a|^2}{1 - 2|a|\cos(t - \varphi) + |a|^2} \frac{(e^{it} - \bar{a})^{n-k}}{(1 - ae^{-it})^n} dt = \left[\frac{(q - a)^{n-k}}{(1 - \bar{a}q)^n} \right]_{q=a},$$

which is equal to $1/(1 - |a|^2)^n$ if $k = n$, and zero if $k < n$, since in this case the function has zeros in a . For the indices $k > n$ the Poisson integral — after simplification with $(1 - \bar{a}e^{it})^n$

— will be

$$\frac{1}{2\pi} \int_{-\pi}^{\pi} \frac{1 - |a|^2}{1 - 2|a| \cos(t - \varphi) + |a|^2} \frac{e^{i(k-n)t}}{(1 - \bar{a}e^{it})^{k-n}(1 - ae^{-it})^n} dt = \left[\frac{q^{k-n}}{(1 - \bar{a}q)^{k-n}(1 - a\bar{q})^n} \right]_{q=a} = \frac{a^{k-n}}{(1 - |a|^2)^k}.$$

Hence the coefficients c_n will be

$$\begin{aligned} c_n &= \frac{1}{\sqrt{1 - |a|^2}} \sum_{k=n}^{\infty} (\Delta\bar{a})^k \frac{a^{k-n}}{(1 - |a|^2)^k} = \frac{1}{a^n \sqrt{1 - |a|^2}} \sum_{k=n}^{\infty} \left(\frac{a\Delta\bar{a}}{(1 - |a|^2)} \right)^k = \\ &= \frac{1}{\sqrt{1 - |a|^2}} \left(\frac{\Delta\bar{a}}{(1 - |a|^2)} \right)^n \sum_{k=n}^{\infty} \left(\frac{a\Delta\bar{a}}{(1 - |a|^2)} \right)^k = \frac{1}{\sqrt{1 - |a|^2}} \left(\frac{\Delta\bar{a}}{(1 - |a|^2)} \right)^n \frac{1}{1 - \frac{a\Delta\bar{a}}{1 - |a|^2}}. \end{aligned}$$

The latest transformation can be done if

$$\left| \frac{a\Delta\bar{a}}{1 - |a|^2} \right| < 1, \quad \text{that is} \quad |\Delta a| < \frac{1}{|a|} - |a|,$$

which is trivial as $|a| < 1$. Hence the coefficients are equal to

$$c_n = \frac{\sqrt{1 - |a|^2}}{1 - |a|^2 - a\Delta\bar{a}} \left(\frac{\Delta\bar{a}}{1 - |a|^2} \right)^n.$$

It can be observed, that if there is a difference between the pole a priori assumed and the analyzed one, it will result in infinite set of representation coefficients with magnitude exponentially decreasing as $n \rightarrow \infty$. The decay rate is equal to

$$\frac{\Delta\bar{a}}{1 - |a|^2},$$

i.e. it is proportional with the difference, more exactly the greater is the difference, the slower is the decay. The coefficients show an additional dependence upon the difference by the factor

$$\frac{1}{1 - |a|^2 - a\Delta\bar{a}},$$

that affects the magnitude and phase globally to every coefficient, however it has no influence on the decay rate. The magnitude of the coefficients is decreased as the difference is

increased. Figure 4.1. represents the relative change in the magnitude of the coefficients as the function of the absolute value of the difference parameterized with the absolute value of the pole (the values 0.999, 0.99, 0.9, 0.8, 0.5, and 0.2 has been used). The decrease can be quite drastic if the concerned pole resides near to the unit circle.

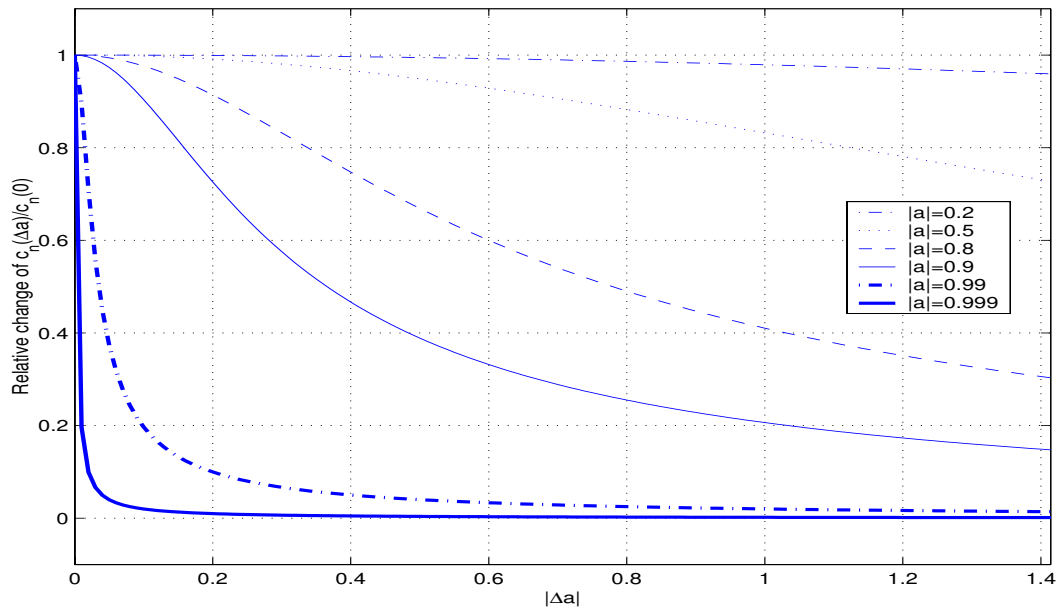


Figure 4.1: Relative change of coefficients as the function of Δa

In the exact case, where no difference on the pole is present, only the first coefficient c_0 differs from zero, as it has been expected by definition. On Figure 4.2 this case has been presented in comparison with the case with difference $\Delta a = 0.3$ with reference pole value 0.6.

The case is more complicated if a generalized orthonormal basis generated upon multiple poles is assumed. With the set of $N \in \mathbb{N}$ distinct poles $(a_0, a_1, \dots, a_{N-1})$, and $n = N\ell + k$ ($k = 0, 1, \dots, N - 1$; $\ell = 0, 1, 2, \dots$) — by using again the mathematical formulation —

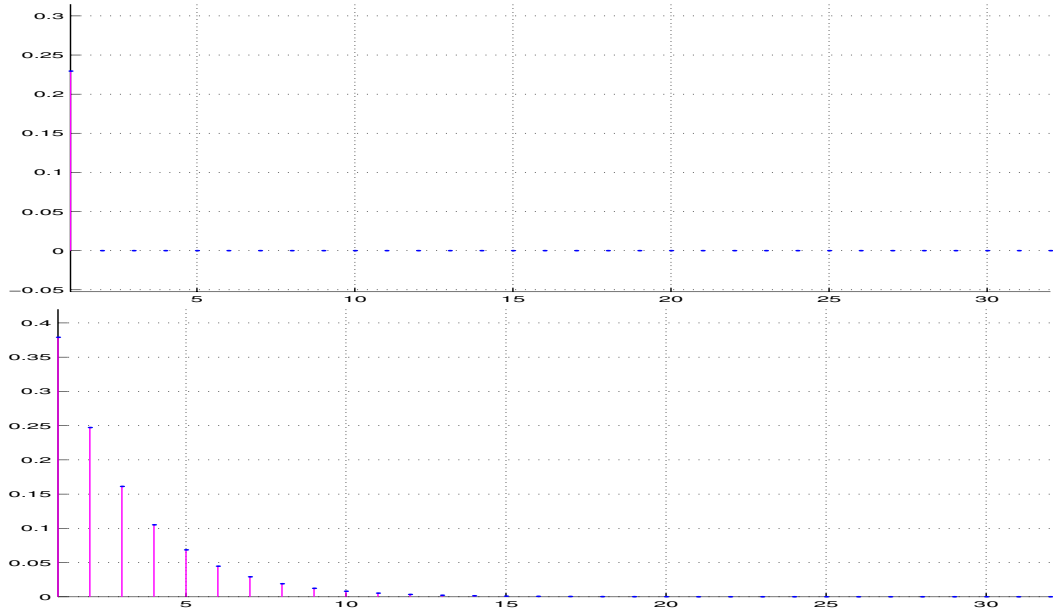


Figure 4.2: GOB coefficients: exact case and difference 0.3

the representation coefficients can be expressed as

$$\begin{aligned}
c_n &\doteq \langle F, \Phi_n \rangle = \\
&= \frac{\sqrt{1 - |a_k|^2}}{2\pi} \int_{-\pi}^{\pi} \sum_{m=0}^{\infty} (\Delta \bar{a}_k)^j \frac{e^{ijt}}{(1 - \bar{a}_k e^{it})^{m+1}} \\
&\quad \frac{\prod_{j=0}^{k-1} (e^{-it} - \bar{a}_j)^{\ell+1} \prod_{j=k}^{N-1} (e^{-it} - \bar{a}_j)^{\ell}}{\prod_{j=0}^k (1 - a_j e^{-it})^{\ell+1} \prod_{j=k+1}^{N-1} (1 - a_j e^{-it})^{\ell}} dt = \\
&= \frac{1}{\sqrt{1 - |a_k|^2}} \sum_{m=0}^{\infty} (\Delta \bar{a}_k)^j \frac{1}{2\pi} \int_{-\pi}^{\pi} \frac{1 - |a_k|^2}{(1 - \bar{a}_k e^{it})(1 - a_k e^{-it})} \\
&\quad \frac{e^{ijt} (e^{-it} - \bar{a}_k)^{\ell} \prod_{j=0}^{k-1} (e^{-it} - \bar{a}_j)^{\ell+1} \prod_{j=k+1}^{N-1} (e^{-it} - \bar{a}_j)^{\ell}}{(1 - \bar{a}_k e^{it})^m (1 - a_k e^{-it})^{\ell} \prod_{j=0}^{k-1} (1 - a_j e^{-it})^{\ell+1} \prod_{j=k+1}^{N-1} (1 - a_j e^{-it})^{\ell}} dt
\end{aligned}$$

Similarly to the simple case, a Poisson integral has been obtained, expressed upon the pole a_k . It can be observed, that the integrand is essentially the same as in the simple case with

the exception of the factor

$$d_{k\ell}(e^{it}) \doteq \frac{\prod_{j=0}^{k-1} (e^{-it} - \bar{a}_j)^{\ell+1} \prod_{j=k+1}^{N-1} (e^{-it} - \bar{a}_j)^\ell}{\prod_{j=0}^{k-1} (1 - a_j e^{-it})^{\ell+1} \prod_{j=k+1}^{N-1} (1 - a_j e^{-it})^\ell}, \quad (4.3.2)$$

which does not depend on m . After the same type of simplifications in the integrand for the cases $m < \ell$ and $m \geq \ell$, and evaluation of the Poisson integral, the following functions will be obtained:

$$\begin{aligned} & \frac{(\bar{q} - a_k)^{\ell-m}}{(1 - a_k \bar{q})^\ell} d_{k\ell}(q) \quad (m < \ell) \\ & \frac{q^{m-\ell}}{(1 - \bar{a}_k q)^{m-\ell} (1 - a_k \bar{q})^\ell} d_{k\ell}(q) \quad (m \geq \ell) \end{aligned}$$

For $q = a$ the case $m < \ell$ results in 0. For the case $m \geq \ell$ the expression of the representation coefficient c_n is equal to

$$c_n \doteq c_{N\ell+k} = \frac{d_{k\ell}(a_k)}{\sqrt{1 - |a_k|^2}} \sum_{m=\ell}^{\infty} \frac{a_k^{m-\ell}}{(1 - |a_k|^2)^m} (\Delta \bar{a}_k)^m,$$

which — with similar considerations as in the simple case — can be transformed into

$$c_n \doteq c_{N\ell+k} = \frac{d_{k\ell}(a_k) \sqrt{1 - |a_k|^2}}{1 - |a_k|^2 - a_k \Delta \bar{a}_k} \left(\frac{\Delta \bar{a}_k}{(1 - |a_k|^2)} \right)^\ell. \quad (4.3.3)$$

It follows from this form, that the use of other poles than the concerned one in the generalized orthonormal basis does not significantly affect its behavior, i.e. in the case of deflection, the representation will be infinite with coefficients exponentially decreasing with decay rate dependent on the difference. Strictly speaking, besides the decay rate there is an additional dependence upon the indexes ℓ through the factors $d_{k\ell}$, however this has no significance on the magnitude of the coefficients, since $|d_{k\ell}(e^{it})| = 1$, i.e. $d_{k\ell}(q)$ is an inner function, while the phase of the coefficients has no influence upon convergence aspects.

Some examples to illustrate the behavior of the GOB coefficients in the case of multiple poles can be found in the next section.

The situation is a bit different if the multiplicity of the pole under analysis is more than one. Let the function $F(q)$ containing a single pole a with multiplicity $m \in \mathbb{N}$ be expressed

with the difference of poles related to the reference poles a_k ($k = 0, 1, \dots, N-1$) as

$$F(q) = \frac{1}{(1 - (\bar{a}_k + \Delta\bar{a}_k)q)^{m_k}}.$$

The series form of this function can be obtained by using the formula

$$\begin{aligned} (1-x)^{-m} &= 1 + mx + \frac{m(m+1)}{2!}x^2 + \frac{m(m+1)(m+2)}{3!}x^3 + \dots = \\ &= \sum_{j=0}^{\infty} \frac{(m+j-1)!}{(m-1)!j!} x^j, \end{aligned} \quad (4.3.4)$$

which is valid for $0 \leq x < 1$ and $m \in \mathbb{N}$; this formula can be proved on the basis of to the binomial theorem applied for negative powers. Applying the formula to (4.3) by substituting $x = q\Delta\bar{a}_k/(1 - \bar{a}_kq)$

$$\begin{aligned} \frac{1}{(1 - (\bar{a}_k + \Delta\bar{a}_k)q)^m} &= \frac{1}{(1 - \bar{a}_kq)^m} \left[1 + m \frac{q\Delta\bar{a}_k}{1 - \bar{a}_kq} + \frac{m(m+1)}{2!} \left(\frac{q\Delta\bar{a}_k}{1 - \bar{a}_kq} \right)^2 + \dots \right. \\ &\quad \left. \dots + \frac{m(m+1) \dots (m+j-1)}{j!} \left(\frac{q\Delta\bar{a}_k}{1 - \bar{a}_kq} \right)^j + \dots \right] = \\ &= \sum_{j=0}^{\infty} \frac{(m+j-1)!}{(m-1)!j!} \frac{(q\Delta\bar{a}_k)^j}{(1 - \bar{a}_kq)^{m+j}}, \end{aligned}$$

which for $m = 1$ results in the formula (4.3.1) obtained for a simple pole.

To compute the coefficients of the representation in a generalized orthonormal basis the above applied procedure can be repeated:

$$\begin{aligned} c_n &\doteq \langle F, \Phi_n \rangle = \\ &= \frac{\sqrt{1 - |a_k|^2}}{2\pi} \int_{-\pi}^{\pi} \sum_{j=0}^{\infty} \frac{(j+m-1)!}{j!(m-1)!} (\Delta\bar{a}_k)^j \frac{e^{ijt}}{(1 - \bar{a}_k e^{it})^{m+j}} \\ &\quad \frac{\prod_{j=0}^{k-1} (e^{-it} - \bar{a}_j)^{\ell+1} \prod_{j=k}^{N-1} (e^{-it} - \bar{a}_j)^{\ell}}{\prod_{j=0}^k (1 - a_j e^{-it})^{\ell+1} \prod_{j=k+1}^{N-1} (1 - a_j e^{-it})^{\ell}} dt = \\ &= \frac{1}{\sqrt{1 - |a_k|^2}} \sum_{j=0}^{\infty} \frac{(j+m-1)!}{j!(m-1)!} (\Delta\bar{a}_k)^j \frac{1}{2\pi} \int_{-\pi}^{\pi} \frac{1 - |a_k|^2}{(1 - \bar{a}_k e^{it})(1 - a_k e^{-it})} \\ &\quad \frac{e^{ijt} (e^{-it} - \bar{a}_k)^{\ell} \prod_{j=0}^{k-1} (e^{-it} - \bar{a}_j)^{\ell+1} \prod_{j=k+1}^{N-1} (e^{-it} - \bar{a}_j)^{\ell}}{(1 - \bar{a}_k e^{it})^{j+m-1} (1 - a_k e^{-it})^{\ell} \prod_{j=0}^{k-1} (1 - a_j e^{-it})^{\ell+1} \prod_{j=k+1}^{N-1} (1 - a_j e^{-it})^{\ell}} dt \end{aligned}$$

Let the notation $d_{k\ell}(q)$ be used according to (4.3.2). The Poisson integral — after performing the suitable simplifications — can be evaluated in the cases as follow, resulting in functions:

- Case 1: ($\ell \geq m - 1$) AND ($j < \ell - m + 1$),

$$\frac{(q - a_k)^{\ell-j-m+1} q^{-(m-1)}}{(1 - a_k \bar{q})^\ell} d_{k\ell}(q),$$

which results in zero if $q = a_k$, since this is a zero of the function with multiplicity $(\ell - j - m + 1)$.

- Case 2: ($\ell \geq m - 1$) AND ($j \geq \ell - m + 1$) OR ($\ell < m - 1$),

$$\frac{q^{j-\ell}}{(1 - \bar{a}_k q)^{j+m-1-\ell} (1 - a_k \bar{q})^\ell} d_{k\ell}(q).$$

which results in value different than zero for $q = a_k$,

$$\frac{a_k^{j-\ell}}{(1 - |a_k|^2)^{j+m-1}}.$$

There are also two cases, that must be considered in obtaining the representations coefficients, the case ($\ell < m - 1$) and ($\ell \geq m - 1$).

In the case ($\ell < m - 1$)

$$\begin{aligned} c_n \doteq c_{N\ell+k} &= \frac{d_{k\ell}(a_k)}{\sqrt{1 - |a_k|^2}} \sum_{j=0}^{\infty} \frac{(j + m - 1)!}{j! (m - 1)!} \frac{a_k^{j-\ell}}{(1 - |a_k|^2)^{j+m-1}} (\Delta \bar{a}_k)^j = \\ &= \frac{d_{k\ell}(a_k)}{a_k^\ell (1 - |a_k|^2)^{m-1/2}} \sum_{j=0}^{\infty} \frac{(j + m - 1)!}{j! (m - 1)!} \left(\frac{a_k \Delta \bar{a}_k}{1 - |a_k|^2} \right)^j. \end{aligned}$$

The infinite sum is convergent according to (4.3.4), the condition of convergence

$$\left| \frac{a_k \Delta \bar{a}_k}{1 - |a_k|^2} \right| < 1,$$

is satisfied, if both the assumed and the analyzed pole is placed within the unit cycle. The coefficient will be

$$c_n \doteq c_{N\ell+k} = \frac{d_{k\ell}(a_k) \sqrt{1 - |a_k|^2}}{a_k^\ell (1 - |a_k|^2 - a_k \Delta \bar{a}_k)^m},$$

which shows some degree of dependency upon the difference Δa_k , because of multiplicity the change is more abrupt than it can be seen on Figure 4.1; the relative change of coefficient can be seen for pole with absolute value 0.9, and multiplicities 1, 2, 3, 4, 5 and 6 on Figure 4.3.

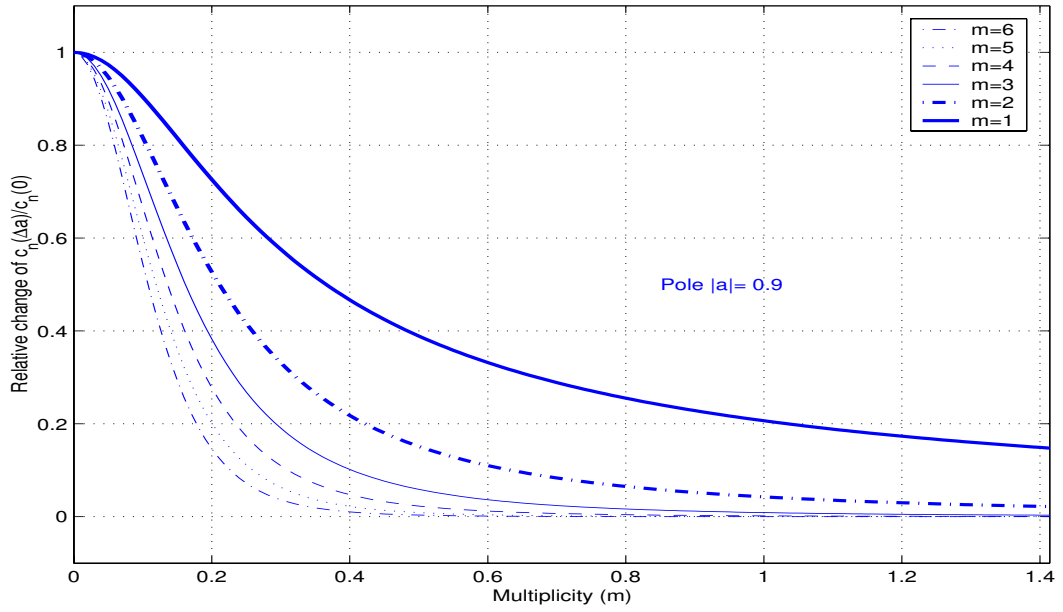


Figure 4.3: Relative change of coefficients as the function of Δa

The second case — ($\ell \geq m - 1$) — is a bit more complicated:

$$\begin{aligned} c_n = c_{N\ell+k} &= \frac{d_{k\ell}(a_k)}{\sqrt{1-|a_k|^2}} \sum_{j=\ell-m+1}^{\infty} \frac{(j+m-1)!}{j!(m-1)!} \frac{a_k^{j-\ell}}{(1-|a_k|^2)^{j+m-1}} (\Delta \bar{a}_k)^j = \\ &= \frac{d_{k\ell}(a_k)}{a_k^\ell (1-|a_k|^2)^{m-1/2}} \sum_{j=\ell-m+1}^{\infty} \frac{(j+m-1)!}{j!(m-1)!} \left(\frac{a_k \Delta \bar{a}_k}{1-|a_k|^2} \right)^j. \end{aligned}$$

The convergence condition of the infinite sum is the same as above, however to evaluate it, the finite sum of the elements of indices 0 to $\ell - m$ must be subtracted from the limit, i.e

by using the notation $x = \frac{a_k \Delta \bar{a}_k}{1 - |a_k|^2}$

$$\begin{aligned} & \frac{1}{(1-x)^m} - \sum_{j=0}^{\ell-m} \frac{m(m+1)(m+2)\dots(m+j-1)}{j!} x^j = \\ & \frac{1}{(1-x)^m} \left(1 - (1-x)^m \sum_{j=0}^{\ell-m} \frac{m(m+1)(m+2)\dots(m+j-1)}{j!} x^j \right) \end{aligned}$$

The rightmost factor of the result is a polynomial of degree ℓ of variable x — i.e. $\frac{a_k \Delta \bar{a}_k}{1 - |a_k|^2}$; let it be denoted by $Q^\ell(x)$. With it the coefficient of the representation c_n will be given as

$$\begin{aligned} c_n \doteq c_{N\ell+k} &= \frac{d_{k\ell}(a_k)}{a_k^\ell (1 - |a_k|^2)^{m-1/2}} \frac{1}{\left(1 - \frac{a_k \Delta \bar{a}_k}{1 - |a_k|^2}\right)^m} Q^\ell \left(\frac{a_k \Delta \bar{a}_k}{1 - |a_k|^2} \right) = \\ &= d_{k\ell}(a_k) \sqrt{1 - |a_k|^2} \frac{\frac{1}{a_k^\ell} Q^\ell \left(\frac{a_k \Delta \bar{a}_k}{1 - |a_k|^2} \right)}{(1 - |a_k|^2 - a_k \Delta \bar{a}_k)^m} \end{aligned} \quad (4.3.5)$$

Comparing this result with that obtained in the case of pole with no multiplicity — see (4.3.3) — it can be observed, that instead of the ℓ -th order of the variable $\frac{a_k \Delta \bar{a}_k}{1 - |a_k|^2}$ a polynomial of degree ℓ has been given, and the weighting factor is also has been modified to degree m , i.e. the number of multiplicity. Essentially the statement has not been changed: in the case of a deflection on a pole relatively to an a priori selected pole set the set of the representation coefficient will become infinite, and the coefficients show an approximately exponential decreasing with decay rate dependent upon the difference.

On Figure 4.4 and 4.5 the case of pole multiplicities greater than one are presented for exact representation of a single real pole ($a = 0.6$), as well as the same with difference $\Delta a = 0.3$. Figure 4.4 presents multiplicity 2, and Figure 4.4 multiplicity 3.

Any function $F(z) \in \mathcal{H}_\perp^2$ is considered to be expressed in partial fraction form

$$F(z) = \sum_{k=0}^{N-1} \sum_{m=1}^{m_k} \frac{A_{km}}{(z - a_k)^m}$$

where N is the number of the distinct poles, $\{a_k\}_{k=0}^{N-1}$ the set of poles, and $\{m_k\}_{k=1}^N$ the multiplicities belonging to them. That is, the function can be expressed as a finite sum of

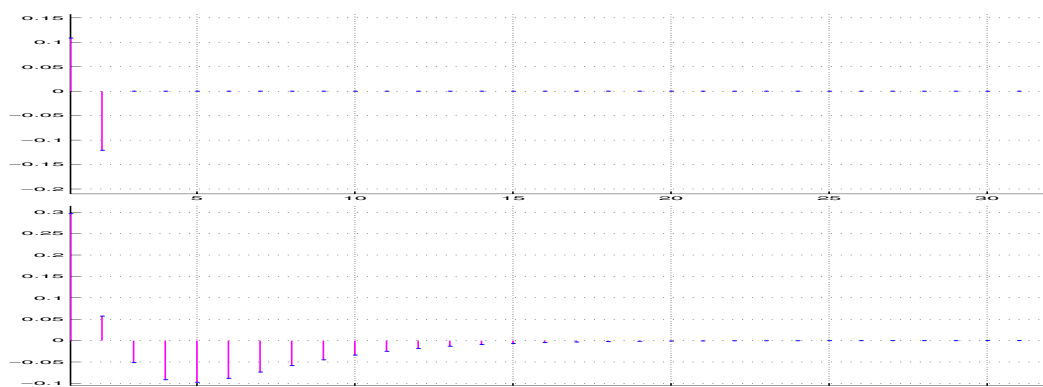


Figure 4.4: GOB coefficients: single pole with multiplicity 2

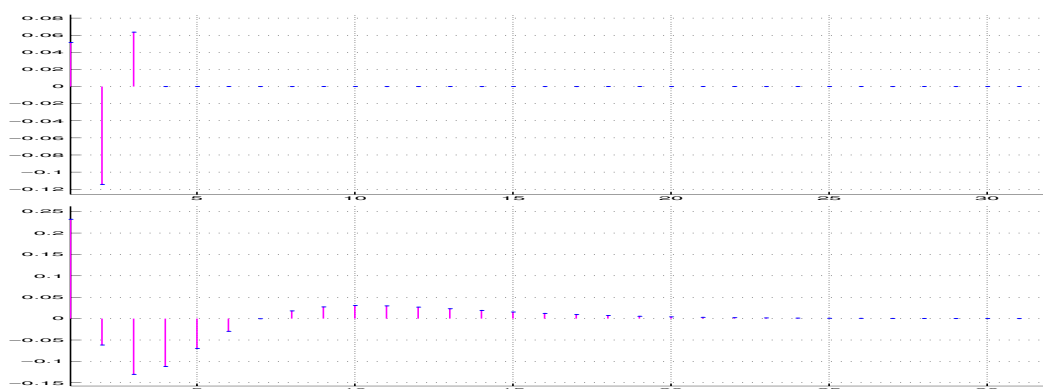


Figure 4.5: GOB coefficients: single pole with multiplicity 3

terms like

$$\frac{A_{km}}{(z - a_k)^m},$$

and the representation in GOB can be performed term by term. This can easily be proved — by returning to the mathematical form — for $F(q) \in \mathcal{H}^2$

$$F(q) = \sum_{k=0}^{N-1} \sum_{j=1}^{m_k} \frac{A_{km}}{(1 - \overline{a_k}q)^m} \quad (4.3.6)$$

By regarding the linearity of the scalar product on the first operand, the representation coefficient c_n can be expressed as

$$c_n = \left\langle \sum_{k=0}^{N-1} \sum_{m=1}^{m_k} \frac{A_{km}}{(1 - \bar{a}_k q)^m}, \Phi_n \right\rangle = \sum_{k=0}^{N-1} \sum_{m=1}^{m_k} A_{km} \left\langle \frac{1}{(1 - \bar{a}_k q)^m}, \Phi_n \right\rangle = \sum_{k=0}^{N-1} \sum_{m=1}^{m_k} A_{km} c_n^{[km]},$$

where

$$c_n^{[km]} \doteq \left\langle \frac{1}{(1 - \bar{a}_k q)^m}, \Phi_n \right\rangle$$

can be considered as the n -th coefficient of the partial representation belonging to the term (4.3.6). The coefficients of the representation are built up as a weighted sum of the partial representation coefficients.

The terms including in the partial fraction of a function F have the form of one of the cases discussed in details above. The results of the discussion can be summarized as follow:

- If the pole under consideration is exactly equal to the a priori assumed one in the GOB (i.e. $\Delta a_k = 0$), the partial representation will contain finite number of elements — exactly m_k ones, the number of the multiplicity of the pole.
- If the pole under consideration deflects from the a priori assumed one in the GOB (i.e. $\Delta a_k \neq 0$), the partial representation will be infinite; the elements with index greater than m_k show a decay as the index is increased with approximately exponential decay rate dependent on the difference to the representing pole actually considered; larger difference results in smaller rate.

This model can be used both in the case of displacement on the existing poles (included all in the pole set assumed in the GOB), and in occurring new ones.

Until this point the poles of a function $F(z) \in \mathcal{H}_\perp^2$ has been mentioned in connection with the GOB representation. However the zero structure is also a significant constituent of the dynamics, hence it is important to include in the analysis. The zeros of an $F(z)$ function are included in the partial fraction form by the coefficients A_{km} , several coefficients based upon

the same pole structure results in several function zeros. Several zero structures does not affect the membership of the function in the class $\mathcal{B}_a^N \mathcal{H}^2$, until the strictly proper character of the function remains valid. As a consequence: the zero structure of a function $F(z)$ can be involved in the detection process through the numerical values of the representation coefficients. This can easily be done in the case of comparing several zero structures within a $\mathcal{B}_a^N \mathcal{H}^2$ class, however it can be rather complicated, if simultaneously a deflection on the poles is happened.

4.3.1 Detection scheme upon the representation coefficients

The simplest method to realize a detection algorithm can be based upon the direct computation of the coefficients of the representation in a generalized orthogonal basis (GOB) defined in Theorem 2.4.6. — constructed upon an a priori fixed set of poles $a = \{a_k \in \mathbb{D}, k = 0, 1, 2, \dots, N - 1\}$. The coefficients can approximately be computed by introducing the argument transform and using the FFT algorithm, as it has been described in Chapter 3.

Some examples are given here to illustrate the behavior of the GOB coefficients. The examples contain variations on the difference of the poles in respect to those applied to build the generalized orthogonal basis, and those belonging to the system to be analyzed. The reference poles used in the examples are as follow:

$$\mathbf{a} = [0.9, 0.99e^{i0.5}, 0.99e^{-i0.5}, 0.98e^{i0.8}, 0.98e^{-i0.8}].$$

The following examples has been generated:

Example 4.3.1. *The same system poles has been used in the example as the reference ones, i.e. the exact case has been represented. The GOB coefficients has been presented on the Figure 4.6 in two forms: the sequence of the coefficients can be seen on the complex plane (left-side diagram), and the real and imaginary parts against the indices (right-side*

diagrams). Finite number of significant coefficients can be detected, a small error can be observed as the consequence of the approximation used by the algorithm to compute the coefficients.

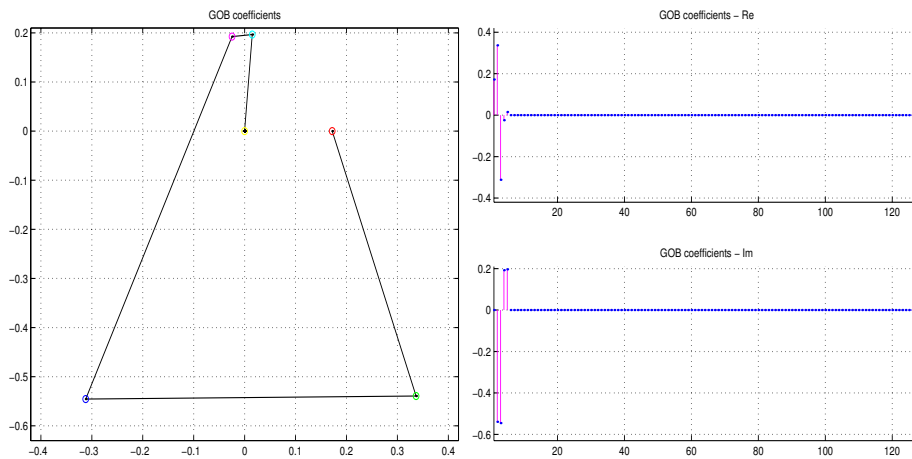


Figure 4.6: Example 4.3.1 — the exact case

Example 4.3.2. The real pole has been perturbed with $\Delta a = 0.2$. The results can be seen on the Figure 4.7 in the same form as in Example 4.3.1. The representation has become infinite with fast decay on the coefficient associated with the perturbed pole.

Example 4.3.3. One of the conjugated complex pole pole pairs has been perturbed such a way, that only the dampedness of the pole changed. The results can be seen on the Figure 4.8. The representation is infinite with fast decay on the coefficient associated with the perturbed poles.

Example 4.3.4. One of the conjugated complex pole pole pairs has been perturbed such a way, that by keeping the original dampedness the tuning of of the pole changed. The results can be seen on the Figure 4.9. The decay is not so fast as in the Example 4.3.3.

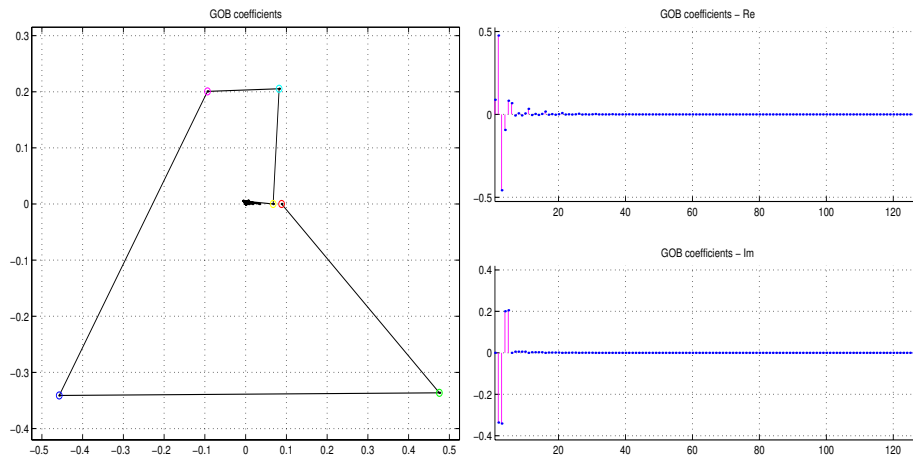


Figure 4.7: Example 4.3.2 — difference on the real pole

Example 4.3.5. *A mixed case is presented, all the poles has been perturbed. The system poles applied are as follow:*

$$\mathbf{a} = [0.8, 0.95e^{i0.45}, 0.95e^{-i0.45}, 0.9e^{i0.6}, 0.9e^{-i0.6}].$$

The results can be seen on the Figure 4.10. An infinite representation can be found with some decay on the coefficients. The differences are considered to be quite big.

As it can be derived form the definition of the GOB (see also the Tables 2.3 and 2.4) the representation coefficients can be divided in groups of N members, where N is the number of the a priori assumed poles. The subsequent groups contain the same poles with successively increasing multiplicity. If the analyzed system possesses exactly the poles that has been presumed, i.e. all of those poles and no other ones are included in the system, the representation will be finite, i.e. a finite set of coefficients will differ from zero, and there exists an index $n \geq N$, from which all the coefficients are zero. The index n is greater than N if at least one pole has multiplicity more than one.

If the poles of the analyzed system does not exactly matches the presumed ones, i.e. one or more poles differ, or new poles have occurred, the representation will become infinite.

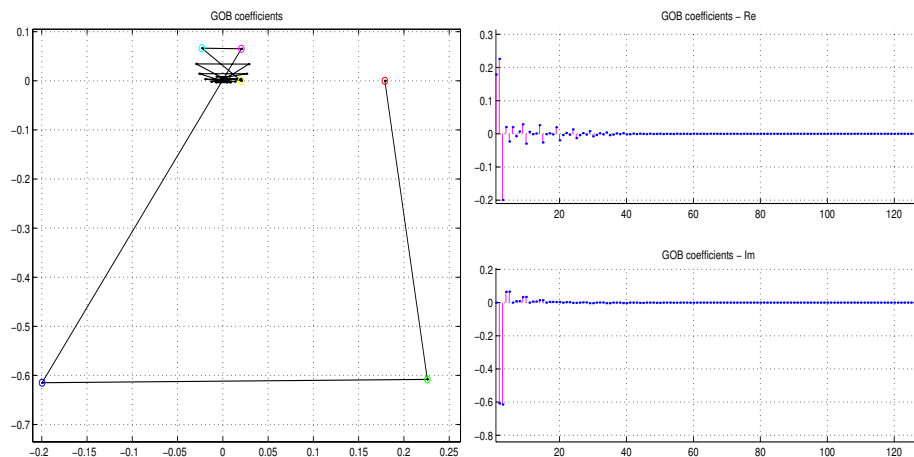


Figure 4.8: Example 4.3.3 — difference on conjugated complex pair

In this case the speed of the decay on the coefficients can give a means for analyzing the measure of the deviation, and making decisions upon it.

In practical cases the data involved in the detection process contain error originating from many sources, e.g.

- Noises in the original signal, originated from physical effects not completely modelled.
- Measurement noise, inaccuracies in the measurement process, quantization errors, bias and variance errors in the preprocessing algorithms.
- Bias error of the representation algorithm, originating e.g. from the truncation of infinite series, as well as quantization and rounding errors in the computations.

These effects will be referred — with some simplification — as *noise*. The noise is usually considered as an additive error concentrated to several points of the process, for example input and output errors are involved in the analysis. In the present discussion these two error types have significance, i.e.

- Input noise: an additive error term cause a deflection on the poles of the system to

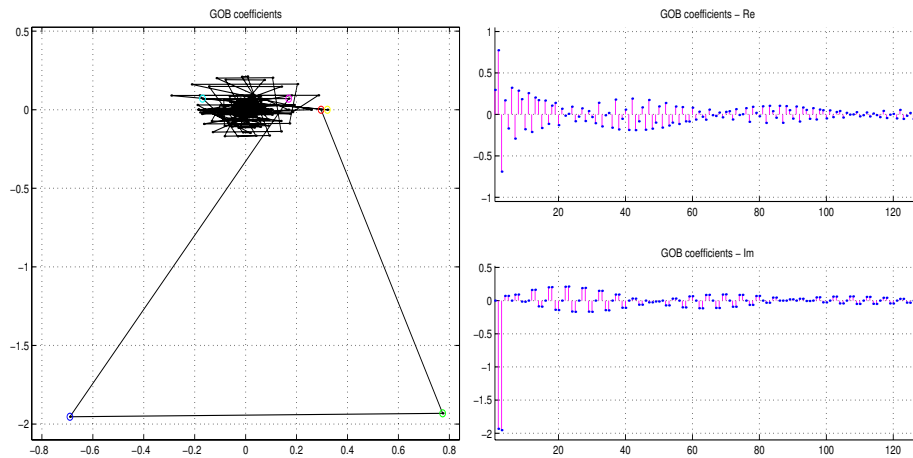


Figure 4.9: Example 4.3.4 — difference on conjugated complex pair

be analyzed.

- Output noise: an additive error is superposed on the representation coefficients.

Of course the input noise results in an error on the coefficients mixed with the output error, hence a difficult task is to separate them. A possibility to do this is originated from the statistics of the noise, based upon a priori assumptions or observations. Hence the decision process which is made upon the coefficients is possible to perform on statistical basis.

The input noise is transferred into the coefficients as it has been shown in the Section 4.3.1. That is, an additive error on a pole results in an infinite set of coefficients with exponential decay. In the case of deterministic deflection on poles are present, the input noise is superimposed on it resulting in modified coefficients on the output. If the statistics of the input noise is known, or assumed, the statistics of any coefficient can be estimated by using the formulas (4.3.3) for the simple case and (4.3.5) for poles with multiplicity. This procedure can be very complicated mainly by assuming multiplicity on poles. A practically tractable way is to estimate the statistics of the "nominal" case, i.e. that belonging to the a priori assumed pole set in GOB, and using them for small deflections around the nominal

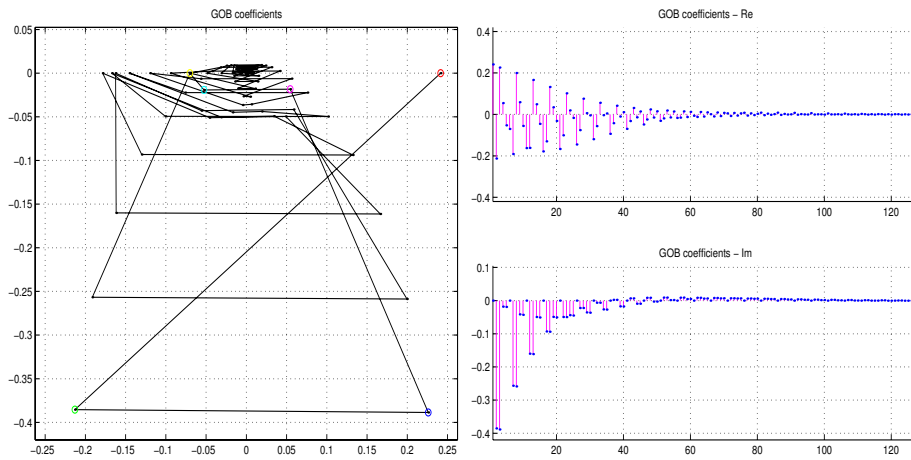


Figure 4.10: Example 4.3.5 — difference on all the poles

case.

Example 4.3.6. *An example is presented to illustrate the cause of noises. The example is based upon the system and representation introduced in the Example 4.3.1. The difference is, that an additive normally distributed noise with zero mean has been applied on the function values involved in the GOB representation. The variance of the noise has been set to 5% relatively to the maximal function value. The results can be seen on the Figure 4.11. It can be observed, that the original coefficients has kept their dominance, a small error can be detected on the remaining ones.*

The output noise include all the errors generated within the representation algorithm. A significant part of it is originated from the truncation of the infinite sums in the practical computations, additional error terms arise from the limited accuracy of data representation (the quantization error). A detailed error analysis exceed the scope of the current work.

A simple decision scheme can be constructed by defining error limits — either on statistical or other way, for example by applying empirical considerations — that are used as thresholds. A typical problem is for example the null-hypothesis test, i.e. decision upon

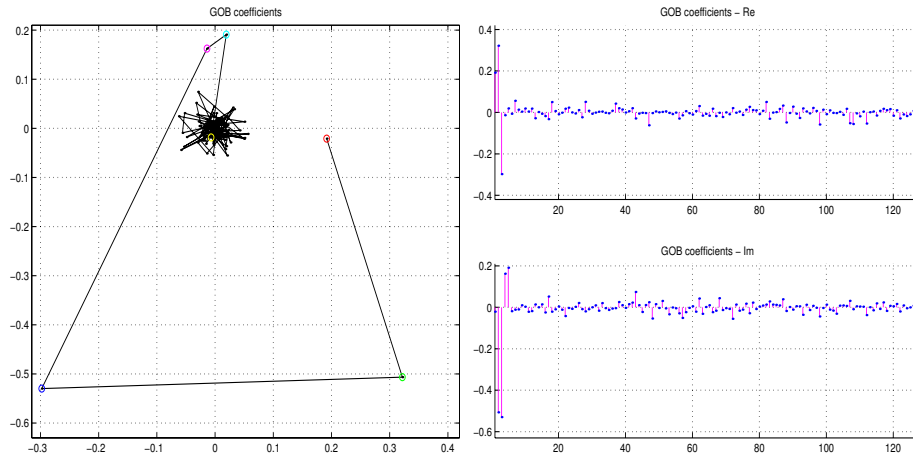


Figure 4.11: Example 4.3.6 — additive noise

whether a coefficient is equal to zero or differs significantly of it. In the presence of output noises the coefficients are not exactly nullified, in this case the error limit can be used as a threshold to decide, which coefficients are significant, and which ones can be considered to be zero.

Numerous detection methods can be generated within the framework of the representation in generalized orthonormal bases, depending on the specific task to be solved, by using different decision rules. Both methods contain common steps that are summarized as follow:

Step 1: A reference system is considered by fixing a finite set of different poles $\mathcal{D} = \{a_k \in \mathbb{D} \mid k = 0, 1, \dots, N - 1\}$, hence the generalized orthogonal basis is defined, as well as the non-uniform frequency scale belonging to the argument function of the GOB, required in the measurements and computations, is derived.

Step 2 The frequency domain measurements of the analyzed function F are performed according to the non-uniform scale belonging to the GOB.

Step 3 The representation of F in the generalized orthogonal basis is generated, i.e. the representation coefficients are computed by using the measurement values arranged in the non-uniform scale. The algorithm of the approximate computing of the coefficients is that described in Chapter 3.

Step 4 The detection problem is solved on the basis of the coefficients computed by applying a decision rule.

Based upon the theoretical background given in Section 4.3 the following standard decision rules, to be used in the Step 4, are specified:

Rule 1: *Detection upon belonging to a class*

1. The simplest question that can be answered, whether the signal analyzed, belongs to the class $\mathcal{B}_a^N \mathcal{H}^2$ generated by the set of a priori selected set of poles. The detection problem is equivalent with the decision whether exactly the first N coefficients of the representation differs from zero. In the presence of noise the goal must be translated to the forms: decision upon whether the first N coefficients differ significantly from zero, or a null-hypothesis test upon the coefficients if indices greater than N .
2. A modified form of the previous task is the detection whether the signal belongs to a broader class in which the poles are considered with higher multiplicity. The detection problem can be translated to this situation: decision upon whether m ($m = 1, 2, \dots$) N -tuples of coefficients differ significantly from zero. The multiplicities of the individual poles can also be derived by analyzing the individual coefficients within the N -tuples.

Rule 2: *Detection upon properties within a class* with the premise that the signal belongs to the class fixed by the a priori assumed poles, based upon the set of the significant coefficients specific can be detected, as

1. Correspondence with a predefined zero structure. The coefficients belonging to one or more specific zero structure can in advance be computed, and these values possibly complemented with error bounds can be used to detect the validity of any structure.
2. Detection of missing poles or multiplicities. Within the set of the significant coefficients some of them can happen to be considered as zero, which give the possibility to detect missing poles, or multiplicities in the extended class.

Rule 3: *Detection of changes relative to the presumed pole set* in the case, when the representation become infinite. This can happen as a consequence of

- displacement of one or more poles,
- occurring one or more new poles.

Based upon the decay rate experienced on the coefficients, the degree of the deviance can — at least qualitatively — be estimated.

Besides these "standard" detection rules numerous other ones can be generated on the basis of additional knowledge — obtained by physical, technological considerations, or purely by the experience — in connection with particular coefficients or groups of them. The detailed study of these type of detection problems exceeds the framework of the current thesis work.

4.3.2 Detection by building reproducing kernel in GOB

A detection method, which does not require the direct computation of the representation coefficients, can be obtained on the basis of reproducing kernel properties of the space $\mathcal{B}_a^N \mathcal{H}^2$, i.e. that generated by the finite Takenaka-Malmquist representation on poles $\{a_k \in \mathbb{D} \mid k = 0, 1, 2, \dots, N - 1, (N \in \mathbb{N})\}$. It can easily be shown, that $\mathcal{B}_a^N \mathcal{H}^2$ space is a reproducing kernel Hilbert space (RKHS). The function $K(z, \mu)$ ($z, \mu \in \mathbb{D}$) is a reproducing kernel in the closed subspace $V \subset \mathcal{H}^2$ if

- for every μ the function $K(z, \mu)$ belongs to V , and
- for all $\mu \in \mathbb{D}$ and every $f \in V$ $f(\mu) = \langle f(z), K(z, \mu) \rangle_z$, where the subscript $z \in \mathbb{D}$ of the scalar product indicates that it is applied to functions of z , referred as the *reproducing property*.

For a detailed introduction to the field of RKHS, and more general definitions see e.g. Chapter 3. of [36], here only some simple results will be recalled. An important theorem describes the connection between a reproducing kernel and orthogonal basis; a simplified form — satisfactory for the current discussion — is presented as follows:

Theorem 4.3.7. *Let $\{\phi_k \mid k \in \mathbb{N}^*\}$ an orthogonal basis in the Hilbert space \mathcal{H} , in that case the reproducing kernel has the form*

$$K(q, s) = \sum_{k=0}^{\infty} \phi_k(q) \overline{\phi_k(s)}.$$

Proof. The function $K(q, s) \in \mathcal{H}$ for any s , hence it can be represented by the orthogonal basis:

$$K(q, s) = \sum_{k=0}^{\infty} \langle K(u, s), \phi_k(u) \rangle \phi_k(q). \quad (4.3.7)$$

According to the reproducing property of $K(q, s)$

$$\langle K(u, s), \phi_k(u) \rangle = \overline{\langle \phi_k(u), K(u, s) \rangle} = \overline{\phi_k(s)},$$

which proves (4.3.7). □

This theorem is also valid in finite dimensional spaces, as it is the space $\mathcal{B}_a^N \mathcal{H}^2$, generating by the finite Takenaka-Malmquist system of dimension N . The next theorem can be stated:

Theorem 4.3.8. *The subspace $\mathcal{B}_a^N \mathcal{H}^2 \subset \mathcal{H}^2$ generated by the finite Takenaka-Malmquist system is a RKHS with reproducing kernel*

$$K(q, s) = \frac{1 - B_N(q) \overline{B_N(s)}}{1 - q\bar{s}}, \quad (4.3.8)$$

where N is the dimension of the system, and $B_N(q)$ is the Blaschke-product defined upon its elements.

Proof. The subspace generated by the N -dimensional Takenaka-Malmquist system — the space of the strictly proper rational functions of maximal order N — is a Hilbert-space, and the Takenaka-Malmquist is an orthonormal basis in it. Hence a reproducing kernel can be constructed according to Theorem 4.3.7:

$$K(q, s) = \sum_{k=0}^{N-1} \Phi_k(q) \overline{\Phi_k(s)},$$

where Ψ_n ($n = 0, 1, \dots, N - 1$) functions are the elements of the basis. By applying the definition of the Takenaka-Malmquist system the k -th term of the sum can be expressed as follows:

$$\Psi_k(q) \overline{\Psi_k(s)} = \frac{1 - |a_k|^2}{(1 - \overline{a_k}q)(1 - a_k\overline{s})} \prod_{j=0}^{k-1} \frac{q - a_j}{1 - \overline{a_j}q} \frac{\overline{s} - \overline{a_j}}{1 - a_j\overline{s}}. \quad (4.3.9)$$

Let the following equivalence be considered:

$$\frac{1 - b_k(q) \overline{b_k(s)}}{1 - q\overline{s}} = \frac{1 - |a_k|^2}{(1 - \overline{a_k}q)(1 - a_k\overline{s})}, \quad (4.3.10)$$

where b_k is the Blaschke-function belonging to a_k defined as

$$b_k(q) = \frac{q - a_k}{1 - \overline{a_k}q}.$$

The equivalence (4.3.10) can easily be proven by substituting the expression of the Blaschke-function with some algebraic manipulations. Applying (4.3.10) to (4.3.9) leads to the next form:

$$\begin{aligned} \Psi_k(q) \overline{\Psi_k(s)} &= \frac{1 - b_k(q) \overline{b_k(s)}}{1 - q\overline{s}} \prod_{k=1}^{n-1} b_k(q) \overline{b_k(s)} = \\ &= \frac{B_{k-1}(q) \overline{B_{k-1}(s)} - B_k(q) \overline{B_k(s)}}{1 - q\overline{s}}. \end{aligned}$$

By summing the N terms, and applying $B_0 = 1$ according to the definition of the Blaschke-product,

$$\frac{1}{1 - q\bar{s}} \sum_{k=0}^{N-1} (B_{k-1}(q)\overline{B_{k-1}(s)} - B_k(q)\overline{B_k(s)}) = \frac{1 - B_N(q)\overline{B_N(s)}}{1 - q\bar{s}},$$

which proves the theorem. \square

For the purposes to obtain an easily usable form of the reproducing kernel, its restriction on the unit circle $K(e^{it}, e^{i\tau})$ has specific significance, which can be expressed with the argument function introduced in Chapter 2:

$$K(e^{it}, e^{i\tau}) = \frac{1 - e^{iN(\beta_N(t) - \beta_N(\tau))}}{1 - e^{i(t-\tau)}}. \quad (4.3.11)$$

It can be observed, that the numerator is equal to zero in the points $t, \tau \in [-\pi, \pi]$ where

$$\beta_N(t) - \beta_N(\tau) = n \frac{2\pi}{N},$$

however the denominator is equal to zero only in

$$t - \tau = 0.$$

By selecting a sequence of points $\{t_n \mid n = 0, 1, \dots, N-1\}$ such that, since the inverse of the argument function exists as it has been shown in Chapter 2,

$$t_n = \beta_N^{-1}(s_n) \quad \text{where} \quad s_n = -\pi + n \frac{2\pi}{N}, \quad (4.3.12)$$

and by using the l'Hôpital rule to resolve the indefinite $0/0$ case when the denominator becomes zero, the reproducing kernel can be expressed as

$$K(e^{it_n}, e^{it_\ell}) = \begin{cases} 0 & \text{if } n \neq \ell, \text{ and} \\ N\beta'_N(t_n) & \text{if } n = \ell. \end{cases} \quad (4.3.13)$$

For future reference let the set of e^{it_n} points be denoted by

$$\mathbb{T}_\beta^N = \{e^{it_n} \mid t_n = \beta_N^{-1}(-\pi + n \frac{2\pi}{N}), n = 0, 1, \dots, N-1\}. \quad (4.3.14)$$

The form 4.3.13 is beneficial in computational point of view, because the derivative of the argument function can easily be computed as the reciprocal of the derivative of its inverse, by using the computable form

$$\left[\frac{d}{ds} \beta_a^{-1}(s) \right]_{s=s_n} = \frac{N}{\sum_{k=0}^{N-1} \frac{1+|a_k|}{|1-\bar{a}_k e^{i\beta_N^{-1}(s_n)}|^2}}$$

as it has been shown in the section 2.4.5.

The sequence of points $\{t_n\}$ results in a non-uniformly spaced lattice in the interval $[-\pi, \pi]$ based upon the values of the inverse argument function computed on points uniformly spaced in the same interval. The variable t — in the technical sense — is identical with a normalized circular frequency relative to the Nyquist-frequency associated with the sampling. Hence the points $\{t_n\}$ can be considered as non-uniformly spaced sample points on the frequency variable.

The application of this discrete form of the reproducing kernel will be obvious in accordance with the following theorem:

Theorem 4.3.9. *Let \mathcal{H} be an RKHS with reproducing kernel $K(t, \tau)$, and let $\{t_n | n = 0, 1, \dots, N-1\}$ a sequence of identical real numbers, where N is the dimension of the space. In the case, when*

$$K(t_n, t_\ell) = \delta_{n\ell}, \quad (4.3.15)$$

the system of functions $K(t, t_n)$ forms an orthonormal basis in \mathcal{H} , and for any function $f \in \mathcal{H}$

$$f(t) = \sum_{n=0}^{N-1} f(t_n) K(t, t_n). \quad (4.3.16)$$

Proof. $K(t, t_n)$ is an orthonormal system, if

$$\langle K(t, t_n), K(t, t_\ell) \rangle = \delta_{n\ell}.$$

furthermore, according to the reproducing property of $K(t, \tau)$

$$\langle K(t, t_n), K(t, t_\ell) \rangle = K(t_n, t_\ell),$$

hence (4.3.15) will be resulted as the condition of the orthonormality. If the number of functions $K(t, t_k)$ is identical to the dimension of \mathcal{H} , the $K(t, t_k)$ is complete, hence it is an orthonormal basis of the space.

Any function $f \in \mathcal{H}$ can be represented in the basis in the form

$$f(t) = \sum_{n=0}^{N-1} c_n K(t, t_n)$$

where the coefficients c_n are given by the orthogonal projection

$$c_n = \langle f(t), K(t, t_n) \rangle \quad (n = 0, 1, \dots, N-1)$$

that are equal to $f(t_n)$ according to the reproducing property of $K(t, t_k)$, hence (4.3.16) is resulted, which completes the proof. \square

The formula (4.3.16) can be considered as the interpolation of function $f \in \mathcal{H}$ upon its discrete points of number corresponding to the dimension of the space (which can of course be infinite, in the situation studied is actually finite). Let an operator be defined as

$$(L_{\mathcal{H}}f)(t) \doteq \sum_{n=0}^{N-1} K(t, t_n) f(t_n), \quad (4.3.17)$$

which is an interpolation operator in the space \mathcal{H} . If the $K(t, t_n)$ system is only orthogonal and not orthonormal, $K(t, t_n)$ can be normed, and the interpolation operator gets the form of

$$(L_{\mathcal{H}}f)(t) \doteq \sum_{n=0}^{N-1} \frac{K(t, t_n)}{K(t_n, t_n)} f(t_n). \quad (4.3.18)$$

This is the case in the Takenaka-Malmquist system discussed above, the reproducing kernel must be normed with the local value of $N\beta'_N$ to result in orthonormality. A detailed theoretical study upon the characteristics of this type of interpolation operators can be found in [66].

The interpolation operator 4.3.18 with the kernel (4.3.13) can be used to solve some types of detection problems. The main idea is, that in this case 4.3.18 is an interpolation

operator only in the space $\mathcal{B}_a^N \mathcal{H}^2$, hence the "quality" of the interpolation gives a good means for detecting the deflection of the analyzed function from this space. A measure of the interpolation quality can be the *discrete scalar product* defined as follows:

Definition 4.3.1. Let f and g be functions belonging to the RKHS $\mathcal{B}_a^N \mathcal{H}^2$ with reproducing kernel $K_N(t, \tau)$, the number

$$[f, g]_N^\beta \doteq \sum_{\zeta \in \mathbb{T}_\beta^N} \frac{f(\zeta) \overline{g(\zeta)}}{K_N(\zeta, \zeta)}. \quad (4.3.19)$$

is called discrete scalar product.

It is easy to show by using the reproducing property of the kernel, that

$$[f, g]_N^\beta = \langle L_N f, L_N g \rangle,$$

i.e. the discrete scalar product can be serve as a measure to compare two interpolations in the subspace concerned.

On the basis of the discrete scalar product an induced norm can also be defined as

$$\|f\|_N^\beta \doteq [f, f]_N^\beta \quad f \in \mathcal{B}_a^N \mathcal{H}^2,$$

that is called *discrete norm*. The norm gives the possibility to measure the interpolation quality of a function alone, without comparing it to another one.

The notions of the discrete scalar product and norm defined by (4.3.19) and (4.3.2), respectively, offer an advantageous means to solve detection problems on the basis of frequency domain measurements belonging to the system analyzed. The measurements should be performed on the non-uniform frequency scale associated with the generalized orthogonal basis, that stands behind the discrete scalar product or norm, i.e. \mathbb{T}_β^N according to (4.3.14). The detection problem is solved as the result of the decision procedure generated by the one of the following criteria:

1. Comparing the discrete norm of the analyzed function F to a threshold $\delta > 0$, and

$$\|\hat{F}\|_N^\beta > \delta.$$

2. Comparing the discrete norm of the difference between the analyzed function F and a reference one $\hat{F} \in \mathcal{B}_a^N \mathcal{H}^2$ to a threshold $\delta > 0$, and

$$\|\hat{F} - F\|_N^\beta > \delta.$$

3. Comparing the discrete scalar product of the analyzed function F and a reference one $\hat{F} \in \mathcal{B}_a^N \mathcal{H}^2$ to a threshold $\delta > 0$

$$\langle \hat{F}, F \rangle_N^\beta > \delta.$$

Exceeding the threshold means the acceptance of the assumption, that the difference or change has occurred. The first criterion is based upon the distance of the function F from a the subspace $\mathcal{B}_a^N \mathcal{H}^2$, hence it measures the difference of F from a class of functions. The last two criteria are based upon the distance of the function F from a reference function belonging the subspace $\mathcal{B}_a^N \mathcal{H}^2$, hence they are considered to be more specific than the first one. Further investigation an examples are presented in [65].

The detection method based upon the decision scheme described above can be performed by the following steps:

- A reference system is considered by fixing a finite set of different poles $\mathcal{D} = \{a_k \in \mathbb{D} \mid k = 0, 1, \dots, N - 1\}$, and in association with this, the computing procedure of the discrete scalar product or norm, as well as the non-uniform frequency scale \mathbb{T}_β^N to be applied in the measurements are derived. (4.3.2).
- The discrete scalar product or norm required in the decision criterion is computed on the basis of frequency domain measurement data of F , produced according to non-uniform scale \mathbb{T}_β^N .
- A decision procedure is performed by comparing the discrete scalar product or norm to a predefined threshold value $\delta > 0$.

The computation of the non-uniform frequency scale can be realized by the algorithms described in Chapter 3. The computation of the discrete scalar product and norm is quite simple, this can be considered as the main advantage of this method. The algorithms for test purposes has been realized in *MATLAB*[®] environment [65].

4.4 Noise suppression, feature enhancement

A typical task in the signal processing is the suppression of noise in signals. In many technical areas noise suppression means rather definite things, e.g. in high fidelity sound reproduction it means reducing the noise producing the electronic components (e.g. thermal noise, semiconductor junction noise, disturbance of external electric and magnetic fields). It is also obvious, that a blurred image is noisy. However, in many fields it is not definitely obvious, what does noise mean. If somebody studies the Brown-processes, the thermal noise is the effect to be considered, and not a disturbing, unwanted thing. Hence it is more acceptable to speak of suppressing unwanted constituents in signals instead of suppressing noise. To decide, what is unwanted is rather "subjective" thing, it depends upon the choice of the analyzer. It is obvious, that general noise suppression method does not exist, the procedure depends upon the goal, and the same can be stated for the goodness, effectiveness, or optimality of the procedures.

The use of knowledge on the poles of a system offers the possibility of an efficient suppression of noises and disturbances acting upon the poles itself. The method is based upon the observation made in the previous session: in the case of any difference on the pole structure — relative to that, a priori assumed — results in infinite number of representation coefficients. By selecting the significant ones and dropping the others (e.g. considering them as zero) and reconstructing the signal on this basis will result in a high level reduction of the noises. The actual values of the coefficients found significant will contain information upon

the "noiseless" signal — these can be considered as the significant features of the signal. These features can be used in further (in most cases automated) decisions, and the image of the reconstructed function can be used for human interpretation.

Dropping the coefficients falling under a predefined noise threshold can also be useful in reducing the algorithmic errors (the output error as they have been mentioned in the previous section) with the purpose to generate detection methods less sensitive to noises.

Chapter 5

Applying GOB representations: identification

In this chapter some aspects of applying generalized orthogonal bases in the identification of systems will be presented. After exploring the modelling capabilities of the GOB representations an iterative scheme to improve an initially assumed model will be presented, operating within the framework of \mathcal{H}^2 representations. Then an extension of the GOB representations toward the field of \mathcal{H}^∞ spaces will be presented, that make these representations suitable to be applied in robust identification problems.

5.1 System identification and nonstandard representations

System identification is the area, that has principally acted in the generation and development of the principle that is now called "nonstandard representations" or "nonstandard basis functions", at least in the systems science. In mathematics this field began to evolve at the beginning of the 20th century in connection with the convergence problems of the Fourier series in several function spaces, for example in \mathcal{L}^∞ . Another motor of the development was the demand for finding several orthogonal systems, which can represent any function belonging to interesting Hilbert spaces — as are the spaces \mathcal{L}^2 and \mathcal{H}^2 — which has led to the construction of the Schauder, Franklin, Walsh, Haar, and other systems;

see for details e.g. in [51], and for the motivation and historical introduction in [70]. In the field of system identification the use of nonstandard bases was also implied because of convergence problems emerged in the spaces applied to find robust solutions instead of the classical optimal ones, namely the \mathcal{L}^∞ and \mathcal{H}^∞ , see the early papers [31], [43], [16], [38], or [7] for a detailed introduction to the field.

However, besides the endeavor to find systems of functions and bases, which are suitable for representation in spaces with infinite norm, there can exist other motivation, e.g. the use of a priori available knowledge of the system in the identification. This idea is not new, most of the conventional identification methods use some amount of a priori assumption upon the system model used. For example, the parametric, e.g. the AR, ARX, ARMA, and ARMAX model based identification methods [26] use more or less strict prescriptions upon the number of parameters to be identified, and the structure in that they are arranged. By applying the concept of the generalized orthogonal bases (GOB) introduced in the Chapter 2 more specialized knowledge can be involved in the identification process, without generating excessive constraints that can extremely restrict the solution. This character is due to the fact, that these methods are not "parametric" in the sense, that the selection of the valid model is not restricted on a set of finite number of parameters.

In the current section the frequency domain identification of discrete-time systems is discussed on the basis of a priori knowledge available upon the poles belonging to them. The frequency domain identification means the derivation (at least approximately) of the transfer function of the system, which can be given on the basis of frequency functions (i.e. the Fourier-transforms) belonging to the input and output signals, or the impulse response of the system. In the classical frequency domain methods the identification process remains within the Fourier framework, i.e. applies representations in the standard trigonometric basis. The use of a priori knowledge upon the system poles involves the use the concept of generalized orthogonal bases. The identification problem of a dynamic system can be

solved by representing its input and output signals, or the impulse response if it is available, in the GOB constructed upon the presumed poles. The derivation of the transfer function on the basis of the input and output representations requires purely algebraic operations, computing a quotient for SISO type, or a matrix fraction for MIMO type systems, with simplifications on the common terms, see for appropriate methods e.g. in [26]. Hence in the context of applying generalized orthogonal bases it is sufficient to focus on the signal representation level, i.e. on the appropriate selection of the presumed pole set, as well as the realization of the signal representation, these areas will be discussed in the following sections.

The system identification methods are based upon measurements performed on the signals belonging to it. This, in the most cases, means the input and output signals, which are not necessarily identical to the de facto inputs and outputs — designed for this purpose — of the system. Inputs are considered the signals, that are determined by conditions originating outside the system, e.g. they can arbitrarily prescribed, while outputs are the signals observed outside the system, and are determined by internal conditions. Measurement means a mapping of a physical quantity upon a numeric scale of real numbers in specific time instances. The result of a measurement is usually considered an momentary value, however the measuring principle can be based upon processing — e.g. integrating, averaging or filtering — of the signal on a finite interval. In the "digital" era measurement also means the transformation of the quantity into numeric form, that means its quantization in a number system of finite accuracy. Besides sampling and quantization in most cases other processing actions are preformed with the purpose to obtain correct measurements. An important preprocessing step in the measurement of analog signals is the use of an anti-aliasing filter, which aims to produce bound-limited signal satisfying the Shannon conditions of sampling.

This characterization is valid for *time-domain* measurements. However, the measurements can be performed against any other physical quantity in the sense, that the measurements are performed depending upon conditions associated with values of a physical quantities different from time. *Frequency-domain* measurements, that has great significance in this thesis, can be considered as typical example for this type. In this case the measurement values are associated with specific values of the frequency associated with the signal itself. Frequency domain measurements are also special in the respect that frequency is not independent from time. Hence the frequency domain measurements should be related to time-domain signals, and the measurement require finite amount of time surely greater than zero — this is followed from the uncertainty principle of Heisenberg [10] — to realize, however the time elapsed between the measurements has no significance. The frequency domain measurements in most cases are realized indirectly on the basis of time-domain measurements by applying spectral methods of the signal processing field.

The result of the measurement (or data acquisition) process is a sequence of numbers, the measurement values, ordered according to the values of another physical quantity, i.e. time, frequency or any other. The spacing on this quantity can be *uniform* or *nonuniform*, depending on the differences between the neighboring points, that can be identical or different, respectively. On the time domain the uniform sampling is more common in the signal processing methods commonly used, this is well fitted to the FFT based spectral methods. Uniform sampling on time domain is a prerequisite to use the description of signals and systems on the unit circle group, i.e. to use the function spaces of \mathcal{H}^2 , and \mathcal{H}^∞ in the description. Besides the uniformity, the Shannon condition should also be satisfied for the sampling. The frequent use of the FFT methods in the signal processing field results in the common use of uniform spacing also on the frequency scale. By using the concept of the generalized orthogonal bases just the benefits of non-uniformly spaced frequency domain data are exploited.

In the following sections the identification problem in the context of using generalized orthogonal bases will be studied by covering the following topics:

- An introduction to the \mathcal{H}^2 identification problems in generalized orthonormal bases will be given.
- The problem how to obtain an appropriate reference poles set to built in the generalized orthogonal basis will be studied: the existing methods for approximate pre-identification of poles will be outlined.
- The possibilities for systematical improving the presumed pole set involved in the generalized orthogonal basis will be discussed: an iterative procedure for finding poles will be proposed.
- The principles of extending the identification procedures based upon the generalized orthogonal bases in the space \mathcal{H}^∞ : the convergence aspects of these representations will be examined.

The last topic somehow differs from the others, however its significance is great: establishes the connection of the GOB based identification methods with the contemporary directions of the robust control and systems theory.

5.2 Identification of functions in \mathcal{H}^2

This section gives a brief introduction to the field of identification of functions belonging to the space $\mathcal{H}^2(\mathbb{D})$ on the basis of a finite set of measurement points arranged on the unit circle.

Any function $F(q)$ belonging to any Hardy space $\mathcal{H}^p(\mathbb{D})$ ($p = 1, 2, \dots, \infty$) can be associated with the *frequency* by its restriction on the unit circle, i.e. the function $F(e^{it})$ is a "frequency-function" or "spectral function", i.e. functions with the independent variable

the *frequency* or any other variable derived from it, e.g. circular frequency, normalized frequency, etc. For any function $F \in \mathcal{H}^p(\mathbb{D})$ the function $F(e^{it})$ ($t \in \mathbb{R}$) is a periodic function belonging to the space $\mathcal{L}^p[-\pi, \pi]$. The parameter t can be considered as a normalized circular frequency relative to the sample frequency f_S associated with the discrete-time signal standing behind the frequency function, as it has been discussed in Section 2.1.

The identification of a function belonging to the space $\mathcal{H}^p(\mathbb{D})$ (typically \mathcal{H}^2 and \mathcal{H}^∞ are considered) based upon measurement values on the unit circle is a standard task in the systems theory, referred as \mathcal{H}^2 approximation and interpolation, see e.g. [11]: least square approximations (Section 3.2), minimum norm interpolations (Section 3.3), the distinguished Nevanlinna-Pick interpolation (3.4), and the optimal Hankel norm approximations (Chapter 4) are frequently applied methods. These now can be referred as classical methods also in the sense, that they do not exceed (even in hidden form) the framework of the standard trigonometric basis.

The objectives set for this thesis in the context of \mathcal{H}^2 identification is to solve the following task: identifying the function $F \in \mathcal{H}^2(\mathbb{D})$ on the basis of measurement values on the unit circle by applying the concept of the generalized orthogonal basis in $\mathcal{H}^2(\mathbb{D})$. The main idea to solve this can be expressed as follows:

1. Generating the representation of the function in the GOB based constructed upon the available a priori knowledge on the pole structure of the function.
2. A good representation contains small number of significant coefficients, hence the GOB should be improved in the way, that the representation be minimal in this respect.

Repeating this procedure until a satisfactory representation is given results in the solution. As the result of the identification process the final set of the representation coefficients can be considered. If this form cannot be used in the control or decision problem to be solved, the rational function or partial fraction form can be generated by algebraic manipulations

(see Section 2.4.3). Of course, this can only be realized in the case of finite set of coefficient, however practically realizable algorithms always result in finite set.

The identification scheme outlined above surely works on systems, that can exactly be associated with finite number N of poles, as in this case the exact representation of the system is finite. By considering poles with multiplicity not greater than one, it is a finite Takenaka-Malmquist representation generated upon the set of poles, in this case the maximal number of the coefficients is N . Finite multiplicity of poles greater than one increases the number of the coefficients with a finite number. Noises corrupting the measured data results in inexact representations resulting infinite number of representation coefficients even in the minimal case. For relatively small noises the use of error bounds and statistical decision principles are adequate methods to find the dominant coefficients.

The criterion of improving the generalized orthogonal basis is obvious: minimal number of representation coefficients should be achieved, the problem is that there is no direct method to find the adequate pole set that ensure this. Hence the problem should be divided in to parts:

- Finding an initial pole set, that resides near to the solution.
- On the basis of modifying the poles constructing an iteration scheme that converges to the solution.

In Section 5.4 an iterative method will be introduced, that is locally convergent in second order, and offers a solution for the problem of improving the GOB representation. However, the "local" nature of the iteration procedure further increases the need of finding an adequate initial approximation for the pole structure. A good initial approximation of the poles seems to be a prerequisite of the success.

In order to find an initial approximation of the system pole, two alternatives are given:

- Reasoning on the basis of structural, and behavioral information originating from the

principles of physics, chemistry, biology, and other disciplines associated with the type of the system to be identified.

- Performing pre-identification of the poles by using formal methods introduced within the field of system identification.

The first alternative can be realized ad hoc, and falls outside the scope of the current thesis. The second approach will be discussed in the Section 5.3.

The representation in a generalized orthonormal basis, i.e. computing the representation coefficients, can be realized by using the estimation algorithm, based upon the argument function, described in the Sections 2.4.5 and 3.1. This algorithm uses the efficient FFT algorithm to approximately evaluate the scalar products belonging to the coefficients on the basis of frequency domain data non-uniformly spaced on the frequency axis. Hence the methods described in Sections 3.3 and 3.4 are also applied.

5.3 Obtaining approximate pole information

The use of rational orthogonal bases supposes some a priori knowledge upon the system poles, which can be acquired by using numerous existing estimation methods. This means, that the classical identification methods has not lost their significance, the GOB based identification methods can mainly be used to improve the knowledge obtained as initial approximation by the classic ones.

Estimating the pole structure and locations is broadly investigated field in the systems science and signal processing. Probably the efforts to estimate the number and location of the poles in connection with the autoregressive (AR) model identification can be considered as the first attempts in this topic in the years 70-80's (see [8] for the historical aspects). A method to estimate the pole structure of a system can be an recursive in order AR model estimation combined with several information criteria (e.g. partial correlation indices, AIC,

BIC, etc.) to stop the iteration [24]. The use of AR, as well as ARX, ARMA, ARMAX, etc. models in this field has led to delicate identification methods, well covered e.g. in [26].

In connection with the autoregressive type methods, the efforts to find high resolution methods to detect harmonic components in noisy signals has led to algorithms that — in the essence — are suitable to derive the poles, e.g. the Prony and the Pisarenko method, see for a survey on them in Chapter 6. of [8].

Based upon the development on the state space methods in the systems science the *subspace methods* was elaborated in the beginning of the 90's, that proved to be highly efficient for both time and frequency domain data, see [41] and [37] for the theory, and [42] for the algorithmic aspects.

The main drawback of both classical identification and subspace methods, that they do not handle of poles with multiplicity greater than one, or they assume a priori fixed multiplicities. This drawback is aimed to step over with the use of GOB-based methods.

5.4 Iterative improving of poles

In this section an iterative method to identify models given in partial fraction form will be presented. This will utilize the benefits of the use of bi-orthogonal rational systems, can handle the multiplicity of the poles, furthermore produces good convergence and easy computability.

The basic model used in the method is the partial fraction representation of a system transfer function $f = f_{\mathbf{a}}$ with poles $\hat{\mathbf{a}} := (\hat{a}_1, \hat{a}_2, \dots, \hat{a}_n) \in \mathbb{C}$, where $\hat{a}_k := 1/\overline{a_k} \in \mathbb{D}$, and $a_k \neq a_\ell$ if $k \neq \ell$ ($k = 1, \dots, n$). Suppose that the multiplicity of a_k is $m_k - 1$, where $m_k \geq 2, m_k \in \mathbb{N}$, and let $\mathbf{m} = (m_1, m_2, \dots, m_n)$. The partial fraction representation can be written as follows:

$$f(q) = f_{\mathbf{a}}(q) = \sum_{k=1}^n \sum_{\ell=0}^{m_k-2} \frac{A_{k\ell} q^\ell}{(1 - \overline{a_k} q)^{\ell+1}} \quad (5.4.1)$$

The identification problem is formulated as the determination of the multiplicities \mathbf{m} , and the corresponding parameters $A_{k\ell}$, \mathbf{a} in (5.4.1) using a set of measured frequency response sample values of f . It is important to stress, that the multiplicities — as it will be clarified latter — are considered not to be fixed, but they will vary in the course of the procedure.

To elaborate the method a discrete scalar product is introduced, and based upon it a bi-orthogonal rational system is defined to represent the function (5.4.1). An iterative scheme will be set up, which starting from an initial pole placement converges into the true poles including their multiplicities. The method has been proved to locally converge in second order. The coefficients of the partial fraction can be computed on the basis of the bi-orthogonal representation. A numerical method can be constructed, which uses discrete values of the transfer function, hence it can be applied as a system identification method based upon frequency domain data.

In the course of this section first a bi-orthogonal system of rational functions will be constructed, to represent the transfer function, on the basis of a discrete scalar product introduced by the discrete Cauchy formula, that is presented at the end as an appendix; then an iteration method will be given with the purpose to estimate both the pole structure and the exact location of the poles.

5.4.1 Construction of a bi-orthogonal system defined by partial fraction

Assume that the system of (5.4.1) has poles all with multiplicity one; in this case it can be represented on a system of rational functions φ_i as follows

$$f_{\mathbf{a}}(q) = \sum_{k=1}^n \frac{A_k}{1 - \bar{a}_k q} = \sum_{\ell \in \mathbb{N}^*} A_{\ell} \varphi_{\ell}(q) \quad (5.4.2)$$

where

$$\varphi_{\ell}(q) := \frac{1}{1 - \bar{a}_{\ell} q}$$

In order to construct the representation, a discrete scalar product

$$[F, G] := [F, G]_N := \frac{1}{N} \sum_{q \in \mathbb{T}_N} F(q) \bar{G}(q) \quad (5.4.3)$$

defined on the discrete group \mathbb{T}_N depending on the parameter $N \in \mathbb{N}^*$ (see Section 5.4.3) will be used. This scalar product can be applied for rational systems analogously to the ordinary – continuous – scalar product, corresponding to the discrete Cauchy formula that is introduced in the Section 5.4.3.

We shall construct discrete bi-orthogonal systems depending on the parameters

$$(a_1, a_2, \dots, a_n) \in \mathbb{D}^n,$$

where $a_i \neq a_j$, if $i \neq j$. Namely for $q \in \mathbb{C}$ and $\ell = 1, 2, \dots, n$ set

$$\varphi_\ell(q) := \frac{1}{1 - \bar{a}_\ell q}, \quad \Phi_\ell(q) := \frac{1 - a_\ell^N}{\omega_\ell(a_\ell)} \omega_\ell(q). \quad (5.4.4)$$

where

$$\omega_\ell(q) = \prod_{\substack{j=1 \\ j \neq \ell}}^n (q - a_j).$$

If $N \geq n$ then the systems (5.4.4) are bi-orthogonal with respect the scalar product $[\cdot, \cdot]_N$, i.e. for any couple $k, \ell \in \{1, 2, \dots, n\}$ we have

$$[\Phi_k, \varphi_\ell]_N = \delta_k^\ell, \quad (5.4.5)$$

where δ_k^ℓ is the Kronecker symbol.

Indeed, by (5.4.22) of Theorem 5.4.2 for $1 \leq k, \ell \leq n$

$$\begin{aligned} [\Phi_k, \varphi_\ell] &= \frac{1}{N} \sum_{\zeta \in \mathbb{T}_N} \frac{\Phi_k(\zeta)}{1 - a_\ell \bar{\zeta}} = \frac{1}{N} \sum_{\zeta \in \mathbb{T}_N} \Phi_k(\zeta) \frac{\zeta}{\zeta - a_\ell} = \\ &= \frac{1}{2\pi i} \int_{\mathbb{T}_N} \frac{\Phi_k(\zeta)}{\zeta - a_\ell} d\zeta = \frac{\Phi_k(a_\ell)}{1 - a_\ell^N} = \delta_k^\ell \end{aligned}$$

hence (5.4.5) is proved.

Following from the bi-orthogonality of φ_ℓ and Φ_ℓ , the coefficients A_ℓ in the representation (5.4.2) can be computed by the scalar product

$$A_\ell = [f, \Phi_\ell]_N.$$

Generalizing this construction to the case of poles with multiplicity larger than one

$$f_{\mathbf{a}}(q) = \sum_{k=1}^n \sum_{\ell=0}^{m_k-2} \frac{A_{k\ell} q^\ell}{(1 - \overline{a_k} q)^{\ell+1}} = \sum_{(k,\ell) \in \mathcal{J}_{\mathbf{n}}} A_{k\ell} \varphi_{k\ell}(q) \quad (5.4.6)$$

where

$$\mathbf{a} = (a_1, a_2, \dots, a_n) \in \mathbb{D}^n \quad (a_i \neq a_j \quad \text{if } i \neq j),$$

and consider the rational functions

$$\varphi_{k\ell}(q) := \frac{q^\ell}{(1 - \overline{a_k} q)^{\ell+1}} \quad (5.4.7)$$

$$(q \in \mathbb{C}, k = 1, 2, \dots, n, \ell = 0, 1, \dots, m_k - 1),$$

where $m_1, m_2, \dots, m_n \in \mathbb{N}^*$, $\mathbf{m} = (m_1, m_2, \dots, m_n)$, $m := m_1 + \dots + m_n$, and

$$\mathcal{J}_{\mathbf{n}} = \{(i, j) : j \in \mathbb{N}, 0 \leq j < m_i, i = 1, \dots, n\}. \quad (5.4.8)$$

Obviously the numbers $\widehat{a}_k := 1/\overline{a_k}$ are the poles of $\varphi_{k\ell}$ with the multiplicity $\ell + 1$.

We show that there exists a collection of polynomials

$$\Phi_{k\ell} = \Phi_{k,\ell}^{\mathbf{m}}(\cdot, \mathbf{a}) \in \mathcal{P}_{m-1} \quad ((k, \ell) \in \mathcal{J}_{\mathbf{m}})$$

such that the systems

$$(\varphi_i, i \in \mathcal{J}_{\mathbf{m}}), \quad (\Phi_i, i \in \mathcal{J}_{\mathbf{m}})$$

are bi-orthogonal with respect the scalar product $[\cdot, \cdot]_N$, if $N \geq m$, i.e.

$$[\Phi_{k\ell}, \varphi_{rs}]_N = \delta_{kr} \delta_{\ell s} \quad ((k, \ell), (r, s) \in \mathcal{J}_{\mathbf{m}}),$$

hence the coefficients $A_{k\ell}$ in the representation (5.4.6) can be expressed by the scalar product

$$A_{k\ell} = [f, \Phi_{k\ell}]_N.$$

Moreover the polynomials $\Phi_{k\ell}$ can be written in the form

$$\Phi_{k\ell} = \omega_k P_{k\ell} \quad ((k, \ell) \in \mathcal{J}_{\mathbf{m}}), \quad (5.4.9)$$

where

$$\begin{aligned} P_{k\ell} &\in \mathcal{P}_{m_k-1}, \\ \omega_k(q) &:= \omega_k(q, \mathbf{a}) := \prod_{\substack{i=1 \\ i \neq k}}^n (q - a_i)^{m_i} \\ &(k = 1, 2, \dots, n, q \in \mathbb{C}). \end{aligned}$$

The polynomials $P_{k\ell}$ can be expressed by the partial sums of the Taylor-series expansion

$$P_k(q) := P_k(q, \mathbf{a}) := \frac{1 - q^N}{\omega_k(q, \mathbf{a})} = \sum_{j=0}^{\infty} p_{kj} (q - a_k)^j \quad (5.4.10)$$

$$(|q - a_k| < r_k, q \in \mathbb{D},$$

$$r_k := \min\{|a_j - a_k| : j = 1, 2, \dots, n, j \neq k\}),$$

namely

$$\begin{aligned} P_{k\ell}(q) &= (q - a_k)^\ell \sum_{j=0}^{m_k - \ell - 1} p_{kj} (q - a_k)^j \\ &(q \in \mathbb{C}, (k, \ell) \in \mathcal{J}_{\mathbf{m}}) \end{aligned} \quad (5.4.11)$$

and by (5.4.10)

$$p_{kj} = \frac{P_k^{(j)}(a_k, \mathbf{a})}{j!} := \frac{1}{j!} \left. \frac{d^j}{dq^j} P(q, \mathbf{a})_k \right|_{q=a_k}.$$

We prove

Theorem 5.4.1. *Let $\mathbf{a} = (a_1, \dots, a_n) \in \mathbb{D}^n$, where $a_i \neq a_j$, if $1 \leq i, j \leq n$ and $i \neq j$ and fix the vector $\mathbf{m} = (m_1, \dots, m_n)$ with $m_j \in \mathbb{N}^*$ and the natural number $N \geq m_1 + \dots + m_n$. Then there exists a unique system of polynomials $\Phi_{k\ell} \in \mathcal{P}_{m-1}$ $((k, \ell) \in \mathcal{J}_{\mathbf{m}})$ such that the systems $\varphi_{k\ell}$ and $\Phi_{k\ell}$ $((k, \ell) \in \mathcal{J}_{\mathbf{m}})$ are bi-orthogonal with respect the scalar product (5.4.3).*

Moreover the polynomials $\Phi_{k\ell}$ can be written in the form (5.4.9) and the coefficients of $P_{k\ell}$ are defined by (5.4.10) and (5.4.11).

Proof. By (5.4.22) of Theorem 5.4.2

$$\begin{aligned} [\Phi_{k\ell}, \varphi_{rs}]_N &= \frac{1}{N} \sum_{\zeta \in \mathbb{T}_N} \frac{\Phi_{k\ell}(\zeta) \bar{\zeta}^s}{(1 - a_r \bar{\zeta})^{s+1}} = \\ &= \frac{1}{N} \sum_{\zeta \in \mathbb{T}_N} \frac{\Phi_{k\ell}(\zeta) \zeta}{(\zeta - a_r)^{s+1}} = \frac{1}{2\pi i} \int_{\mathbb{T}_N} \frac{\Phi_{k\ell}(\zeta)}{(\zeta - a_r)^{s+1}} d\zeta = \\ &= \frac{1}{s!} \left. \frac{d^s}{dq^s} \frac{\Phi_{k\ell}(q)}{1 - q^N} \right|_{q=a_r} \end{aligned}$$

and consequently the systems in question are bi-orthogonal if and only if

$$\frac{1}{s!} \left. \frac{d^s}{dq^s} \frac{\Phi_{k\ell}(q)}{1 - q^N} \right|_{q=a_r} = \delta_k^r \delta_\ell^s \quad (5.4.12)$$

for any couple $(k, \ell), (r, s) \in \mathcal{J}_m$. Thus the $\Phi_{k\ell} ((k, \ell) \in \mathcal{J}_m)$ polynomials are the fundamental polynomials of the weighted Hermite interpolation problem

$$(\rho_N \Phi)^{(j)}(a_i) = b_{ij} \quad ((i, j) \in \mathcal{J}_m),$$

where $\rho_N(q) := (1 - q^N)^{-1}$ ($q \in \mathbb{C}$) is the weight function and b_{ij} are given numbers. From (5.4.12) it follows that $\Phi_{k\ell}$ is of the form

$$\Phi_{k\ell}(q) = P_{k\ell}(q) \prod_{\substack{j=1 \\ j \neq k}}^n (q - a_j)^{m_j} = P_{k\ell}(q) \omega_k(q)$$

($q \in \mathbb{C}$), and by (5.4.12)

$$(\rho_N \omega_k P_{k\ell})^{(j)}(a_k) = \delta_j^\ell j! \quad (\ell \leq j < m_k). \quad (5.4.13)$$

This is equivalent to

$$\sum_{i=0}^j \binom{j}{i} (\rho_N \omega_k)^{(j-i)}(a_k) P_{k\ell}^{(i)}(a_k) = \delta_j^\ell j!$$

($\ell \leq j < m_k$). Thus $P_{k\ell}^{(i)}(a_k) = 0$, if $i < \ell$ and

$$\sum_{i=\ell}^j \frac{(\rho_N \omega_k)^{(j-i)}(a_k)}{(j-i)!} \frac{P_{k\ell}^{(i)}(a_k)}{i!} = \delta_j^\ell \quad (\ell \leq j < m_k). \quad (5.4.14)$$

We consider the infinite system of linear equations with respect to $p_{k0}, p_{k1}, \dots, p_{ki}, \dots$:

$$\sum_{i=0}^j \frac{(\rho_N \omega_k)^{(j-i)}(a_k)}{(j-i)!} p_{ki} = \delta_0^j \quad (j \in \mathbb{N}). \quad (5.4.15)$$

The coefficient of p_{kj} in j -th equation is $(\rho_N \omega_k)(a_k) \neq 0$, consequently this system has a unique solution. Comparing this with (5.4.13) and (5.4.14) we get

$$\frac{P_{k\ell}^{(i)}(a_k)}{i!} = p_{k(\ell-i)} \quad (i \geq \ell).$$

It is clear that the Taylor-coefficients of the function

$$P_k(q) := \frac{1 - q^N}{\omega_k(q)} = \sum_{j=0}^{\infty} p_{kj} (q - a_k)^j \quad (|q - a_k| < r_k)$$

satisfy (5.4.15) and Theorem 5.4.1 is proved. \square

To evaluate the numbers p_{kj} we introduce the function

$$S_k(q) := \frac{P'_k(q)}{P_k(q)} = \sum_{j=0}^{N-1} \frac{1}{q - \epsilon_N^j} - \sum_{\substack{j=1 \\ j \neq k}}^n \frac{1}{q - a_j},$$

($|q - a_k| < r_k$), where $\epsilon_N^j = e^{i2\pi \frac{j}{N}}$. Hence by

$$P_k^{(\ell+1)}(a_k) = \sum_{j=0}^{\ell} \binom{\ell}{j} P_k^{(j)}(a_k) S_k^{(\ell-j)}(a_k) \quad (\ell \in \mathbb{N})$$

we get the following recursion:

$$p_{k(\ell+1)} = \frac{1}{\ell+1} \sum_{j=0}^{\ell} p_{kj} s_{k(\ell-j)} \quad (\ell \in \mathbb{N}), \quad (5.4.16)$$

where

$$\begin{aligned} s_{ki} &:= \frac{S_k^{(i)}(a_k)}{i!} = \\ &= \sum_{j=0}^{N-1} \frac{(-1)^i}{(a_k - \epsilon_N^j)^{i+1}} - \sum_{\substack{j=1 \\ j \neq k}}^n \frac{(-1)^i}{(a_k - a_j)^{i+1}}, \end{aligned} \quad (5.4.17)$$

($i \in \mathbb{N}$). On the basis (5.4.16) and (5.4.17) the coefficients p_{kj} can be computed.

5.4.2 Iteration on pole structure and parameters

In this section an iteration method will be constructed to compute the poles – including their multiplicities – of a rational function by applying the partial fraction model introduced by (5.4.6). This algorithm is locally convergent in second order and uses the values of the rational function only in the points of \mathbb{T}^N , i.e. uniformly spaced sample values of the frequency response of the underlying system.

To compute the vector $\hat{\mathbf{a}} = (\hat{a}_1, \dots, \hat{a}_n) \in \mathbb{D}^n$ we use the system

$$\Phi_{k\ell}^{\mathbf{m}}(\cdot, \mathbf{a}) \quad ((k, \ell) \in \mathcal{J}_{\mathbf{m}}).$$

Let $N \geq m := m_1 + m_2 + \dots + m_n$. Then by Theorem 5.4.1 the systems

$$\Phi_{k\ell}^{\mathbf{m}}(\cdot, \mathbf{a}), \quad \varphi_{k\ell}(\cdot, \mathbf{a}) \quad ((k, \ell) \in \mathcal{J}_{\mathbf{m}}),$$

depending on $\mathbf{a} \in \mathbb{D}^n$, are bi-orthogonal with respect to the scalar product (5.4.3). Denote

$$\begin{aligned} \phi_k(\cdot, \mathbf{a}) &:= \Phi_{k(m_k-1)}^{\mathbf{m}}(\cdot, \mathbf{a}) \\ \phi_k^-(\cdot, \mathbf{a}) &:= \Phi_{k(m_k-2)}^{\mathbf{m}}(\cdot, \mathbf{a}) \end{aligned} \tag{5.4.18}$$

and introduce

$$F_k(\mathbf{a}) := [\phi_k(\cdot, \mathbf{a}), f_{\mathbf{a}}]_N, \quad F_k^-(\mathbf{a}) := [\phi_k^-(\cdot, \mathbf{a}), f_{\mathbf{a}}]_N$$

($k = 1, \dots, n$), the conjugate coefficients of the bi-orthogonal expansion of the functions (5.4.18). This expansion will be infinite, unless it is applied on the exact pole locations. In that case the expansion will contain $m_k - 1$ nonzero terms, hence we have

$$F_k(\mathbf{a}) = 0, \quad F_k^-(\mathbf{a}) = \bar{\lambda}_k = \bar{A}_{k(m_k-2)} \quad (\neq 0)$$

for ($k = 1, \dots, n$).

An iteration process can be given by introducing the functions

$$\begin{aligned} G_k(\mathbf{a}) &:= a_k + \frac{1}{m_k - 1} \frac{F_k(\mathbf{a})}{F_k^-(\mathbf{a})} \quad (k = 1, \dots, n), \\ G &:= (G_1, \dots, G_n). \end{aligned} \tag{5.4.19}$$

The iteration process is given by

$$\mathbf{a}^{\nu+1} := G(\mathbf{a}^\nu) \quad (\nu \in \mathbb{N}, \mathbf{a}^0 \in \mathbb{D}^n). \quad (5.4.20)$$

It can be proven that the iteration procedure (5.4.20) is locally convergent in second order, i.e. there exists an $r > 0$, $K > 0$ such that if for the initial value $\|\mathbf{a}^0 - \mathbf{a}\| < r$, then

$$\|\mathbf{a}^{\nu+1} - \mathbf{a}\| \leq K \|\mathbf{a}^\nu - \mathbf{a}\|^2 \quad (\nu \in \mathbb{N}). \quad (5.4.21)$$

The proof is based upon the characteristics of the first and second order partial derivatives of function (5.4.19). Namely it can be proved, that the Jacoby matrix $\partial_\ell G_k(\mathbf{a})$ of the function is zero, moreover the second partial derivatives $\partial_{sr} G_k(\mathbf{a})$ ($s \neq r$) are equal to 0, and $\partial_{ss} G_k(\mathbf{a})$, $\partial_{kk} G_k(\mathbf{a})$ are finite; that implies (5.4.21).

The realization of the iteration process requires an initial pole location \mathbf{a}^0 , which is advantageous to be near enough to the true location. The possibly applicable methods to do this has been outlined in section 5.3.

The input data required by the method – due to the discrete scalar product that has applied – are discrete points of the frequency response of system to be identified. These types of data can easily be acquired by FFT procedures from time-domain data, or – if it is possible to realize – by direct frequency response measurements.

5.4.3 The discrete Cauchy formula

In the method presented we have needed a discrete analogue of the Cauchy integral formula. Remember, that if $F \in \mathcal{A}$ then for any $a \in \mathbb{D}$ and $n \in \mathbb{N}$ (see e.g. [19])

$$\frac{1}{2\pi i} \int_{\mathbb{T}} \frac{F(\zeta)}{(\zeta - a)^{n+1}} d\zeta = \frac{F^{(n)}(a)}{n!}.$$

Replacing \mathbb{T} by the discrete group

$$\mathbb{T}_N := \{e^{i2\pi \frac{k}{N}} : k = 0, 1, \dots, N-1\} \quad (N \in \mathbb{N}^*)$$

and the integral by the sum

$$\frac{1}{2\pi i} \int_{\mathbb{T}_N} F(\zeta) d\zeta := \frac{1}{N} \sum_{\zeta \in \mathbb{T}_N} F(\zeta) \zeta$$

we get a similar formula for polynomials. For function $F \in \mathcal{A}$ obviously

$$\lim_{N \rightarrow \infty} \frac{1}{2\pi i} \int_{\mathbb{T}_N} F(\zeta) d\zeta = \frac{1}{2\pi i} \int_{\mathbb{T}} F(\zeta) d\zeta.$$

Denote \mathcal{P}_n the set of complex polynomials of degree n . Then the following analogue of the Cauchy integral formula holds.

Theorem 5.4.2. *Let $n \in \mathbb{N}$, $N \in \mathbb{N}^*$ be fixed numbers and denote $P \in \mathcal{P}_{N+n-1}$ a polynomial.*

i) Then for any $a \in \mathbb{D}$ we have

$$\frac{1}{2\pi i} \int_{\mathbb{T}_N} \frac{P(\zeta)}{(\zeta - a)^{n+1}} d\zeta = \frac{1}{n!} \frac{d^n}{dq^n} \frac{P(q)}{1 - q^N} \Big|_{q=a}. \quad (5.4.22)$$

ii) Furthermore if a_0, a_1, \dots, a_n are distinct points in \mathbb{D} , then

$$\frac{1}{2\pi i} \int_{\mathbb{T}_N} \frac{P(\zeta)}{(\zeta - a_0) \dots (\zeta - a_n)} d\zeta = \sum_{j=0}^n \frac{1}{\omega_j(a_j)} \frac{P(a_j)}{1 - a_j^N}, \quad (5.4.23)$$

where

$$\omega_j(q) := \prod_{\substack{\ell=0 \\ \ell \neq j}}^n (q - a_\ell) \quad (q \in \mathbb{C}, j = 1, 2, \dots, n)$$

are the fundamental polynomials of Lagrange interpolation.

Proof. First we prove (5.4.22) for $n = 0$. To this end write $P \in \mathcal{P}_{N-1}$ in the form

$$P(q) = \sum_{j=0}^{N-1} c_j q^j \quad (q \in \mathbb{C}).$$

Observe that for $\zeta \in \mathbb{T}_N$ we have $\zeta^N = 1$ and consequently

$$\begin{aligned} \frac{\zeta}{\zeta - a} &= \frac{1}{1 - a\bar{\zeta}} = \frac{1}{1 - a^N} \frac{1 - (a\bar{\zeta})^N}{1 - a\bar{\zeta}} = \\ &= \frac{1}{1 - a^N} \sum_{j=0}^{N-1} a^j \bar{\zeta}^j \quad (\zeta \in \mathbb{T}_N). \end{aligned}$$

Using the orthogonality of the discrete trigonometric system we get

$$\begin{aligned} \frac{1}{2\pi i} \int_{\mathbb{T}_N} \frac{P(\zeta)}{\zeta - a} d\zeta &= \frac{1}{N} \sum_{\zeta \in \mathbb{T}_N} P(\zeta) \frac{\zeta}{\zeta - a} = \\ &= \frac{1}{1 - a^N} \sum_{j=0}^{N-1} c_j a^j = \frac{P(a)}{1 - a^N} \end{aligned}$$

and for $n = 0$ (5.4.22) is proved.

To show (5.4.23) write $P \in \mathcal{P}_{n+N-1}$ in the form

$$P(q) = Q(q)(q - a_0) \dots (q - a_n) + R(q),$$

where $R \in \mathcal{P}_n$, $Q \in \mathcal{P}_{N-2}$. Applying Lagrange interpolation formula to R we get

$$\begin{aligned} \frac{P(q)}{(q - a_0) \dots (q - a_n)} &= Q(q) + \frac{R(q)}{(q - a_0) \dots (q - a_n)} = \\ &= Q(q) + \sum_{j=0}^n \frac{R(a_j)}{q - a_j} = Q(q) + \sum_{j=0}^n \frac{P(a_j)}{q - a_j}. \end{aligned}$$

Since $Q \in \mathcal{P}_{N-2}$, the orthogonality of the discrete trigonometric system implies

$$\int_{\mathbb{T}_N} Q(\zeta) d\zeta = 0,$$

and applying (5.4.22) in the case $n = 0$ we get (5.4.23).

Observe that the right hand side in (5.4.23) can be expressed by the divided differences of the function

$$G(q) := \frac{P(q)}{1 - q^N} \quad (q \in \mathbb{D}).$$

Namely (5.4.23) is equivalent to

$$\frac{1}{2\pi i} \int_{\mathbb{T}_N} \frac{P(\zeta)}{(\zeta - a_0) \dots (\zeta - a_n)} d\zeta = G(a_n, \dots, a_1, a_0). \quad (5.4.24)$$

(Compare eg. [21], pp. 247.)

Since for any $G \in \mathcal{A}$

$$G(a_n, \dots, a_1, a_0) \rightarrow \frac{G^{(n)}(a)}{n!} \quad \text{as } a_j \rightarrow a,$$

$j = 0, 1, \dots, n$, therefore (5.4.22) follows from (5.4.24). \square

Taking the limit in (5.4.22) as $N \rightarrow \infty$ we obtain the continuous variant of the formula.

5.4.4 Realization and examples

The algorithm presented above has been implemented in a *MATLAB*[®] procedure named *psc*. An initial pole set and the multiplicities belonging to it, as well as the error bound of the iteration can be specified as input for the procedure. As output the final pole set is given. To illustrate the algorithm, three examples are presented, both ones operating on the same pole set, that consist of one real pole and a conjugated complex pair. The real pole has multiplicity 1 in both experiment, the multiplicity of the complex poles is 1 in the first experiment and 2 in the 2nd and 3rd one. The exact pole values are as follow:

$$\mathbf{a} = [0.9, 0.99e^{i0.5}, 0.99e^{-i0.5}].$$

The root mean square of the absolute difference of the consecutive pole values is used as error term to stop the iteration. The value 10^{-5} has been used as error bound in the experiments.

In the first experiment the iteration has been started from the initial pole positions

$$\mathbf{a}^{(0)} = [0.7, 0.9e^{i0.7}, 0.9e^{-i0.7}],$$

and the assumed multiplicities has been

$$\mathbf{m} = [2, 2, 2].$$

On Figure 5.1 the movement of the poles can be seen on the complex plane and in the form of diagrams containing the real and the imaginary part of the poles against the iteration number, as well as the values of the error term has been presented. Fast convergence to the correct position can be observed.

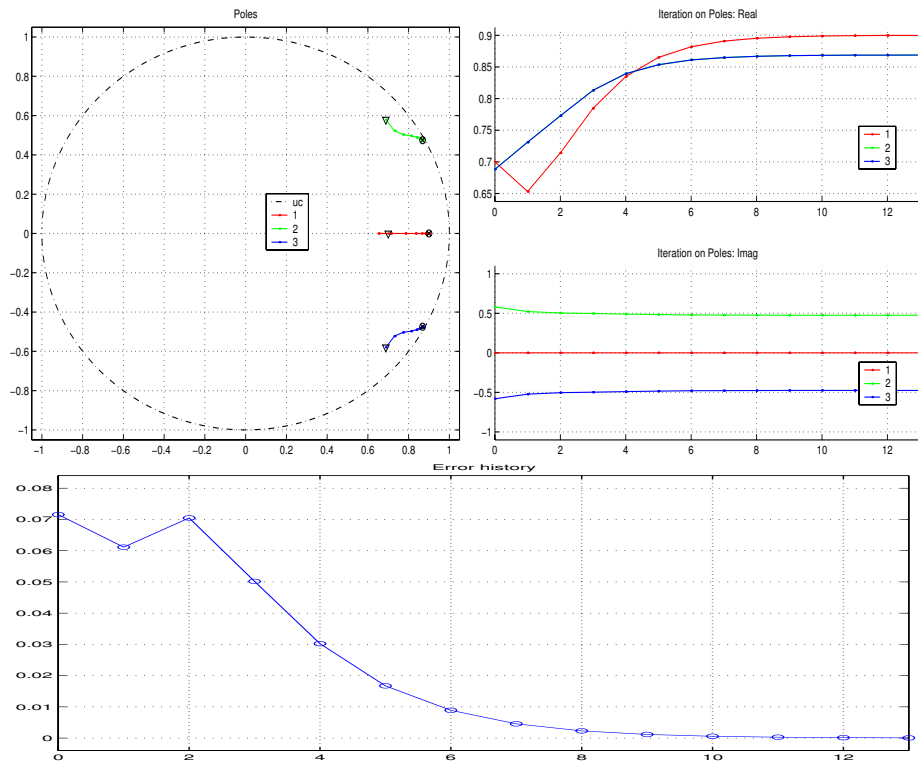


Figure 5.1: Iteration on poles

In the 2nd experiment the multiplicities of the complex poles have been increased to 2, the initial pole positions and the assumed multiplicities have been

$$\mathbf{a}^{(0)} = [0.85, 0.9e^{i0.7}, 0.9e^{-i0.7}]$$

$$\mathbf{m} = [2, 3, 3].$$

The results can be seen on Figure 5.2 in the same structure as above. Fast convergence to the correct position can be observed.

In the 3rd experiment the initial positions of the complex poles have been set to greater

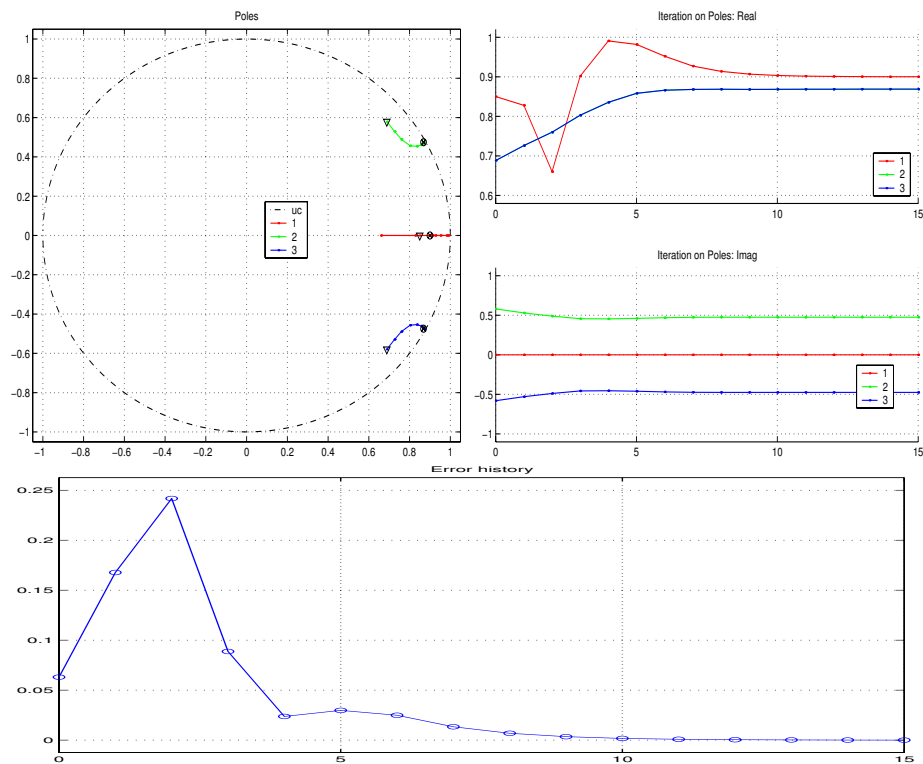


Figure 5.2: Iteration on poles

distance from the exact positions:

$$\mathbf{a}^{(0)} = [0.85, 0.9e^{i0.9}, 0.9e^{-i0.9}]$$

$$\mathbf{m} = [2, 3, 3].$$

The results can be seen on Figure 5.3. The poles have gone away outside the unit circle. In these positions the algorithm does not work well. No solution has been found, and the error function has not been presented on the figure.

5.5 \mathcal{H}^∞ representations in generalized orthogonal basis

In this section the extension of the results achieved in the field of using representations in generalized orthogonal bases in the identification of signals and systems will be given from

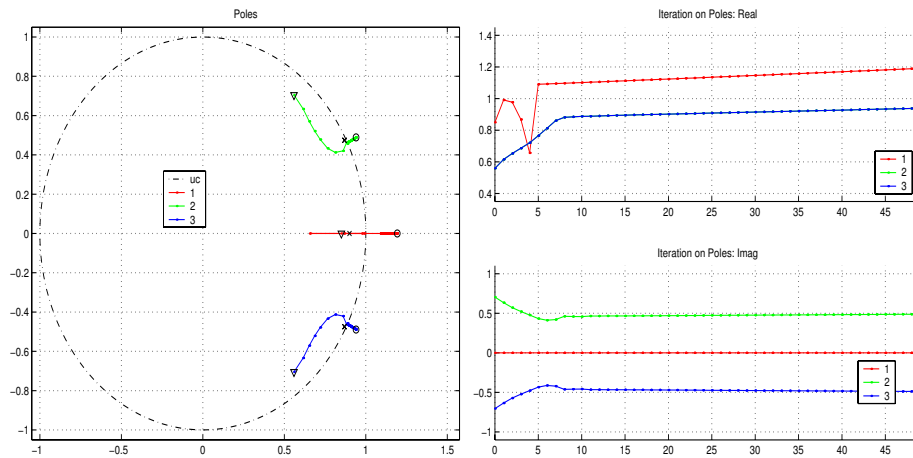


Figure 5.3: Iteration on poles

the space \mathcal{H}^2 to \mathcal{H}^∞ . This is essential in the respect of applying these results in the robust design methods of the control, detection, and other significant fields of the systems science. The method followed to do this, will be the study of convergence of the representations in the \mathcal{H}^∞ space. If convergence is proven, the representations in a GOB will be valid in \mathcal{H}^∞ sense, hence the methods based upon them will become legitim also in that space.

It is well known fact, that a sequence convergent in quadratic norm in a function space is not necessarily converges in maximum norm, i.e. uniformly. A well-known example is the problem of he uniform convergence of the Fourier-series: the Fourier-series itself does not, however the sequence of their partial sums does converge in $\mathcal{L}^\infty[-\pi, \pi]$. The forming of partial sums is the simplest form of the application of *summation schemes* with the purpose of improving convergence. The use of summation in connection with identification and control in the robust field has been elaborated e.g. in [48], [20], [7] by applying the notion of the so-called ϕ -summation.

The idea of ϕ -summation is essentially a generalization of "windowing" widely used in the field of signal processing. The ϕ -function is a continuous, even, compactly supported

function with $\phi(0) = 1$. The series $\sum_{k=-\infty}^{\infty} g_k$ is called to be ϕ -summable if the sequence

$$U_n^\phi g := \sum_{k=-\infty}^{\infty} \phi\left(\frac{k}{n}\right) g_k \quad n \in \mathbb{N}^*$$

converges as $n \rightarrow \infty$. It can be proved that if ϕ is compactly supported continuous function of bounded variation, and $\phi(0) = 1$, than for every convergent series

$$\lim_{n \rightarrow \infty} U_n^\phi g = \sum_{k=-\infty}^{\infty} g_k$$

See proof in [75]. In this case the ϕ -summation is called to be regular.

Some examples for summation procedures are enumerated as follow

- Fejér summation

$$\phi(x) := \begin{cases} 1 - |x| & \text{if } |x| \leq 1 \\ 0 & \text{if } |x| > 1 \end{cases}$$

- de la Vallée-Poussin summation

$$\phi(x) := \begin{cases} 1 & \text{if } |x| \leq 1/2 \\ 2(1 - |x|) & \text{if } 1/2 < |x| \leq 1 \\ 0 & \text{if } |x| > 1 \end{cases}$$

- Ragozinsky summation

$$\phi(x) := \begin{cases} \cos(\pi x/2) & \text{if } |x| \leq 1 \\ 0 & \text{if } |x| > 1 \end{cases}$$

A more exhaustive introduction to the several ϕ -summation schemes and their characteristics can be found e.g. in [7].

It was shown in [50] that using the summation procedure

$$U_m^\varphi(F) = \sum_{k=0}^{N-1} \sum_{\ell=0}^{\infty} \varphi\left(\frac{\ell N}{m}\right) \langle F, \Phi_{\ell N+k} \rangle \Phi_{\ell N+k}$$

generated by the function φ we get an approximation process which converges in L^∞ norm if $m \rightarrow \infty$. By applying the procedure of computing the coefficients of a function representation, introduced in Section 2.4.5, the coefficients in a ϕ -summation form can be also be computed by using the FFT technique. This fact is expressed in the following theorem:

Theorem 5.5.1. *The Fourier coefficients of F with respect to the generalized orthogonal basis can be expressed by the trigonometric Fourier coefficient of the functions f_k*

$$f_k(s) = F(e^{i\beta_a^{-1}(s)}) \overline{\Phi_k(e^{i\beta_a^{-1}(s)})} \rho(s) \quad s \in \mathbb{R}, k = 0, 1, \dots, N-1$$

i.e.

$$\langle F, \Phi_{\ell N+k} \rangle = [f_k, \epsilon_{\ell N}] \quad (k = 0, 1, \dots, N-1, \ell \in \mathbb{Z}).$$

The approximating model $U_m^\varphi F$ is of the form

$$(U_m^\varphi F)(e^{it}) = \sum_{k=0}^{N-1} \Phi_k(e^{it}) T_{m,k}(\beta_a(t)) \quad (t \in \mathbb{R}),$$

where the functions

$$T_{m,k}(s) := \sum_{\ell=0}^{\infty} \varphi\left(\frac{\ell N}{m}\right) [f_k, \epsilon_{\ell N}] \epsilon_{\ell N}(s)$$

$$s \in \mathbb{R}, k = 0, 1, \dots, N-1, m = 1, 2, \dots$$

can be obtained by inverse Fourier transform.

Proof. From the definition of the system Φ it follows that

$$U_m^\varphi F = \sum_{k=0}^{N-1} \Phi_k \sum_{\ell=0}^{\infty} \varphi\left(\frac{\ell N}{m}\right) \langle F, \Phi_{\ell N+k} \rangle B_a^\ell$$

By using the expression of f_k and the notation

$$[f_k, \epsilon_{\ell N}] =: \frac{1}{2\pi} \int_{-\pi}^{\pi} f_k(s) e^{-i\ell N s} ds,$$

we get

$$(U_m^\varphi F)(e^{it}) = \sum_{k=0}^{N-1} \Phi_k(e^{it}) \sum_{\ell=0}^{\infty} \varphi\left(\frac{\ell N}{m}\right) [f_k, \epsilon_{\ell N}] \epsilon_{\ell N}(\beta_a(t)). \quad (5.5.1)$$

Hence Theorem 5.5.1 follows immediately. \square

To express the statement of the \mathbb{L}^∞ convergence let us use the notation

$$M_p(\hat{\varphi}) := \int_{-\infty}^{\infty} |t|^p |\hat{\varphi}(t)| dt < \infty \quad (p \geq 0)$$

for the p -th momentum of the Fourier transform $\hat{\varphi}$ of $\varphi : \mathbb{R} \rightarrow \mathbb{R}$.

Theorem 5.5.2. *Let φ be a compactly supported even continuous function with $\varphi(0) = 1$ and $M_1(\hat{\varphi}) < \infty$. Then there exists a constant $C > 0$ depending only on $a \in \mathbb{D}^N$ and φ (and independent on m) such that*

$$\|U_m^\varphi F\|_{\mathcal{H}^\infty} \leq C \|F\|_{\mathcal{H}^\infty} \tag{5.5.2}$$

where $F \in \mathcal{H}^\infty, m = 1, 2, \dots$.

Moreover, for any functions F belonging to the disc algebra we have

$$\lim_{m \rightarrow \infty} \|U_m^\varphi F - F\|_{\mathcal{H}^\infty} = 0. \tag{5.5.3}$$

We remark that if $M_2(\hat{\varphi}) < \infty$ then the order of approximation can be estimated by the modulus of continuity of the corresponding functions.

To compute the coefficients in the Kautz expansion we can use FFT algorithms and the approximating model $U_m^\varphi F$ can be evaluated by inverse Fourier transform.

Proof. It will be shown, that U_n^φ can be expressed by the corresponding trigonometric summation operator

$$V_m^\varphi g := \sum_{n \in \mathbb{Z}} \varphi\left(\frac{n}{m}\right) [g, \epsilon_n] \epsilon_n \quad (m = 1, 2, \dots).$$

Indeed, it is known ([75]) that the trigonometric Fourier coefficients of

$$g^{(N)}(t) := \frac{1}{N} (g(t + 2\pi i/N) + g(t + 4\pi i/N) + \dots + g(t + 2N\pi i/N))$$

satisfy $c_n := [g^{(N)}, \epsilon_n] = [g, \epsilon_{N\ell}]$, if $n = \ell N$ and $c_n = 0$ otherwise. Consequently

$$V_m^\varphi(g^{(N)}) = \sum_{\ell=Z} \varphi\left(\frac{\ell N}{m}\right) [g, \epsilon_{\ell N}] \epsilon_{\ell N}.$$

Hence by (5.5.1)

$$(U_m^\varphi F)(e^{it}) = \sum_{k=0}^{N-1} \Phi_k(e^{it}) V_m^\varphi(f_k^{(N)})(\beta_a(t)). \quad (5.5.4)$$

is given.

It is known (see [49]) that there is a constant C_φ depending only on φ such that

$$\|V_m^\varphi(g)\|_\infty \leq C_\varphi \|g\|_\infty \quad (m = 1, 2, \dots,)$$

Since $\|g^{(N)}\|_\infty \leq \|g\|_\infty$ and

$$\|f_k\|_\infty \leq \|F\|_{\mathcal{H}^\infty} \|\Phi_k\|_{\mathcal{H}^\infty} \|\rho_a\|_\infty,$$

from (5.5.4) we get

$$\|U_m^\varphi f\|_{\mathcal{H}^\infty} \leq \sum_{k=0}^{N-1} \|\Phi_k\|_{\mathcal{H}^\infty} \|V_m^\varphi(f_k)\|_\infty \leq C \|F\|_{\mathcal{H}^\infty}$$

where

$$C = C_\varphi \|\rho_a\|_\infty \sum_{k=0}^{N-1} \|\Phi_k\|_{\mathcal{H}^\infty}^2$$

and (5.5.2) is proved. Claim (5.5.3) follows from (5.5.2) by a well-known density argument. \square

This theorem proves the convergence in \mathcal{H}^∞ by applying the ϕ -summation scheme, this fact is enough to state: the representations based upon generalized orthogonal bases can legally used in \mathcal{H}^∞ sense. The procedure to estimate the modified coefficients is also has given. However, in the practically applied algorithms — where finite number of coefficients are involved — there is no reason to apply the ϕ -summed coefficients, hence it can be considered as a principal, however — in the respect of the theory — undoubtedly significant result.

Chapter 6

New results

The new scientific results achieved during the research — subject of this thesis work — are summarized in the theses numbered from 1 to 6 given as follow.

6.1 Thesis I.

The use of signal representations in function spaces specifically constructed by applying *a priori* knowledge of the system has been proposed in the identification, detection, noise suppression, and other related areas emerging in association with the application of signal processing and systems science.

If the *a priori* knowledge is used to define the form of the functions taking place in the representing functions set, the representation will be sensitive to the matching of function analyzed with the assumed characteristics itself. Hence the representation coefficients will be suitable for making selective decisions upon whether the concerned signal possess the assumed characteristics, or no, as well based upon quantitative relations the measure of the matching with them can also be judged.

This idea has been introduced in the Chapter 1, and elaborated in in Sections 4.1 and 4.2 of Chapter 4.

6.2 Thesis II.

A method has been constructed for the purpose to approximately compute the coefficients of a representation of a function belonging to the space $\mathcal{H}^2(\mathbb{D})$ in a generalized orthonormal basis defined by a set of poles $\{a_k \in \mathbb{D} \mid k = 0, 1, 2, \dots, N-1\}$. The method is based upon a non-uniformly spaced partition of the frequency domain — belonging to the discrete-time form of the underlying band-limited signal, and normalized to cover the interval $[-\pi, \pi]$ — by applying the inverse of the argument function corresponding to the Blaschke-product defined on the poles. The method uses the FFT algorithm to compute the coefficients.

The coefficients $c_n = c_{N\ell+k}$ of the representation of $F \in \mathcal{H}^2(\mathbb{D})$ in the generalized orthonormal basis $\{\Phi_n\}$ can approximately computed by accomplishing the following steps:

- Deriving a scale containing M uniformly spaced samples on the interval $[-\pi, \pi]$ of parameter s , i.e. $\{s_0, s_1, \dots, s_M\}$ for $m = 0, 1, \dots, (M-1)$.
- Approximately computing the values of the inverse argument function β_a , i.e. $\{t_0, t_1, \dots, t_M\}$ by $t_m = \beta_a^{-1}(s_m)$ for $m = 0, 1, \dots, (M-1)$.
- Computing the function

$$f_k(s) = F(e^{i\beta_a^{-1}(s)}) \overline{\Phi_k(e^{i\beta_a^{-1}(s)})} \beta_a'(s),$$

on the points s_m as well as $t_m = \beta_a^{-1}(s_m)$ by the use of $F(t_m)$ measurements for the indices $k = 0, 1, \dots, (N-1)$ and $m = 0, 1, \dots, (M-1)$.

- On the basis of the expression of coefficients with the function $f_k(s_m)$

$$\langle F, \Phi_{\ell N+k} \rangle = \frac{1}{2\pi} \int_{-\pi}^{\pi} f_k(s) e^{-i\ell N s} ds.$$

N number of M -point FFTs is performed according to

$$d_{kj} = \frac{1}{M} \sum_{m=-M/2}^{M/2-1} f_k(s_m) e^{-i2\pi \frac{jm}{M}}.$$

resulting in $\{d_{kj}\}$ finite sequences of Fourier coefficients, where $k = 0, 1, \dots, (N - 1)$ and $j = 0, 1, \dots, (M - 1)$.

- Decimating the sequences of the coefficients by N , and ordering the elements of the N number of sequences into a single sequence of the representation coefficients by applying $\ell = j/N$,

$$c_{\ell N+k} = d_{k,\ell N} \quad (k = 0, 1, \dots, N - 1) \quad \text{and} \quad (\ell = 0, 1, \dots, M/N - 1)$$

The method has been introduced in the Chapter 2, and elaborated until algorithmic level in the Chapter 3 in the thesis, and has been published in the conference paper [55].

6.3 Thesis III.

A method has been elaborated to detect phenomena in correspondence with the structure of a system on the basis of the representation of the signals belonging to it in the generalized orthonormal basis generated upon the *a priori* assumed pole set associated with the system. The detection method is based upon the fact, that the representation of a function belonging to the subspace $\mathcal{B}_{a|N} \mathcal{H}^2(\mathbb{D})$ generated by the finite Takenaka-Malmquist system defined upon the presumed poles is finite, i.e. finite number of the representation coefficients differ from zero. In the case of differences on the pole structure, i.e. a deflection occurs on the concerned function from the presumed subspace, the representation becomes infinite.

It has been shown, that the coefficients in an infinite representation beyond the indices corresponding to the multiplicity of the poles exponentially tend to zero with a decay rate proportional to the difference.

A detection scheme has been set up on the basis of the representation coefficients to detect

- changes on the pole placement,

- occurring new poles,
- disappearing existing poles, as well as
- changes on the zero structure

of system under analysis. The detection is realized by decision algorithms upon the values of the coefficients by using deterministic limits or statistical considerations.

The detailed description can be found in the Chapter 4 of the of the thesis, and has been published in conference papers [65, 63].

6.4 Thesis IV.

In connection with the identification of systems by representing the signals belonging to them in generalized orthogonal bases a method for the refinement of the a priori assumed pole structure has been constructed. The method establishes a convergent iteration scheme upon the modification of the poles — involved also their multiplicities — in the direction determined by a *biorthogonal* system with the generalized orthonormal basis in respect to a *discrete scalar product*. The iteration on the poles $\mathbf{a} = \{a_0, a_1, \dots, a_{n-1}\}$ with multiplicities $\mathbf{m} = \{m_0, m_1, \dots, m_{n-1}\}$ is defined by

$$\mathbf{a}^{\nu+1} := G(\mathbf{a}^\nu) \quad (\nu \in \mathbb{N}, \mathbf{a}^0 \in \mathbb{D}^n)$$

where

$$G_k(\mathbf{a}) := a_k + \frac{1}{m_k - 1} \frac{F_k(\mathbf{a})}{F_k^-(\mathbf{a})} \quad (k = 1, \dots, n) \quad G := (G_1, \dots, G_n).$$

and

$$F_k(\mathbf{a}) := [\Phi_{k(m_k-1)}^{\mathbf{m}}(\cdot, \mathbf{a}), f_{\hat{\mathbf{a}}}]_N, \quad F_k^-(\mathbf{a}) := [\Phi_{k(m_k-2)}^{\mathbf{m}}(\cdot, \mathbf{a}), f_{\hat{\mathbf{a}}}]_N.$$

The functions $\{\Phi_{k\ell}\}$ form a bi-orthogonal system with the generalized orthogonal basis $\varphi_{k\ell}$ with respect to a discrete scalar product $[\cdot, \cdot]_N$ defined upon N number of measurement

points, i.e.

$$[\Phi_{kl}, \varphi_{rs}] = \delta_{kl} \delta_{rs}$$

The discrete scalar product has been defined on the basis of the discrete form of the Cauchy integral. A method for the construction of the functions Φ_{kl} is also given.

The detailed description can be found in Section 5.4 of the Chapter 5 of the thesis, and has been published in the conference paper [62].

6.5 Thesis V.

A measurement method has been proposed, based upon non-uniformly spaced frequency values, computed from the inverse argument function — belonging to the Blaschke-product defined upon a predefined pole set — of a uniformly spaced set of values in the interval $[-\pi, \pi]$. This non-uniformly spaced set of frequency-domain measurements forms the starting point of the representation methods in generalized orthonormal bases (see Thesis II), however it has benefits in any other signal processing method connected to spectral functions, since

- for signals belonging to the subspace $\mathcal{B}_{a|N} \mathcal{H}^2(\mathbb{D})$ generated by the Blaschke-product this scale results in optimal arrangement of sample points on the spectral function, since these points are reference points of an exact interpolation operator.
- for signals residing near to the subspace $\mathcal{B}_{a|N} \mathcal{H}^2(\mathbb{D})$ the scale results in suboptimal — however advantageous — arrangement of sample points on the spectral function.

Applying this non-uniform scale the spectral function of signals satisfying the conditions of the above cases can be represented better even by using less sample points, than the classic methods applying uniform spacing in sampling.

The detailed description can be found in Sections 3.3 and 3.4 of the Chapter 3 of the thesis, and published in the conference paper [64].

6.6 Thesis VI.

By applying the ϕ -summation schemes the convergence of the representations based upon generalized orthonormal bases has been extended from the \mathcal{H}^2 space to \mathcal{H}^∞ . Based upon the definition of the ϕ -summation operator

$$U_m^\varphi(F) = \sum_{k=0}^{N-1} \sum_{\ell=0}^{\infty} \varphi\left(\frac{\ell N}{m}\right) \langle F, \Phi_{\ell N+k} \rangle \Phi_{\ell N+k}$$

where $\{\Phi_n\}$ are the members of a generalized orthonormal basis, φ is the function of a summation-procedure; and the definition

$$M_p(\hat{\varphi}) := \int_{-\infty}^{\infty} |t|^p |\hat{\varphi}(t)| dt < \infty \quad (p \geq 0)$$

the following theorem has been proven:

Theorem 6.6.1. *Let φ be a compactly supported even continuous function with $\varphi(0) = 1$ and $M_1(\hat{\varphi}) < \infty$. Then there exists a constant $C > 0$ depending only on $a \in \mathbb{D}^N$ and φ (and independent on m) such that*

$$\|U_m^\varphi F\|_{H^\infty} \leq C \|F\|_{H^\infty}$$

where $F \in H^\infty$, $m = 1, 2, \dots$. Moreover, for any functions F belonging to the disc algebra we have

$$\lim_{m \rightarrow \infty} \|U_m^\varphi F - F\|_{H^\infty} = 0.$$

The detailed description can be found in Section 5.5 of the Chapter 5 of the thesis, and has been published in the conference paper [55].

Bibliography

- [1] A.Edelmayer, J. Bokor, and L. Keviczky, *An H_∞ approach to robust detection of failures in dynamical systems*, Proc. of 33rd IEEE Conf. on Decision and Control (Orlando, FL), Dec 1994, pp. 3037–3039.
- [2] ———, *A scaled L_2 optimization approach for improving sensitivity of H_∞ detection filters for LTV systems*, Proc. of 2nd IFAC Symp. on Robust Control Design, ROCOND'97 (Budapest, Hungary), 1997, pp. 543–548.
- [3] A.Edelmayer, J. Bokor, F. Szigeti, and L. Keviczky, *Robust detection filter design in the presence of time varying system perturbations*, Automatica **33** (1997), no. 3, 471–475.
- [4] M. Basseville and A. Benveniste, *Detection of abrupt changes in signals and dynamical systems*, Lecture notes in control and information sciences, vol.77, Springer-Verlag, New York, Berlin, Heidelberg, 1985.
- [5] M. Basseville and I. Nikiforov, *Detection of abrupt changes – theory and applications*, Prentice-Hall, Inc., Englewood Cliffs, NJ, 1993.
- [6] J. Bokor, *Approximate identification for robust control*, Preprints of the 2nd IFAC Symposium on Robust Control Design (Budapest, Hungary) (Cs. Bányász, ed.), 1997, ROCOND'97, pp. 25–36.
- [7] ———, *Approximate identification for robust control*, Annual Reviews in Control **22** (1998), 187–198.

- [8] J. V. Candy, *Signal processing: the modern approach*, McGraw-Hill Book Company, New York, St. Louis, San Francisco, 1988.
- [9] C. T. Chou, M. Verhagen, and R. Johanson, *Continuous-time identification of siso systems using laguerre functions*, IEEE Trans, Signal Processing **47** (1999), no. 2, 349–362.
- [10] C. K. Chui, *An introduction to wavelets*, Academic Press, Inc., Boston, San Diego, New York, 1992.
- [11] C. K. Chui and G. Chen, *Signal processing and systems theory*, Springer-Verlag, New York, Berlin, Heidelberg, 1987.
- [12] L. Cohen, *Time-frequency analysis*, Prentice Hall PTR, Englewood Cliffs, New Jersey, 1995.
- [13] T.H. Cormen, C.E. Leiserson, and R.L. Rivest, *Introduction to algorithms*, Massachusetts Institute of Technology, Boston, MA, 1990.
- [14] I. Daubechies, *Ten lectures on wavelets*, CBMS-NSF regional conference series in applied mathematics; 61, SIAM, Philadelphia, Pennsylvania, 1992.
- [15] T.J. de Hoog, Z. Szab, P.S.C. Heuberger, P.M.J. Van den Hof, and J. Bokor, *Minimal partial realization from generalized orthonormal basis function expansions*, Automatica **38** (2002), no. 4, 655–669.
- [16] P.M.J. Van den Hof, P.S.C. Heuberger, and J. Bokor, *System identification with generalized orthonormal basis functions*, Proc. of the 33rd Conference on Decision and Control (Lake Buena Vista, FL), 1994, CDC'94, pp. 3382–3387.
- [17] B. Fisher and A. Medvedev, *Laguerre shift identification of a pressurizer process*, Proc. of the American Control Conference (Philadelphia, PA), vol. 3, 1998, ACC'98, pp. 1933–1937.

- [18] ———, *Laguerre domain estimation of time-delays in narrowband ultrasonic echoes*, Proc. of the 14th IFAC World Congress (Beijing, P. R. China), vol. H, 1999, pp. 361–366.
- [19] J. B. Garnett, *Bounded analytic functions*, Academic Press, New York, London, Toronto, Sydney, San Francisco, 1981.
- [20] L. Gianone, J. Bokor, and F. Schipp, *Approximate \mathcal{H}_∞ identification using partial sum operators in a disc algebra basis*, IEEE Transaction on Automatic Control **43** (1996), no. 8, 1117–1122.
- [21] P. Henrici, *Applied and computational complex analysis*, John Wiley & Sons, New York, London, Sidney, Toronto, 1987.
- [22] P. S. C. Heuberger and P. M. J. Van den Hof, *The hambo transform: A signal and system transform induced by generalized orthonormal basis functions*, Proc. 13th IFAC World Congress (San Francisco, CA), 1996, pp. 357–362.
- [23] W. H. Kautz, *Transient synthesis in the time domain*, IRE Trans. Circuit Theory **CT-1** (1954), 29–39.
- [24] L. Keviczky, J. Bokor, S. Veress, and I. Nagy, *Application of ar and arma methods for diagnostics of a nuclear power plant*, Proc. 8th IFAC/IFORS Symp. on Identification and System Parameter Estimation (Beijing, China), 1988, pp. 947–952.
- [25] E. Kreyszig, *Introductory functional analysis with applications*, John Wiley & Sons, New York, 1989.
- [26] L. Ljung, *System identification: theory for the user*, Prentice-Hall, Inc., Englewood Cliffs, NJ, 1987.
- [27] L. Lovász and P. Gács, *Algorithms*, Műszaki Könyvkiadó, Budapest, Hungary, 1978, (in hungarian).
- [28] P. M. Mäkilä, *Approximation of stable systems by Laguerre filters*, Automatica **26** (1990), no. 2, 333–345.

- [29] ———, *Laguerre series approximation of infinite dimensional systems*, *Automatica* **26** (1990), no. 6, 985–995.
- [30] ———, *Approximation of stable systems and optimal approximation*, *Automatica* **27** (1991), no. 4, 663–676.
- [31] ———, *Laguerre methods and H_∞ identification of continuous-time systems*, *Int. J. Control* **56** (1991), no. 3, 689–707.
- [32] ———, *Worst case input-output identification*, *Int. J. Control* **57** (1992), 673–689.
- [33] P. M. Mäkilä and J. R. Partington, *Robust approximate modelling of stable linear systems*, *Int. J. Control* **58** (1993), 665–683.
- [34] F. Malmquist, *Sur la détermination d'une classe de fonctions analytiques par leur valeurs dans un ensemble donné de points*, *Comptes Rendus du Sixième des mathématiciens scandinaves (Kopenhagen, Denmark)*, 1925, pp. 253–259.
- [35] R. S. Mangoubi and A. M. Edelmayer, *Model based fault detection: the optimal past, the robust present, and a few thoughts on the future*, *Proc. of 4th IFAC Symposium on Fault Detection Supervision and Safety for Technical Processes, SAFEPROCESS'2000 (Budapest, Hungary)*, June 2000, pp. 64–75.
- [36] L. Máté, *Wilbert space methods in science and engineering*, Akadémiai Kiadó, Budapest, 1989.
- [37] Th. McKelvey, H. Akçay, and L. Ljung, *Subspace-based multivariable system identification from frequency response data*, *IEEE Autom. Control* **AC-41** (1996), 960–979.
- [38] B.M. Ninness and F. Gustafsson, *A general construction of orthonormal bases for system identification*, *Proc. of 33rd IEEE Conf. on Decision and Control (Orlando, FL)*, Dec 1994, pp. 3388–3393.
- [39] ———, *A unifying construction of orthonormal bases for system identification*, *Tech. Report EE9432, Department of Electrical Engineering, University of Newcastle, Newcastle, NSA, Australia*, 1994.

- [40] ———, *A unifying construction of orthonormal bases for system identification*, IEEE Transactions on Automatic Control **42** (1997), no. 4, 515–521.
- [41] P. Van Overschee and B. De Moor, *Subspace algorithms for the stochastic identification problem*, Proc. of 30th IEEE Conf. on Decision and Control, CDC'91 (Brighton, UK), 1991, pp. 1321–1326.
- [42] ———, *N4sid: subspace algorithms for the identification of combined deterministic-stochastic systems*, Automatica **30** (1994), 75–93.
- [43] J. R. Partington, *Robust identification and interpolation in H_∞* , Int. J. Control **54** (1991), no. 5, 1281–1290.
- [44] ———, *Robust identification in H_∞* , Journal of Mathematical Analysis and Applications **100** (1992), 428–441.
- [45] P.M.J. Van den Hof P.S.C. Heuberger, O.H. Bosgra, *A generalized orthonormal basis for linear dynamical systems*, IEEE Trans. on Automatic Control **AC-40** (1994), no. 3, 451–465.
- [46] W. Rudin, *Real and complex analysis*, 1 ed., Series in Higher Mathematics, McGraw-Hill, New York, 1966.
- [47] ———, *Functional analysis*, McGraw-Hill, New York, 1973.
- [48] F. Schipp and J. Bokor, *L^∞ system approximation algorithms generated by ϕ summations*, Automatica **33** (1997), no. 11, 2019–2024.
- [49] ———, *Approximate identification in Laguerre and Kautz bases*, Automatica **34** (1998), no. 4, 463–468.
- [50] F. Schipp, L. Gianone, J. Bokor, and Z. Szabó, *Identification in generalized orthonormal basis - a frequency domain approach*, Proc. of the 13th IFAC World Congress (San Francisco, CA), 1996, pp. 387–392.
- [51] F. Schipp, W. R. Wade, and P. Simon, *Walsh series, an introduction to dyadic harmonic analysis*, Adam Hilger Ltd., Bristol, New York, 1990.

- [52] A. Soumelidis, *Applications of wavelet type constructions in vehicle dynamics*, Proceedings of the 5th Mini Conference On Vehicle Dynamics, Identification and Anomalies (Budapest, Hungary), 1996, VSDIA'96, pp. 421–425.
- [53] A. Soumelidis, J. Bokor, P. Gáspár, and T.T. Hai, *Virtual instrument tools for signal processing and system identification based failure detection in complex plants*, Chemical Engineering World **XXXI** (1996), no. 7, 49–52.
- [54] A. Soumelidis, J. Bokor, L. Keviczky, A. Edelmayer, P. Gáspár, Zs. Cski, and E. Varga, *Toward an intelligent evolutionary signal processing based failure monitoring and diagnostic system for complex plants*, Proc. of 2nd IFAC Symposium on Fault Detection Supervision and Safety for Technical Processes (Espoo, Finland), 1994, SAFEPROCESS'94, pp. 760–765.
- [55] A. Soumelidis, J. Bokor, and F. Schipp, *Representation and approximation of signals and systems using generalized Kautz functions*, Proc. of the 36th Conference on Decision and Control (San Diego, CA), 1997, CDC'97, pp. 3793–3796.
- [56] A. Soumelidis and A. Edelmayer, *Modelling of complex systems for control and fault diagnostics: a knowledge based approach*, Engineering systems with intelligence. Concepts, tools and applications, ed. S. Tzafestas, pp. 152–132, Kluwer Academic Publ., Amsterdam, Holland, 1991, EURISCON'91, Corfu, Greece, 1991.
- [57] A. Soumelidis, P. Gáspár, and J. Bokor, *Inverted pendulum: an environment for intelligent control design and tests*, 3rd IFAC Symposium on intelligent components and instruments for control applications (Annecy, France), 1997, SICICA'97, pp. 421–425.
- [58] ———, *An inverted pendulum tool for teaching linear optimal and model based control*, Periodica Polytechnica Ser. Transp. Eng. **25** (1997), no. 1-2, 9–19.
- [59] A. Soumelidis, G.Z. Kovács, J. Bokor, P. Gáspár, L. Palkovics, and L. Gianone, *Automatic detection of the lane departure of vehicles*, 8th IFAC Symposium on Transportation Systems (Chania, Greece), 1997, pp. 1096–1101.

- [60] A. Soumelidis and I. Nagy, *Intelligent modelling of complex physical systems: application in diagnostics of NPPs*, Proc. of the 11th IFAC World Congress (Tallin, USSR), vol. 7, 1990, pp. 13–17.
- [61] A. Soumelidis, I. Nagy, and J. Bokor, *Analyzing time-varying and transient vibration properties in technological systems*, 5th International Congress on Sound and Vibration (Adelaide, Australia), 1997, pp. 2071–2078.
- [62] A. Soumelidis, M. Papp, F. Schipp, and J. Bokor, *Frequency domain identification of partial fraction models*, accepted for publication on the 15th IFAC World Congress (Barcelona, Spain), 2002, pp. –.
- [63] A. Soumelidis, F. Schipp, and J. Bokor, *Detection of changes on signals and systems based upon representations in orthogonal rational bases*, submitted to 36th Conference on Decision and Control (Las Vegas, Nevada, USA), 2002, CDC'2002, pp. –.
- [64] ———, *Frequency domain representation of signals in rational orthogonal bases*, submitted to Mediterranean Control Conference (Lissabon, Portugal), 2002, MED'2002, pp. –.
- [65] A. Soumelidis, Z. Szabó, and J. Bokor, *Fault detection in lightly damped systems using rational orthonormal functions*, Proc. of 4th IFAC Symposium on Fault Detection Supervision and Safety for Technical Processes, SAFEPROCESS'2000 (Budapest, Hungary), June 2000, pp. 548–553.
- [66] Z. Szabó, *\mathbb{L}^p norm convergence of rational operators on the unit circle*, Mathematica Pannonica **9** (1998), no. 2, 281–292.
- [67] ———, *Rational orthonormal functions and applications*, Ph.D. thesis, Eötvös Loránd University of Budapest, 2001.
- [68] Z. Szabó, J. Bokor, and F. Schipp, *Nonlinear rational approximation using generalized orthonormal basis*, Proc. of the European Control Conference (Brussels, Belgium), vol. 6 Part B, 1997, ECC'97, pp. 25–36.

- [69] G. Szegő, *Orthogonal polynomials*, 4 ed., AMS, New York, 1981.
- [70] B. Szőkefalvi-Nagy, *Real functions and function series*, 6 ed., Tankönyvkiadó, Budapest, 1977, (in hungarian).
- [71] S. Takenaka, *On the orthogonal functions and a new formula of interpolation*, Japanese Journal of Mathematics **II** (1925), 129–145.
- [72] I. Vajk, A. Soumelidis, Cs. Bányász, and L. Keviczky, *Adaptive controllers as virtual instruments*, Proceedings of the 1st IFAC Conference on System Identification (Budapest, Hungary), 1994, SYSID'94, pp. 291–296.
- [73] B. Wahlberg, *System identification using Laguerre models*, IEEE Trans. on Automatic Control **AC-36** (1991), 551–562.
- [74] ———, *System identification using Kautz models*, IEEE Trans. on Automatic Control **AC-39** (1994), 1276–1282.
- [75] A. Zygmund, *Trigonometric series vol. 1-2*, Cambridge University Press, Cambridge, 1959.